INFORMATION TO USERS

This manuscript has been reproduced from the microfilm master. UMI films the text directly from the original or copy submitted. Thus, some thesis and dissertation copies are in typewriter face, while others may be from any type of computer printer.

The quality of this reproduction is dependent upon the quality of the copy submitted. Broken or indistinct print, colored or poor quality illustrations and photographs, print bleedthrough, substandard margins, and improper alignment can adversely affect reproduction.

In the unlikely event that the author did not send UMI a complete manuscript and there are missing pages, these will be noted. Also, if unauthorized copyright material had to be removed, a note will indicate the deletion.

Oversize materials (e.g., maps, drawings, charts) are reproduced by sectioning the original, beginning at the upper left-hand corner and continuing from left to right in equal sections with small overlaps.

Photographs included in the original manuscript have been reproduced xerographically in this copy. Higher quality 6" x 9" black and white photographic prints are available for any photographs or illustrations appearing in this copy for an additional charge. Contact UMI directly to order.

Bell & Howell Information and Learning
300 North Zeeb Road, Ann Arbor, MI 48106-1346 USA
800-521-0600

BRINE PERCOLATION, FLOODING AND SNOW ICE FORMATION ON ANTARCTIC SEA ICE

A

THESIS

Presented to the Faculty

of the University of Alaska Fairbanks

in Partial Fulfillment of the Requirements

for the Degree of

DOCTOR OF PHILOSOPHY

By

Ted Maksym, B.Sc.(Hons.)

Fairbanks, Alaska

May 2001

BRINE PERCOLATION, FLOODING AND SNOW ICE FORMATION ON ANTARCTIC SEA ICE

By

Ted Maksym

RECOMMENDED:

Advisory Committee Chair

Department Head

APPROVED:

Dean, College of Science, Engineering and Mathematics

Dean of the Graduate School

1-9-01

Date

Abstract

Modelling studies of brine percolation, flooding, and snow ice formation on Antarcic sea ice were undertaken to (1) determine the influence of brine transport processes on the salinity, porosity, and stable isotopic composition of snow ice and the underlying ice, (2) explain the range of salinities and isotopic composition observed in ice cores, and to provide a better estimate of the contribution of snow ice to the thickness of the winter pack ice, (3) better understand the microstructural controls on brine percolation and its effects on the properties of sea ice, and (4) understand the effects of meteorological forcing on snow ice formation and development of the ice cover.

Snow ice thickness is most dependent on snow accumulation rates. Once snow ice begins to form on a floe, most of the subsequent thickening is due to snow ice formation. Results show that percolation in winter sea ice is most likely an inhomogeneous process. Flooding most likely occurs rapidly through localized regions of high permeability, such as in large, open brine drainage channels or cracks.

Simulations of the freezing of a flooded slush layer show that focussing of thermohaline convection may form porous drainage channels in the ice and snow. These channels allow rapid desalination of the slush and exchange of $H_2{}^{18}O$ depleted brine with sea water. Significant positive shifts in $\delta^{18}O$ are possible in the slush layer. This process can explain the range of $\delta^{18}O$ observed in ice cores. Based on these results, a cutoff of $\delta^{18}O < -2‰$ is recommended for snow ice identification in the Ross, Amundsen, and Bellingshausen seas. Such a cutoff puts the amount of snow ice observed at 6-18% of the ice thickness.

Although flooding appears to occur through spatially restricted regions of the ice, the precise nature of the flow and factors controlling onset of percolation are unclear.

Contents

List of Figures

List of Tables

Acknowledgements

Paying due credit to all who, even in a small way, contributed to the completion of a thesis is an important task, as it has been said that the oft-most read part of a thesis is the acknowledgements [*Heavner*, 1999]. In the more than six years that have passed since I began this journey, many people have come and gone who have, in their various ways, shaped this work.

First and foremost, I want to thank my advisor, Martin Jeffries, who made this thesis possible. His guidance, support, and encouragement have been instrumental in the completion of this work. As much as anything, the freedom he allowed me to pursue my own ideas has helped shape not only this thesis, but also myself as a scientist. His faith in my ideas and ability has been of singular importance in preserving my love of science.

The rest of my committee, Willy Weeks, Hajo Eicken, Matthew Sturm, and Keith Echelmeyer all deserve credit for their contributions. Willy, for first introducing me to the field of sea ice, and showing how genuinely interesting this stuff can be. Hajo and Matthew, for many stimulating discussions about arcane aspects of snow and sea ice, and showing me that some people actually do care about the small stuff. Matthew especially deserves mention as a source of inspiration to pursue a scientific career, for his indefatigable interest in snow and ice and his belief that one should have the courage to be wrong. I must also thank Will Harrison, who acted as a surrogate committee member, welcomed me into his home when I first came to Alaska, and always was ready with a good Newfie joke (although usually the same one). He and Keith reminded me of the pitfalls of modelling and helped to keep me honest.

For keeping me solvent during the past six years, I must thank the National Science

Foundation who provided funding through NSF grant OPP 9316767. Roger Smith, director of the Geophysical Institute, also provided generous support.

I must also thank all the user consultants at the Arctic Region Supercomuting Center for all their help over the years fixing technical difficulties and for the "dorm room", and all the fine folks at Coca-Cola for keeping me awake down the home stretch. To everyone who sailed with me aboard the *Nathaniel B. Palmer*, I thank you for making those months of darkness some of the most enjoyable adventures I have had.

Lastly, I must thank all those who have made my time in Alaska one of the best chapters of my life. Rob and the Swiss truffle, my fellow viz lab trolls, have made what has really been my home more bearable. Tina has put out her best efforts to keep me distracted from work every so often. Most of all I want to thank everyone from Crane Court: Laura (and her website), Bevin, Matt and Carrie, Pig and Toad, Lisa and family, D 'n' T, Jesus and pals, and everyone else who made it the best neighbourhood I've ever had, even if I only stopped by once and a while. As Laura once told me at the Crane Court bonfire, this is truly a magical place.

Of all the Crane Courters, the sincerest thanks must go to Ryan. He has been a loyal friend since my arrival in Fairbanks. His kindness, good humour, and philosophy of hard work and clean living have taught me that there is more to grad school than grad school.

But above all, I want to thank Alison who put her own life on hold and suffered through all the long-distance plane flights, outdoor plumbing, and missed graduation deadlines. For her steadfast support, "gentle" encouragement, and yeomen kindness in the final sleepless weeks, I owe more than I can repay (and a Passat). Most of all, I thank her for staying even when the snow fell.

Preface

Parts of Chapter 3 and Chapter 4 of this thesis have been published in the following peer-reviewed articles:

Maksym, T. and M. O. Jeffries, Phase and compositional evolution of the flooded layer during snow ice formation on Antarctic sea ice, *Ann. Glaciol.*, in press, 2001.

Maksym, T. and M. O. Jeffries, A one-dimensional percolation model of flooding and snow ice formation on Antarctic sea ice, *J. Geophys. Res.*, *105*, 26,313-26331, 2000.

The author participated in the collection of data used herein aboard the R/V *Nathaniel B. Palmer* on cruises NBP95-3 and NBP95-5 in 1995.

Chapter 1

Introduction

1.1 Snow ice and the climate system

Snow ice is, in short, frozen slush. Not so glamorous, perhaps, yet it is an important geophysical phenomenon in the cryosphere and climate system. While interpretations vary, I will define snow ice here strictly as ice which forms when a saline slush layer freezes at the surface of sea ice. When a sea ice floe is depressed below sea level, typically from the weight of it's snow cover, brine and/or sea water may percolate to the ice surface, flooding the snow pack to create slush. Upon freezing, a porous, saline ice layer is formed. Recent observations in all regions of the Southern Ocean indicate that this is a major mechanism for Antarctic sea ice thickening. Despite widespread occurrence, there are few detailed *in situ* observations of this process, and little is known about the dependence of the process on ice thermo-physical and morphological properties or its effects on the evolution of these properties and the overall ice mass balance.

Flooding and snow ice formation have many implications on both small and large scales, from its effects on ocean-atmosphere heat transfer, salinity fluxes to the upper ocean, effects on sea ice remote sensing signatures, and the primary productivity of the Southern Ocean. Snow ice formation may be of significant global importance in climate change, providing a buffer to the effects of warming and enhanced moisture transport in the Antarctic [*Eicken et al.*, 1995]. In order to assess the larger impacts of flooding and snow ice formation on these processes, one must understand the evolution of snow ice on

smaller scales, ranging from the centimeter scale of the internal brine network, to that of individual ice floes. In the absence of detailed time series field observations, computer modelling is a valuable tool in the evaluation of the role various thermo-physical processes play in flood-freeze cycles and their effect on the evolution of the ice mass balance. In this work, modelling studies of sea water percolation and snow ice formation are presented in an attempt to assess their role in the evolution of Antarctic sea ice.

The Ross, Amundsen, and Bellingshausen (RAB) seas appear to be a region of exceptional snow ice production, with the ubiquitous occurrence of flooding and snow ice throughout the growth season. This three part study will focus on the winter production of snow ice in this region. The first part explores the small scale evolution of the flooded layer and underlying ice to examine the role of brine exchange in controlling the ice porosity and the transport of salt within the ice. An attempt is made to explain the wide range of ice $\delta^{18}O$ and salinity values observed in the field and to aid in making a better estimate of snow ice quantities observed in ice cores. In the second part, a simple flooding and snow ice growth model is used to evaluate the importance of ice permeability and climatic forcing on Antarctic ice development. Finally, the interplay between ice microstructure and brine percolation is examined in more detail and the implications of heterogeneous percolation and snow ice formation on the evolution of individual ice floes is explored.

1.2 Ice growth processes

Antarctic sea ice can be divided into three distinct types based on its growth processes: frazil, congelation, and snow ice. Frazil ice forms under the turbulent conditions of wind and wave action through the "pancake cycle" [*Wadhams et al.*, 1987; *Lange et al.*, 1989]. During initial ice formation, ice platelets suspended in the water column begin to aggregate, eventually consolidating into small circular floes, or pancakes. These floes continue to interact and increase in size and adhere to one another. As they grow, the floes damp the wave field until the individual cake floes can consolidate and form sheet ice. Rafting of pancakes is common. This process leads to sea ice with a granular texture, with individual grains sizes of one to several millimeters. The consolidation process generally limits the thickness of pancakes to about 40 cm [*Lange et al.*, 1990; *Worby et al.*, 1998].

As the Antarctic ice pack is exposed to the intrusion of storms and ocean swell, this is the predominant mode of ice formation in many regions [*Wadhams et al.*, 1987; *Lange et al.*, 1989; *Lange and Eicken*, 1991; *Jeffries et al.*, 1997].

Once the initial ice pack has formed, or in quiescent conditions, ice growth proceeds by congelation growth, whereby columnar crystals grow downward at the base of the floe. Congelation ice is easily identified by its long wide columns and cellular substructure. This mode of growth is somewhat less common, representing generally 20-40% of the total thickness [*Lange and Eicken*, 1991; *Jeffries et al.*, 1997; *Worby et al.*, 1998], though in the relatively sheltered inner Ross Sea, it may exceed 60% [*Jeffries and Adolphs*, 1997]. Dynamic thickening through rafting or ridging of both frazil and congelation ice is exceedingly common; few ice cores are observed that don't exhibit multiple layering [see e.g., *Lange et al.*, 1990; *Worby et al.*, 1996; *Jeffries and Adolphs*, 1997; *Jeffries et al.*, 1997]. Snow ice formation is distinct from the other two processes in that thickening of the ice occurs at the top of the floe. The freezing front is poorly defined, since an ice matrix (snow grains) exists across it's thickness. This allows a temperature gradient to develop across the slush layer and freezing to take place throughout the entire layer. Consequently, as the ice congeals, pockets of brine are readily entrapped, hence the salinity of a snow ice layer may be quite high. Thorough freezing of the flooded layer is dependent on the presence of pathways for the drainage of brine from the slush. Snow ice, like frazil, has a granular substructure. Typically it is less dense [*Leppäranta*, 1983] and more saline than frazil ice. Snow ice is generally found at the top of ice cores, although a modest amount is found in buried layers as a result of deformation [*Jeffries et al.*, 1997, 1998b]. Snow ice, as defined herein, is different from other types of sea ice with a meteoric ice (i.e. snow) fraction. These include superimposed ice, which forms from the re-freezing of snow melt [*Kawamura et al.*, 1997; *Jeffries et al.*, 1994] as well as ice that has snow incorporated directly into the ice matrix during growth.

1.3 Role of snow ice in sea ice processes

Snow ice formation has a broad range of impacts on the physical characteristics of Antarctic sea ice and ocean-ice-atmosphere exchange. Most importantly, flooding of the

ice surface moves the freezing front from the ice/ocean interface to the base of the snow pack while significantly reducing the effective snow depth [*Jeffries et al.*, 2001]. This causes an increase in the heat flux through the snow layer, greatly enhancing the rate of ice growth. Concomitantly, the growth at the bottom of the floe ceases until slush freeze-up is complete, or if there is significant oceanic heat flux, there may be substantial basal melt. This thins the ice, increasing the relative snow load, therefore enhancing flooding and snow ice formation. This process has been likened to a "conveyor belt" method of ice growth [*Jeffries et al.*, 1997] where frazil or congelation ice is continually replaced by snow ice, eventually resulting in ice composed completely of snow ice [e.g., *Jeffries et al.*, 1994]. If conditions are such that the slush layer does not freeze, this cycle may cause the disintegration of the ice cover, as hypothesized by *Jacobs and Comiso* [1993].

The influence of flooding on the snow cover is largely manifested in a decrease in snow thickness, and hence, a reduction in insulation of the ice, but it also has important effects on the snow pack microstructure itself. Capillary suction will wick brine in the snow up above sea level. This results in a wet saline layer that persists even after the flooded layer has frozen [*Sturm et al.*, 1998; *Massom et al.*, 1997, 1998]. In the presence of brine, snow grains will coarsen, leading to a somewhat higher thermal conductivity at the base of the snow pack [*Crocker*, 1984]. The bottom layer of the snow is usually composed of low conductivity depth hoar [*Sturm et al.*, 1998; *Massom et al.*, 1997, 1998], so flooding will tend to remove the least conductive strata of the snow pack [*Sturm et al.*, 1998]. All these processes work to enhance the heat flux through the snow pack making flooding an effective means of enhancing ice growth rates, both within the flooded layer, and at the ice/ocean interface once the flooded layer has frozen. As a negative feedback, however, the steepened temperature gradient due to thinner snow may enhance the development of depth hoar, acting to reduce heat loss from the ice [*Sturm et al.*, 1998].

Flooding of the snow pack with sea water provides a substantial heat flux to the ice surface, warming the underlying ice and thereby increasing the ice brine volume. Brine pockets and tubes enlarge and become more connected, enhancing the hydraulic connectivity between the flooded layer and the ocean. This allows a continuous exchange of brine through the ice as the slush freezes, providing a significant fraction of the salt flux to the upper ocean in second year pack ice [*Lytle and Ackley*, 1996]. This brine exchange is also

a significant source of nutrients for inter-ice algal communities [*Fritsen et al.*, 1994, 1998].

Flood-freeze cycles have an effect on microwave remote sensing signatures of sea ice. The presence of slush and brine wicking up into the snow pack will tend to increase the radar backscatter due to high dielectric contrast between dry and saline snow [*Lytle et al.*, 1996]. As the slush freezes and decreases in salinity [*Lytle and Ackley*, 1996], backscatter may drop by as much as 10 dB, though in practice it may only be 2 or 3 dB [*Drinkwater and Lytle*, 1997].

All of these processes will be affected by the small scale behaviour of flooding and snow ice formation. The fluid dynamics of flooding and freezing affect the transport of brine and nutrients through the ice and snow and affect the salinity distribution, and hence, the porosity of the ice. The permeability of the ice will determine the prevalence of snow ice formation and its impact on the snow and ice thickness distribution. In order to fully understand the complex physical and biological processes and interactions taking place in Antarctic sea ice, one must understand the small scale behaviour of brine percolation and re-freezing of slush.

1.4 Mechanisms of snow entrainment into sea ice

In assessing the impact of snow ice production, it is important to be able to distinguish snow ice, as defined here, from sea ice that has a meteoric ice content by other means. Meteoric ice is ice of atmospheric origin, such as snow or frozen rainwater. For a snow ice layer, then, the meteoric ice fraction represents only the snow component, whereas the term "snow ice" refers to the entire layer. This distinction is important as it is the snow ice thickness that represents the contribution of flood-freeze events to the thickening of the ice pack.

Entrainment of snow into sea ice may occur in a number of ways (Figure 1.1). During initial and young ice formation (Figure 1.1a-d) a small amount of snow may be entrained. During frazil ice formation (Figure 1.1a), falling snow may act as seed crystals and be incorporated directly into growing pancakes. As the pancakes develop (Figure 1.1b), floe-floe interactions can cause the squirting of sea water onto the ice surface, where new or falling snow will turn to slush and eventually freeze. This process is quite common [e.g.,

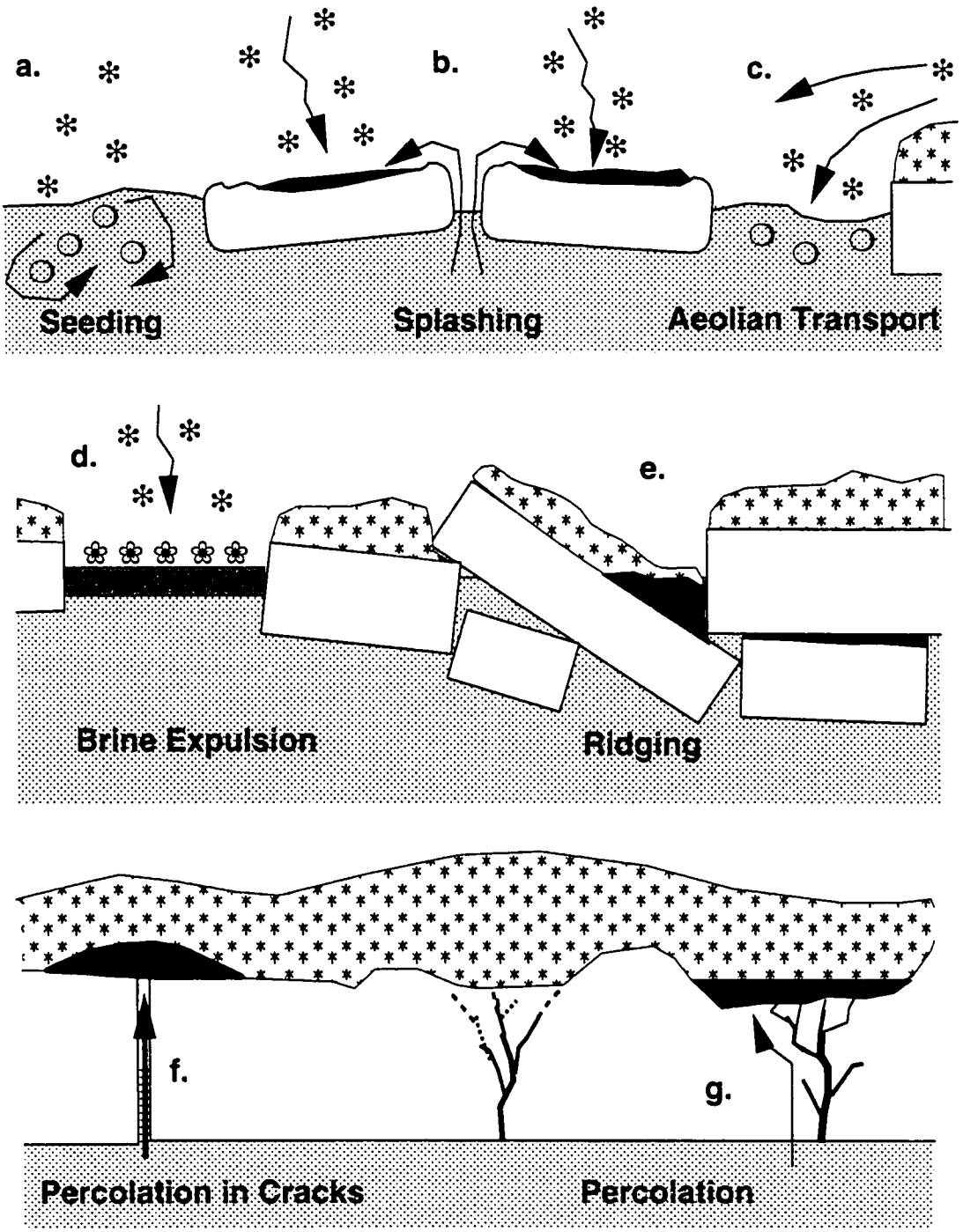

Figure 1.1: Snow entrainment processes in sea ice.

Massom et al., 1998] in the outer pack ice. Snow may also be blown into open leads from the thicker pack ice (Figure 1.1c) and seed frazil growth. Finally, during growth of new ice, or nilas, brine rejected onto the surface leads to the formation of very saline "frost flowers" [*Martin et al.*, 1996]. New snow will be wetted by these frost flowers and may eventually re-freeze (Figure 1.1d). All these processes are probably of minor importance; for instance, for typical frazil growth rates in an open lead of about 20 cm day^{-1}, snow fall would have to be quite vigourous to have a significant impact on the meteoric ice fraction. In any case, averaged over the entire ice pack, where much of the new ice growth will occur in the absence of snowfall, this effect is likely negligible. Flooding of the surface of pancakes may be more important, but in most cases, only one or two centimeters of snow ice are likely to form by this method. This could explain only a fraction of ice layers with a meteoric ice fraction. These four processes are of limited geophysical interest, in that they do not affect ice growth processes in any substantive way.

Ridging and rafting (Figure 1.1e) can be a significant source of flooding and snow ice formation [*Ackley*, 1986]. Ice at the edge of sea ice ridges is often out of local isostatic balance and depressed below sea level. Sea water readily floods the snow in the depressions due to the poor consolidation of the ridge. Ice blocks may also be rafted under the ice sheet. Any snow on the surface of the blocks will form buried snow ice layers. The most common mode of flooding, however, is the percolation of sea water and brine up through relatively level ice (Figures 1.1f-g). Sea water may seep up through narrow cracks in the ice and spread laterally at the surface. Alternatively, brine and sea water may percolate through the interconnected channels and pore space of sea ice. It is this last mechanism which is believed to be the most common and responsible for the greater fraction of snow ice observed, and has been implicitly assumed in most studies [*Crocker and Wadhams*, 1989; *Hudier et al.*, 1995; *Jeffries and Adolphs*, 1997; *Jeffries et al.*, 1998a, b; *Golden et al.*, 1998]. For this to take place, the internal pore space, or brine network, of the ice must be well connected across the entire thickness of the ice to allow fluid to flow. This is often true in the warm, lower layers of the ice sheet, but near the colder, upper surface the pores may become disconnected, rendering the ice impermeable (Figure 1.1g.). Hence, spatial and temporal variations in pore space geometry may have an important impact on brine percolation and surface flooding. Most investigators have not addressed the physical

processes involved in brine percolation beyond noting that for flooding to occur, the sea ice must be permeable [*Eicken et al.*, 1995; *Jeffries et al.*, 1998a, b].

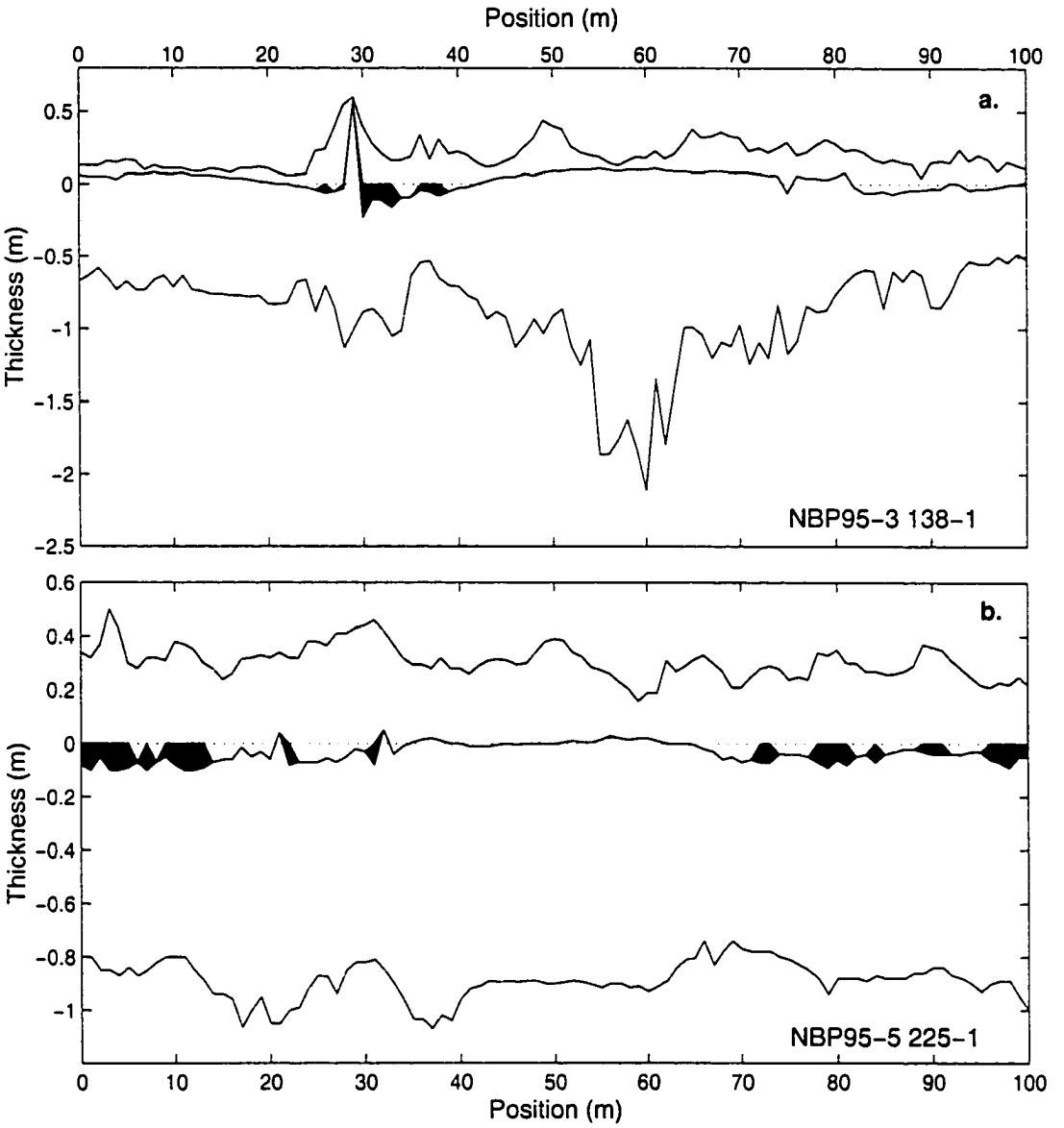

Figure 1.2: Snow depth and ice thickness profiles. Thickness profiles for two selected floes in the Ross Sea sampled in 1995 at (a) 75.2°S, 179.9°E, and (b) 69.5°S, 179.7°W. Snow cover is shaded gray. Sea level is indicated by the dotted line at zero depth. Areas that were flooded prior to drilling are shaded black.

Two typical floes sampled in the Ross Sea in 1995 illustrate the variability in snow and ice thickness and flooding in Figure 1.2. Flooding occurs on the flanks of a ridge of floe 138-1 where the ice surface is below sea level (Figure 1.2a). After meter 80, there is no flooding despite a negative freeboard. Note the bowing of the floe due to the weight of the ridge sail and the buoyancy of the large keel in the middle of the floe. Floe 225-1 (Figure 1.2b) is an essentially unridged floe, yet flooding is common along its length. This flooding is most likely due to percolation through interconnected brine space in the ice. Note that the flooding is not uniform along the floe, indicating that in some regions the ice was impermeable. Furthermore, the flooding was apparently restricted from spreading laterally to some extent. Both floes have significant snow depth variability. The importance of this variability is perhaps best illustrated by re-plotting the snow and ice thicknesses scaled by the inverse of the thermal conductivity (Figure 1.3). This gives the thermal resistance, a measure of the insulating barrier provided by the ice and snow layers. This provides a dramatic illustration of the importance of the insulating effect of the snow and the effect that an inhomogeneous snow cover may have on the evolution of the underlying ice.

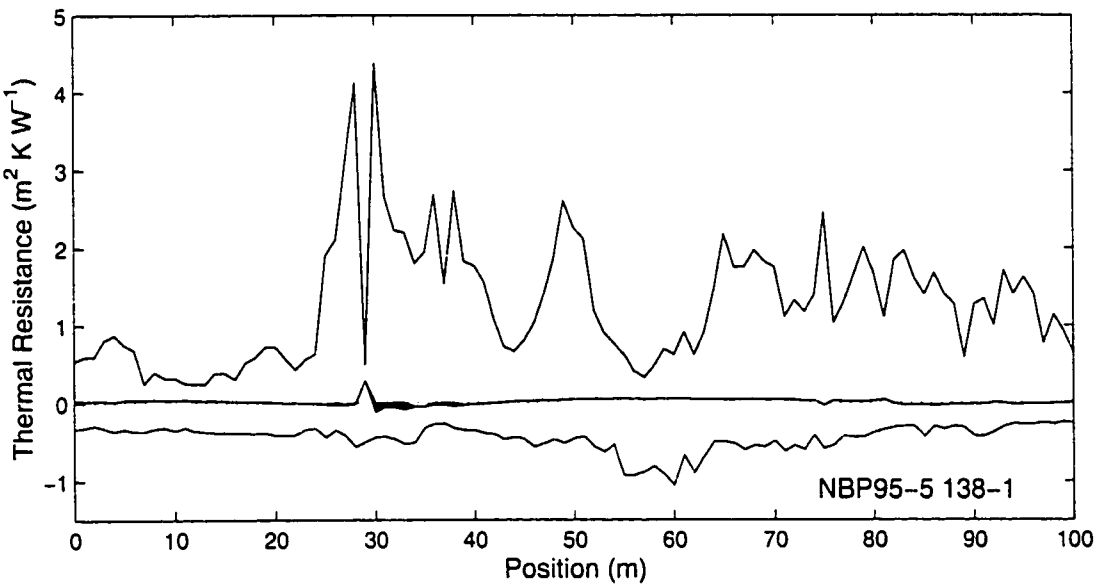

Figure 1.3: Thermal insulation effect of snow. Snow depth and ice thickness profile of Figure 4a with the thicknesses scaled by the inverse of the thermal conductivity

1.5 Percolation in sea ice

1.5.1 Field observations of percolation and flooding

Only a few studies documenting in situ observations of flooding and snow ice formation exist [*Weeks and Lee*, 1958; *Lytle and Ackley*, 1996; *Hudier et al.*, 1995; *Golden et al.*, 1998; *Takizawa*, 1985]. Ironically, although this process is primarily an Antarctic one, the first detailed observations of brine infiltration were made in the Arctic [*Weeks and Lee*, 1958], and to this day, this study remains one of the most thorough. Their observations of flooding at Hopedale, Labrador, based on slush salinity and density, show that the infiltrating fluid was brine displaced from within the ice by sea water. This indicates that the fluid flow takes place through the internal pore space of the ice rather than through larger scale cracks. The flow was limited by low permeability, as the observed slush level lagged behind the theoretical water level for several days. Significant settling of the snow cover was evident. One interesting result of their study was the strong vertical c-axis alignment in the re-frozen slush. *Weeks and Lee* [1958] observed significant desalination of the slush during freezing. This is consistent with other studies [*Lytle and Ackley*, 1996; *Takizawa*, 1985], indicating that there is good hydraulic communication of the brine with the underlying ice and ocean. *Weeks and Lee* [1958] observed a marked increase in the salinity of the underlying ice, occurring either during sea water infiltration of the ice or desalination of the flooded layer. This is in contrast to *Lytle and Ackley* [1996] who observed little change in the salinity of the underlying ice during freeze-up in the Weddell Sea. *Fritsen et al.* [1994] estimate that the brine in the slush layer was replaced several times before freezing. *Hudier et al.* [1995], working in the Sea of Okhotsk, observed significant effects on the salt transfer between the ice and ocean. These observations indicate that brine exchange processes may have a significant effect on the microstructural evolution of the ice.

Golden et al. [1998] have suggested that in colder ice the brine pathways are poorly connected and render the ice effectively impermeable to brine flow. Once the ice warms above a threshold value (approximately -5°C), the ice becomes permeable and flooding occurs. This phenomenon has been observed in the East Antarctic pack ice [*Golden et al.*, 1998]. Clearly, understanding the evolution of the pore space is an important part of

understanding the role of percolation in flooding and thickening of ice floes.

1.5.2 Brine space microstructure

The pore space geometry in sea ice is spatially and temporally inhomogeneous. In congelation ice, brine is trapped between ice lamellae as the ice grows, and tends to form oblately tubular inclusions along plate and crystal boundaries [e.g., *Bennington*, 1987; *Perovich and Gow*, 1996; *Cole and Shapiro*, 1998]. These may be a few millimeters long with poor connectivity in cold ice [*Cole and Shapiro*, 1998] or a centimeter or more long and well connected in warm ice [*Weissenberger et al.*, 1992]. Typically, these inclusions are very small, having a horizontal dimension of a fraction of a millimeter. In very warm ice the brine space may be well connected along crystallographic boundaries [*Perovich and Gow*, 1996, Figure 10]. In frazil ice the entrapped brine forms a convoluted network of pathways along the grain boundaries [*Weissenberger et al.*, 1992, Figure 3].

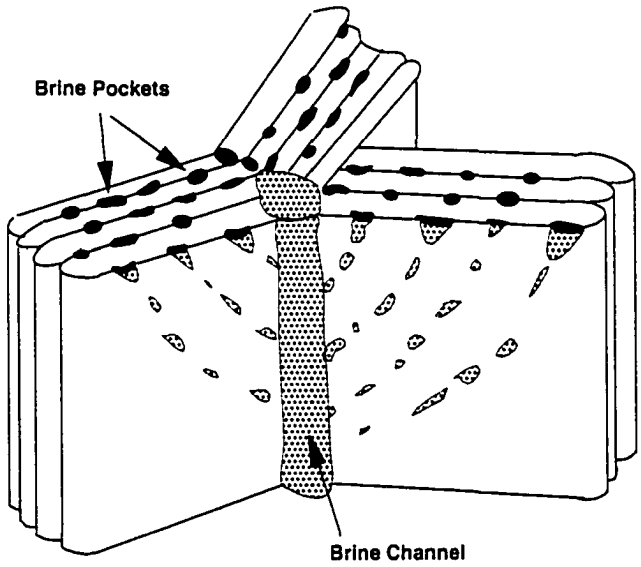

Figure 1.4: Schematic of brine drainage. Porosity structure of congelation ice (after *Wakatsuchi* [1983])

During initial ice growth, thermohaline convection in the porous basal layer causes focussing of brine flow into many small channels [*Worster*, 1997] (Fig. 1.4). These tubes are fed by brine from pockets entrapped along plate boundaries during ice growth. The

number of tubes depends on the growth rate of the ice [*Saito and Ono*, 1980] with tube diameters ranging from less than a millimeter up to a few millimeters [*Lake and Lewis*, 1970; *Freitag*, 1999; *Eicken et al.*, 2000]. Similar features will also form during consolidation of frazil ice [J.-L. Tison, personal communication, 2000]. As the ice thickens, larger tubes appear but become more widely spaced [*Lake and Lewis*, 1970; *Wakatsuchi*, 1983]. In very thick ice, tubes a centimeter or more in diameter with radial feeder structures can occur [*Lake and Lewis*, 1970; *Cole and Shapiro*, 1998]. All these features may form parts of a complicated interconnected network of pores. This network may render the ice permeable, either in the bulk pore space, through individual drainage tubes, or in isolated areas of cracked or high-porosity ice. *Freitag* [1999] has shown that it is the larger diameter pores, which make up a small fraction of the total pore space, which are responsible for the bulk of the permeability. Because of the vertical alignment of pores and drainage tubes, one can expect that the ice permeability will be highly anisotropic. This is generally true in congelation ice [*Freitag*, 1999], with a vertical permeability typically 10 times or more than the horizontal permeability. In granular ice, this anisotropy is reduced.

Since the pore volume is controlled by the ice temperature and salinity [*Cox and Weeks*, 1983], fluid flow is both affected by, and affects, the evolution of the pore space. Therefore a consideration of the temporal and spatial inhomogeneities of the brine space network and corresponding permeability is necessary for a proper treatment of the effects of brine percolation on ice properties, and vice versa.

1.6 Snow ice observations in the Southern Ocean

Snow ice is a ubiquitous feature of marginal seas, where the ice is typically thin and there is substantial snow fall. Snow ice has been studied in the Baltic sea [*Leppäranta*, 1983; *Saloranta*, 2000], the Sea of Okhotsk [*Takizawa*, 1985; *Hudier et al.*, 1995; *Ukita et al.*, 2000], and the Labrador Sea [*Weeks and Lee*, 1958]. In the Antarctic, where snow accumulation rates over the pack ice are relatively high [*Giovinetto et al.*, 1992], snow ice formation is a major contributor to the ice mass balance. Snow ice has been observed in all regions of the Southern Ocean [*Kawamura et al.*, 1997; *Eicken et al.*, 1994; *Allison and Worby*, 1994; *Jeffries and Adolphs*, 1997; *Jeffries et al.*, 1997, 1998b, 2001; *Rapley and*

Lytle, 1998].

Data were collected in the RAB seas on four cruises aboard the R/V *Nathaniel B. Palmer* between 1993 and 1995, spanning the months of May to October (Figure 1.5). Snow ice was ubiquitous in all regions and at all times, though evidence of flooding was fairly rare except for September-October 1994. Analysis of ice cores indicate that 12-38% of the total thickness may be snow ice (Figure 1.6), although there is large inter-annual variability [*Jeffries et al.*, 2001]. Snow ice percentages in Figure 1.6 are identified as granular ice layers with $\delta^{18}O < 0‰$, [e.g., *Jeffries et al.*, 2001; *Lange et al.*, 1990; *Allison and Worby*, 1994]. In addition, observations from East Antarctica [*Worby et al.*, 1998] and from the Weddell Sea [*Eicken et al.*, 1994] are shown. For the Weddell Sea, the percentage of snow ice is estimated from $\delta^{18}O$ data presented by *Eicken* [1998], and includes some second year ice. Also shown in Figure 1.6 are annual means of snow ice from the results of a dynamic-thermodynamic ice model [*Fichefet and Morales Maqueda*, 1999]. Note that this model produced substantially less snow ice than is observed, although this value was highly dependent on precipitation estimates.

The smaller amounts of snow ice observed in East Antarctica and the Weddell sea can in part be attributed to low snow accumulation, as evidenced by generally positive ice freeboards [*Massom et al.*, 1998; *Eicken et al.*, 1994]. In the RAB seas, mean freeboard values were very close to zero [*Jeffries and Adolphs*, 1997; *Jeffries et al.*, 1998b], indicative of a high potential for flooding. Snow ice production is more prevalent in this region than elsewhere in the Southern Ocean, and in contrast to the Weddell Sea and East Antarctica, can form readily at any time in the growth season [*Jeffries et al.*, 2001]. This work will focus primarily on flooding and snow ice formation in late fall - early spring in the RAB seas.

The source of the regional variation in snow ice formation shown in Figure 1.6 can be seen readily by examining precipitation patterns in the RAB Seas. Figure 1.7 shows the average April-November precipitation for 1993-1995 from the National Center for Environmental Prediction (NCEP) reanalysis data. This compares reasonably well with estimates from extrapolation of the continental precipitation [*Giovinetto et al.*, 1992] and European Centre for Medium-range Weather Forecasts (ECMWF) reanalysis moisture budget [*Bromwich et al.*, 1998]. Snowfall rates are low in the inner Ross Sea, where little

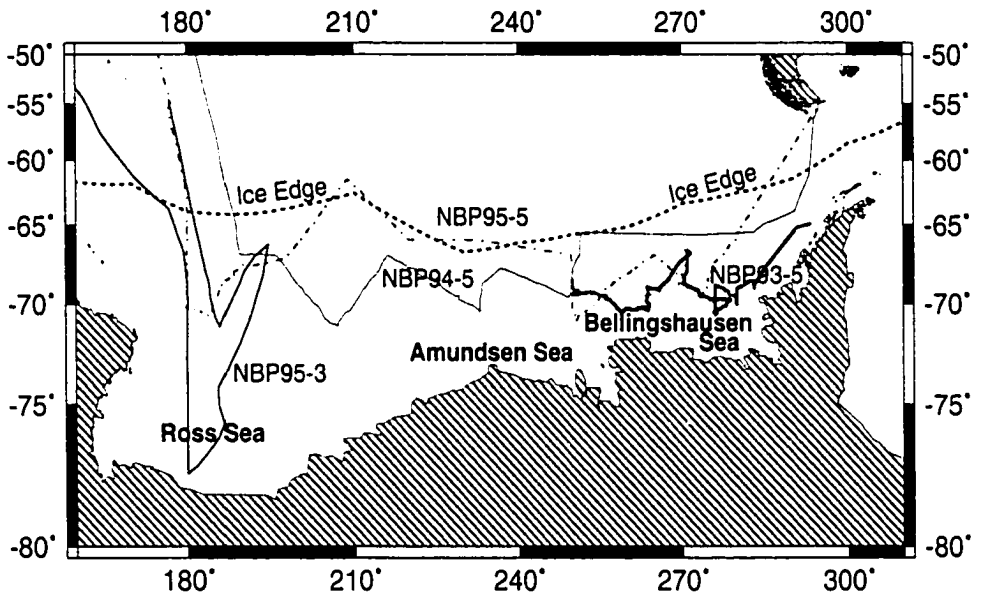

Figure 1.5: Cruise tracks in the Ross, Amundsen and Bellingshausen (RAB) seas. Measurements were gathered on four cruises of the *Nathaniel B. Palmer* between 1993 and 1995. The approximate ice edge is shown for September 1995.

snow ice is found, and increase steadily towards the ice edge. Precipitation is highest along the coast in the Amundsen Sea and near the Antarctic Peninsula, which are regions of perennial ice. Note that there is anomalous precipitation in some areas due to spectral wave distortion of the NCEP model, most noticeably near Terra Nova Bay in the Ross Sea.

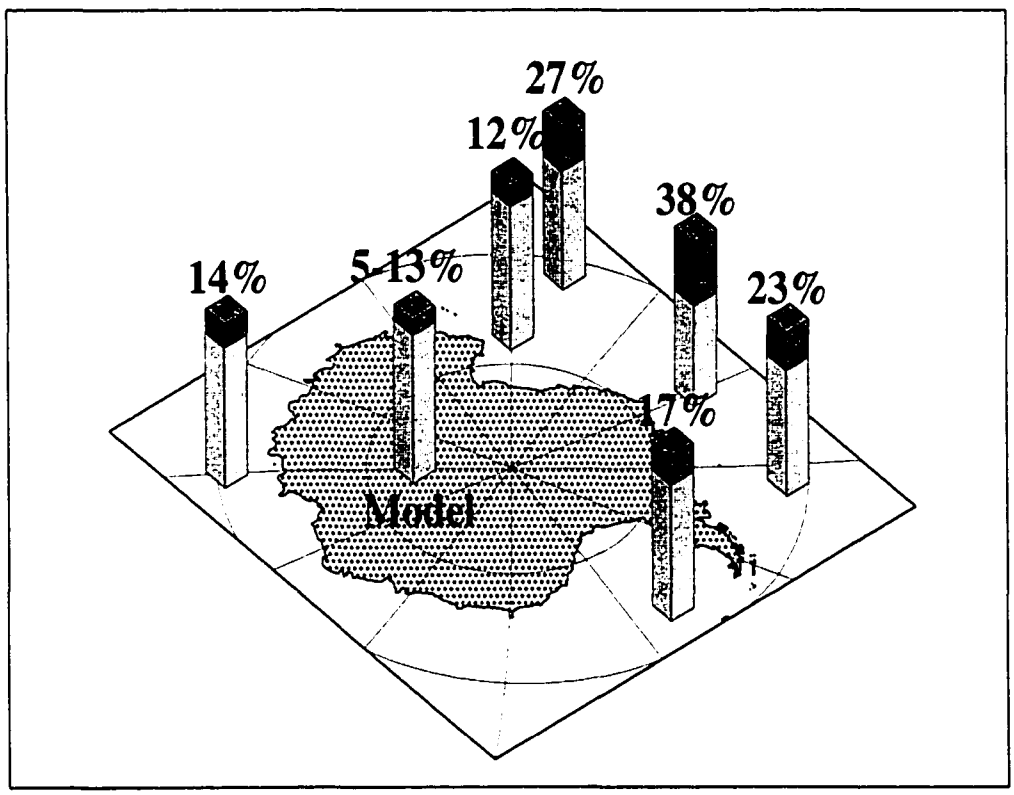

Figure 1.6: Winter snow ice distribution in the Southern Ocean. Snow ice contribution to sea ice thickness for various regions is given as a percentage of total ice thickness. An annual mean snow ice contribution for the Southern Ocean from a dynamic-thermodynamic model [*Fichefet and Morales Maqueda*, 1999] is shown over the continent.

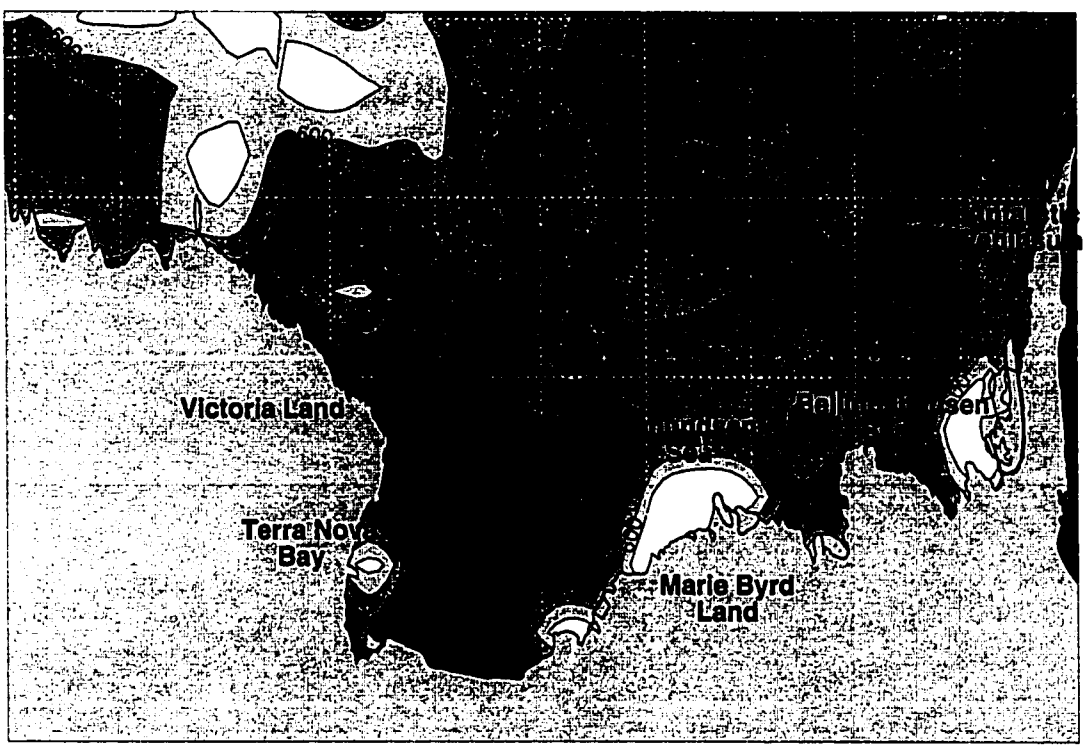

Figure 1.7: Snowfall in the RAB seas. Smoothed precipitation field from NCEP reanalysis for April-November 1993-1995. Units are kg m^{-2}.

Chapter 2

Oxygen isotopes and snow ice identification: How much snow ice is there anyway?

2.1 Isotopic signatures of sea ice in the Ross, Amundsen and Bellingshausen seas

Naturally, in assessing the role of snow ice in the development and mass balance of sea ice, a good estimate of the amount of snow ice present is necessary. Snow ice has a granular structure that has been traditionally characterized as polygonal crystals [*Weeks and Lee*, 1958; *Eicken et al.*, 1994; *Tison et al.*, 1998]. However, in practice, the structure may closely resemble the fine grained orbicular structure of frazil ice [e.g *Jeffries et al.*, 1994] and is difficult to clearly distinguish from frazil ice. Therefore, it is common practice to use stable oxygen isotopes to identify snow ice [*Jeffries and Adolphs*, 1997; *Jeffries et al.*, 1997, 1998b; *Lange et al.*, 1990; *Eicken et al.*, 1994; *Worby and Massom*, 1995; *Ukita et al.*, 2000].

The ratio of the stable isotopes of oxygen, ^{18}O and ^{16}O, in a water (or ice) sample is most conveniently described by the $\delta^{18}O$ value. This is given as the isotopic ratio relative to that of Vienna Standard Mean Ocean Water (VSMOW):

$$\delta^{18}O = \left[\frac{(^{18}O/^{16}O)_{\text{sample}}}{(^{18}O/^{16}O)_{\text{VSMOW}}} - 1\right] \times 1000‰. \quad (2.1)$$

As air masses move poleward, the heavy isotope $H_2{}^{18}O$ preferentially rains out so that precipitation is progressively depleted in the heavy isotope closer to the pole, resulting in highly negative $\delta^{18}O$ values in antarctic precipitation. In the RAB Seas, average snow $\delta^{18}O$ values range between -13.2‰ and -21.5‰ [*Jeffries et al.*, 1998a]. In contrast, $\delta^{18}O$ values of the sea water average -1‰. This sea water value is very low compared to other measurements for the Ross Sea in summer [*Jacobs et al.*, 1985] or the Weddell Sea [*Lange et al.*, 1990; *Eicken*, 1998], which tend to be much closer to 0‰. *Jeffries et al.* [1994] suggested that this reflects the incorporation of precipitation into the surface waters. Frazil and congelation ice form from sea water, so the $\delta^{18}O$ of these structural facies should have $\delta^{18}O$ values no less than -1‰. Because of the different vibrational energies of the two stable oxygen isotopes, $H_2{}^{18}O$ freezes more readily than $H_2{}^{16}O$. Except for very high growth rates, there is some fractionation during freezing, depleting ^{18}O in the liquid phase, and raising the $\delta^{18}O$ value of the ice. For a maximum fractionation coefficient, ϵ_{eff}, of about 2.7‰ [*Eicken*, 1998], resultant $\delta^{18}O$ values can be as high as +1.7‰ (from $\epsilon_{eff} = \delta_{si} - \delta_w$, the difference between the $\delta^{18}O$ values of sea ice and the sea water from which it formed). As snow ice is a mixture of snow and sea-water, $\delta^{18}O$ of snow ice should be negative. This fact is used as the basis for identification of snow ice layers, with any granular layer with $\delta^{18}O < 0$ identified as snow ice [e.g. *Jeffries et al.*, 1997; *Worby and Massom*, 1995].

The distribution of all $\delta^{18}O$ and salinity measurements with depth for the four cruises in the RAB seas (Figure 1.5) is similar to that given by *Eicken* [1998] for the Weddell sea (Figure 2.1). The frazil and congelation layers form a tightly grouped backbone of $\delta^{18}O$ values running from $\delta^{18}O \sim 0$ at the surface to $\delta^{18}O \sim 1$ at a depth of 1m. This increase represents an increase in fractionation as the ice growth rate slows. Near the surface, where ice growth rates are high, ϵ_{eff} is reduced, and the isotopic composition is closer to that of the parent sea water. Note that the mode is about 1‰ lower than that given by *Eicken* [1998], or approximately the difference between the sea water $\delta^{18}O$ of

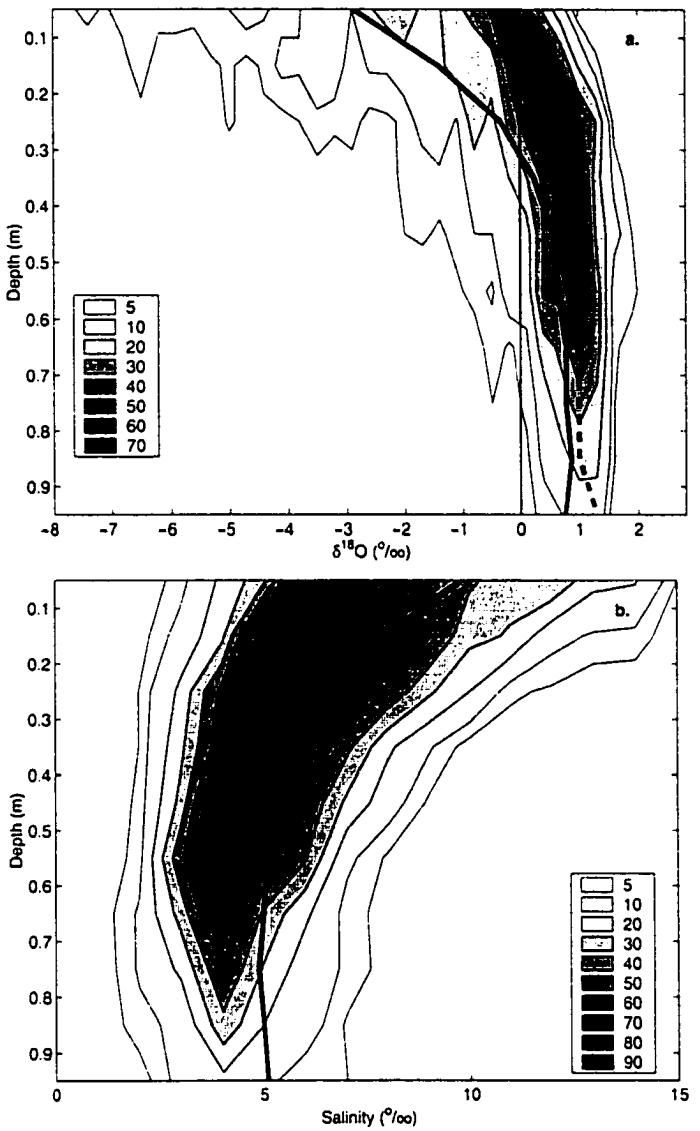

Figure 2.1: $\delta^{18}O$ and salinity profiles. (a) Distribution of $\delta^{18}O$ measurements as a function of ice core depth for all cruises in the Ross, Amundsen and Bellingshausen Seas. The distribution is given by the number of measurements that fall within a specified interval. Intervals are 0.3‰ along the x-direction and 0.1 m in the y-direction. The thick solid line is the mean $\delta^{18}O$ profile. The dotted line gives the mode of the distribution with depth. (b) Distribution of ice salinity as a function of depth for all cores. The x-interval is 1‰. The mean salinity profile is given by the solid line.

the Weddell and RAB Seas. We expect that the $\delta^{18}O$ values of ice formed through the freezing of sea water will be normally distributed about the mean. Hence, the difference between the mode and the mean of the $\delta^{18}O$ distributions primarily represents the effect of meteoric ice and snow ice. As we can expect, snow ice is found primarily in the upper regions of the ice cores. The salinity profile is C- or S- shaped, similar to those described by *Eicken* [1992]. The high salinity values at the top of the cores are primarily due to snow ice formation.

The difficulty in identification of ice type from crystal texture is illustrated in Figure 2.2. Snow ice samples (i.e., $\delta^{18}O < 0‰$) are divided into those that were suspected of being snow ice based on crystal texture, and those that were thought to be frazil. Although those layers originally identified as snow ice tended to actually be snow ice according to oxygen isotope analysis, many of those identified as frazil turned out, in fact, to be snow ice as well. Both types exhibited a wide range of $\delta^{18}O$ values, but there was a substantial amount of granular ice with only slightly negative values. It is these layers which present a puzzle. If snow ice is produced through the freezing of a slush layer composed of 50% sea water and 50% snow the mean $\delta^{18}O$ value should be about -9‰, with a maximum of about -5‰. Such a criterion would reject most of the snow ice identified with a criterion of $\delta^{18}O < 0‰$. Using a criterion of $\delta^{18}O < -1‰$, equivalent to no fractionation during frazil ice growth, would reduce the observed amount of snow ice by about 40% (Figure 2.3). This small change alone is very significant, as it would not only diminish the importance of flooding and snow ice formation in the winter thickening of the ice pack, and in turn enhance the role of frazil formation, but would imply a substantial reduction in snow accumulation estimates [*Jeffries et al.*, 2001]. There are also a small number of congelation ice layers that had negative $\delta^{18}O$ values. These layers, because of their columnar crystal structure, cannot be the result of snow ice formation. This suggests that some frazil ice layers might also have a negative $\delta^{18}O$ and a cutoff for snow ice identification of 0‰ may not be accurate.

Several authors have calculated the fraction of meteoric ice present in ice cores [*Lange et al.*, 1990; *Eicken et al.*, 1994; *Jeffries et al.*, 2001]. Meteoric ice, as opposed to snow ice, refers only to the snow component entrained in the ice cover. Assuming snow ice is

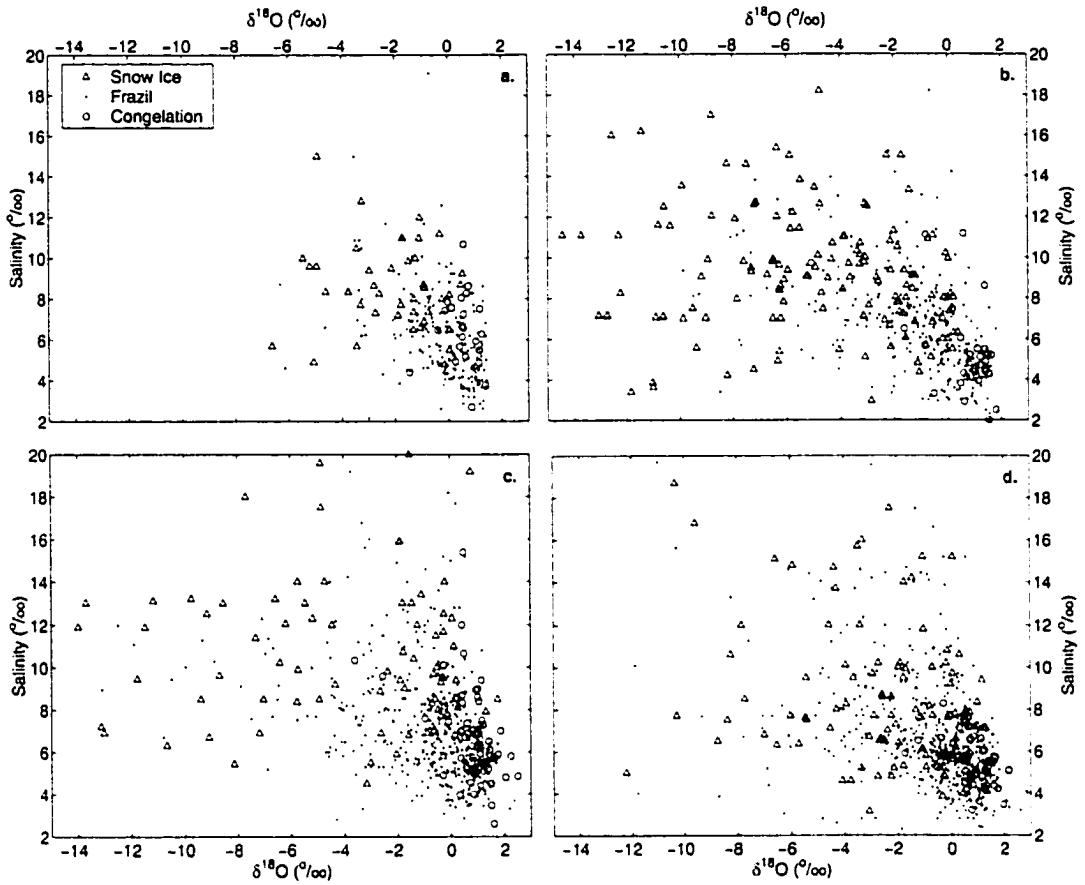

Figure 2.2: Salinity vs. $\delta^{18}O$. Scatter plots of ice salinity versus $\delta^{18}O$ for cores obtained during autumn and winter cruises of the *R. V. Nathaniel B. Palmer* in the Ross, Amundsen and Bellingshausen Seas. (a) Aug-Sept 1993, (b) Sept-Oct 1994, (c) May-June 1995, and (d) Aug-Sept 1995. The different symbols indicate the ice type as determined from ice texture alone : Δ snow ice, o congelation ice, · frazil. In standard practice, snow ice is defined as granular ice with a negative $\delta^{18}O$ value. For clarity, only half of the congelation and frazil data points with $\delta^{18}O > 0$ are shown. For (c) and (d) there were several samples with $\delta^{18}O$ or salinity values outside of the range shown.

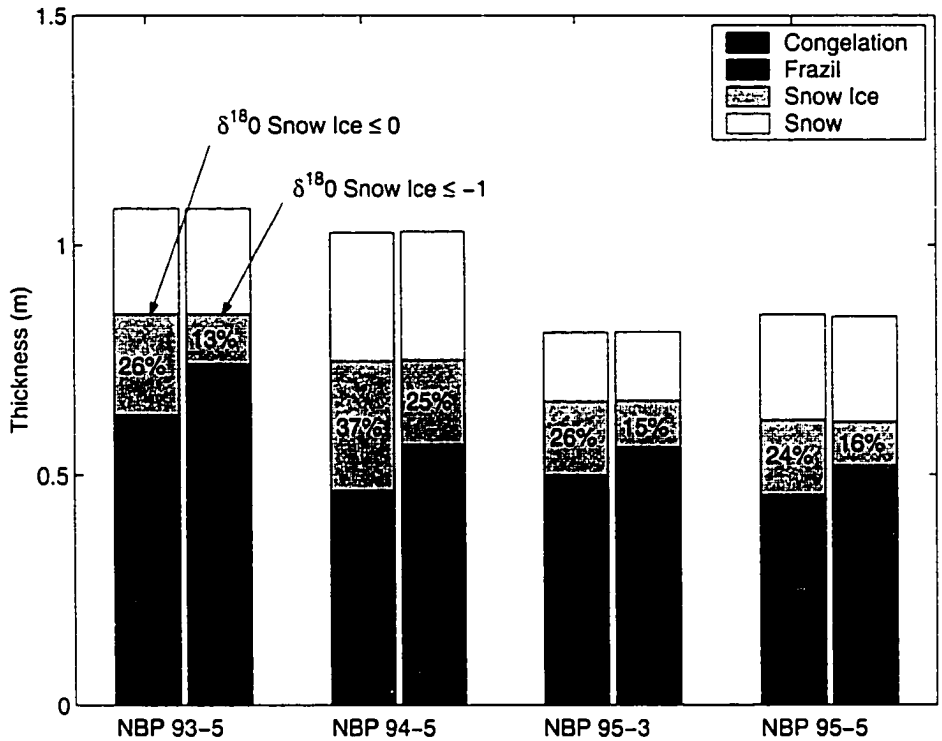

Figure 2.3: Ice core structure from the RAB seas. Each ice texture is given as the mean thickness of that ice type per core. Also given is the mean snow depth. Amounts of snow ice are given using a snow ice criterion of $\delta^{18}O = 0‰$ and $\delta^{18}O = -1‰$.

composed only of snow and sea water, we may calculate the meteoric ice fraction, f_{sn}, by

$$f_{sn} = \frac{\delta_{si} - \delta_w}{\delta_{sn} - \delta_w}, \tag{2.2}$$

where δ_{si}, δ_{sn}, and δ_w are the $\delta^{18}O$ values for the snow ice, snow, and sea water, respectively. Here, δ_w is an effective value for sea water, since some fractionation will take place during freezing and brine drainage from the slush layer. Taking $\delta_w = 0‰$, a mean value for the RAB seas data gives snow fractions of 17% for those ice layers with $\delta^{18}O < 0‰$. *Eicken et al.* [1994] report a meteoric fraction of 22% for the upper ice layers of Weddell sea ice. If we assume that ice layers with $\delta^{18}O < -1‰$ are snow ice, (2.2) gives $f_{sn} = 24\%$. Since initial meteoric ice fractions in slush should be 30-50%, based on observed snow densities, either there is some post-genetic isotopic exchange occurring between the flooded

layer and the ice and ocean below, or some snow is entrained into sea ice by other means. In either case we are left with the difficulty of estimating the contribution of flooding and snow ice formation to the mass balance of sea ice.

Examining the probability distribution functions (PDFs) of $\delta^{18}O$ values (Figure 2.4a) is of little help in discriminating ice types. Congelation ice has a fairly narrow distribution with a peak at 1.2‰, and very few measurements with negative values. Granular ice has a similar distribution at the upper end, with a slightly lower peak of 0.8‰. This difference is probably due to the higher growth rates experienced by individual frazil crystals in supercooled sea water [*Eicken*, 1998]. The other side of the distribution shows a gradual tail towards very negative $\delta^{18}O$ values. This is due to the contribution of snow ice, but unfortunately, there is no clear dividing line between the snow ice and frazil portions of the distribution. Hence, it is difficult to distinguish snow ice from frazil ice that has a meteoric ice component entrained by means other than flooding, and frazil ice that has a low $\delta^{18}O$ value due to rapid freezing of sea water.

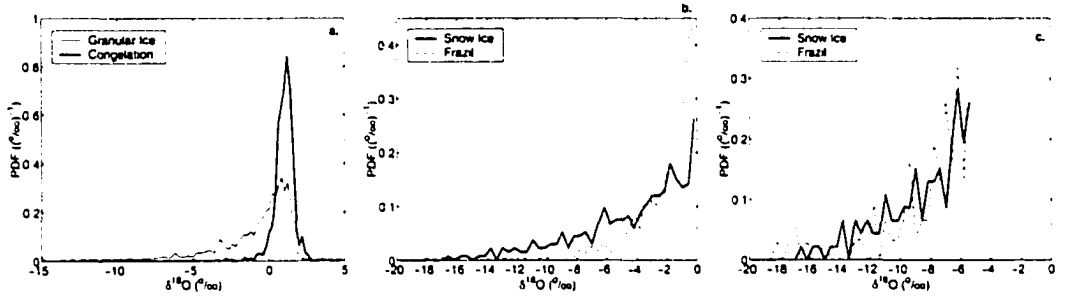

Figure 2.4: $\delta^{18}O$ probability density functions (PDF). $\delta^{18}O$ distributions for all ice samples taken on the four autumn and winter cruises in the RAB seas: (a), distribution of all congelation and granular ice samples, (b) normalized distribution of $\delta^{18}O$ values for granular ice samples divided according to a preliminary identification based on ice texture alone, (c) as in (b), but with a maximum $\delta^{18}O$ cutoff of -5‰.

Dividing granular ice samples according to the preliminary identification from crystal structure alone reveals two very different distributions (Figure 2.4b). While both groups have more measurements closer to 0‰, the samples identified as snow ice have a much flatter distribution. The majority of samples identified as frazil have $\delta^{18}O > -2‰$. If we assume that one is as likely to identify a snow ice sample correctly as not, we should expect that these two distributions would be similar. That this is not the case suggests

that many of these samples may, in fact, not have formed via the flooding process. The PDFs for these two sets of samples closely match only when the cutoff is moved to -5‰. Using (2.2) with this as a cutoff for snow ice gives $f_{sn} = 50\%$, consistent with *Lytle and Ackley* [1996], and measurements of slush in the RAB seas. Such a low cutoff would reduce the estimate of snow ice contribution to total ice thickness to a mere 4%.

2.2 Estimating a cutoff $\delta^{18}O$ criterion for sea ice with a meteoric fraction

2.2.1 Fractionation during freezing of sea water

How then, are we to estimate the contribution of flooding and re-freezing to the mass balance of sea ice? To do this we must assess the various processes that affect the oxygen isotope profile. The first step is to determine a reasonable criterion for discriminating ice with a meteoric component from ice grown entirely from sea water. To do this we must estimate the minimum $\delta^{18}O$ that can be expected in new sea ice.

The distributions of $\delta^{18}O$ in Figure 2.1 can be divided according to crystal structure to examine the effects of growth regime on the isotopic signature of the ice (Figure 2.5). Only those samples with $\delta^{18}O > -1‰$ are included, as this is the minimum value for ice grown from sea water with $\delta^{18}O = -1‰$, which is the mean value for the RAB seas in winter. For both congelation and granular ice, the mean and mode of the distribution match quite closely for all depths, consistent with a normally distributed variance that might be expected for growth under random variations in growth conditions. The isotopic composition of frazil ice is approximately 0.5‰ below that of congelation ice. This is consistent with the results of *Eicken* [1998], implying a generally lower ϵ_{eff} for frazil ice. This may be due in part to the low degree of fractionation in frazil crystals formed rapidly in slightly super-cooled water.

The isotopic composition of growing sea ice can be estimated following *Eicken* [1998]. From Burton-Prim-Slichter (BPS) theory [*Burton et al.*, 1953] for the incorporation of impurities into a solid at a freezing interface, the fractionation coefficient of pure ice can

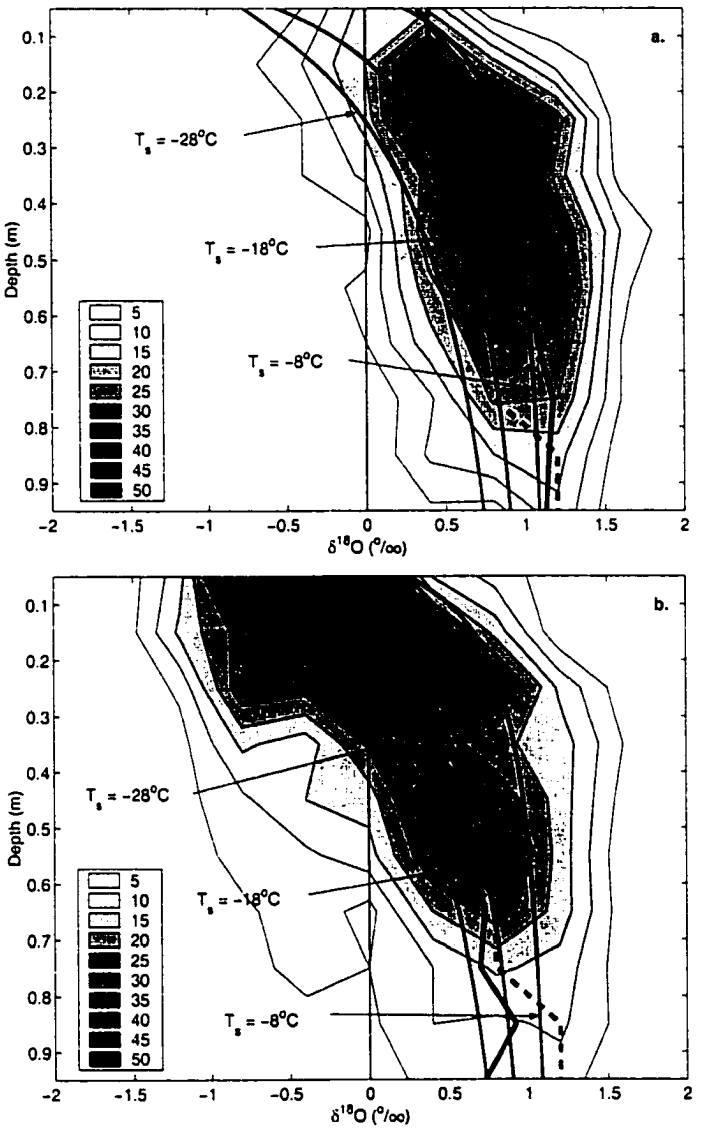

Figure 2.5: Isotopic composition variation with depth. Distribution of $\delta^{18}O$ measurements with depth for ice layers with a $\delta^{18}O$ > -1‰. (a) Congelation ice layers, (b) granular ice layers. As before, the thick solid line is the mean $\delta^{18}O$ profile. The dotted line gives the mode of the distribution with depth. Also shown is the modelled $\delta^{18}O$ profile for a range of surface temperatures (thin solid lines) T_s is the surface temperature. Contours have the same meaning as in Figure 2.1 (x-interval is 0.4‰)

be determined from

$$\epsilon_{eff,i} = \left[\frac{\alpha_{eq}}{\alpha_{eq} + (1 - \alpha_{eq})\exp(\frac{-z_{bl}v_i}{D})} - 1\right]. \quad (2.3)$$

where $\alpha_{eq} = R_i/R_b$, the fractionation factor, is given by the isotopic ratios in the solid and liquid phase, z_{bl} is the boundary layer thickness of BPS theory, v_i is the ice growth velocity, and D is the diffusivity of $H_2^{18}O$. *Eicken* [1998] modified this theory for sea ice by including a factor to account for the incorporation of brine into sea ice as it grows by

$$\epsilon_{eff,si} = (1 - k_{eff})\epsilon_{eff,i}, \quad (2.4)$$

where k_{eff} is the salt segregation coefficient as given by *Cox and Weeks* [1988]. The ice growth velocity can be estimated by

$$v_i = \frac{k_{si}}{\rho_{si}L_{si}}\frac{(T_f - T_a)}{(Z_i + a)} - \frac{F_w}{\rho_{si}L_{si}}, \quad (2.5)$$

where k_{si}= 1.9 W $m^{-1}K^{-1}$ is the thermal conductivity, ρ_{si} = 920 kg m^{-3} is the density, $L_{si} = 2.88\times10^5$ J kg^{-1} is the latent heat of fusion for an ice salinity of 5‰, T_f and T_a are the ocean and air temperatures, Z_i is the ice thickness, and F_w = 5 W m^{-2} is the ocean heat flux. a is a correction for the difference between air and ice surface temperature [*Leppäranta*, 1993]. A value of 5 cm for a produces good agreement with the results of *Worby and Allison* [1991].

Using (2.3)-(2.5), theoretical $\delta^{18}O$ curves for new sea ice are shown in Figure 2.5 for various surface temperatures, -18°C being the average winter temperature for the Ross Sea in 1995. This range of temperatures represents the approximate range of growth conditions that might be experienced by a growing ice sheet in the RAB seas in winter. The upper end of this range is likely more appropriate for greater depths (thicker ice) when a snow cover will raise the ice surface temperature. Although the data exhibit a broader range of $\delta^{18}O$ values than the model predicts, this can in part be attributed to the wide variability in $\delta^{18}O$ for the source water, which ranged from -1.7 to 0.8‰ [*Jeffries et al.*, 2001]. The model reproduces the general shape of the profiles well, from near equilibrium values for ϵ_{eff} at greater depth (slower growth), and steepening sharply near the surface.

The important result of the fractionation model is that it predicts $\delta^{18}O < 0$ in the near surface ice layers for rapid growth conditions, with a lower bound of -0.8‰. This could explain up to 72% of the congelation layers with $\delta^{18}O < 0$‰. A cutoff criterion of 0‰ may then be inappropriate for the identification of snow ice layers. Using a cutoff of -0.8‰ would exclude 29% of the identified snow ice layers. Such a criterion should be used with caution, however, due to the range of growth conditions and sea water isotopic composition that can occur in the Southern Ocean. Nevertheless, it partially explains many anomalous measurements for congelation ice and accounts for a substantial fraction of granular ice that has slightly negative $\delta^{18}O$ values. This process, however, cannot account for any sample that had a $\delta^{18}O$ value less than that of the parent sea water. This leaves a substantial fraction of samples that may be snow ice, yet exhibit snow fractions substantially lower than what is expected due to the freezing of a slush layer.

2.2.2 Isotopic signatures due to sampling errors

Another possible cause of slightly negative $\delta^{18}O$ values is mixing of isotopic signatures of distinct layers during sampling. Ice core samples were divided into sections up to 5 cm in length for oxygen isotope analysis (see e.g., *Jeffries et al.* [1994]). Usually, distinct boundaries could be seen between individual granular layers to guide the sampling for isotope analysis. However, the possibility remains that some granular ice samples may have consisted of both frazil and snow ice layers. The isotopic signature of such a sample would then be a weighted average of that of the two separate layers based on the relative fraction of each ice type in the sample. If a sample then contains a small fraction of snow ice, its $\delta^{18}O$ value could well be slightly below 0‰, despite a positive $\delta^{18}O$ value for the frazil component.

To assess this affect, the fraction of granular layers with slightly negative $\delta^{18}O$ values lying immediately above frazil layers is determined. These are examined because they are layers that form the boundary between snow ice and frazil ice. If we let frazil ice be granular ice with $\delta^{18}O > 0$‰, then 53% of those layers with $-1‰ < \delta^{18}O < 0‰$ lie immediately above a frazil layer. Using a cut-off of $\delta^{18}O > -1‰$ for frazil ice (see Section 2.2.1), 69% of those layers with $-2‰ < \delta^{18}O < -1‰$ lie immediately above a frazil layer. This indicates that a substantial fraction, though not all, of the granular ice layers with

$\delta^{18}O > -2‰$ may be a mixture of frazil and snow ice. Only a maximum of 19% of those layers with $\delta^{18}O < -2‰$ are such boundary layers.

Since ice cores were sampled according to crystal structure boundaries, a mixture of isotopic signatures is unlikely to occur in all these samples. In congelation ice samples, which cannot contain a snow ice component, 34% of those layers immediately below granular ice have $\delta^{18}O < 0‰$. All but one of the overlying granular layers also had a negative $\delta^{18}O$ value. Of the few congelation samples that had $\delta^{18}O < -1‰$, 83% lay beneath a granular layer with a meteoric ice component. This indicates that some process other than sampling error is most likely responsible for moderately negative $\delta^{18}O$ values in sea ice. For ice with $\delta^{18}O > -1‰$, rapid freezing during growth may explain many of the measurements. For those layers with $\delta^{18}O < -1‰$, most must either be snow ice, or have a snow fraction entrained by other physical processes during evolution of the ice cover.

In the next section, a model of a slush layer is presented which attempts to explain the evolution of the isotopic composition and drainage of salt during freeze-up.

2.3 Key results of isotopic analysis

- Crystal structure is a poor tool for identification of snow ice so the use of stable isotopes is necessary.
- Due to a low sea water $\delta^{18}O$ value for the RAB seas in winter, rapid growth conditions can produce ice with $\delta^{18}O < 0‰$. This can explain at most 40% of sampled ice layers with $\delta^{18}O < 0‰$, and estimates of snow ice contribution to ice thickness should be reevaluated.
- Mixing of layers of different composition during sampling is unlikely to account for a large fraction of the moderately negative isotopic values observed.
- Those samples with $\delta^{18}O < -1‰$ must contain a meteoric ice component. While many can clearly be identified as snow ice, the provenance of samples with $\delta^{18}O$ values between approximately -5 and -1‰, or 74% of the possible snow ice layers, is unclear.

Chapter 3

Phase and compositional evolution of the flooded layer

3.1 Isotopic exchange and brine drainage

During the freezing of a slush layer, significant morphological and compositional changes can occur. First, the porosity is typically dramatically reduced, from 50% or more to below 10%. Concurrently, there is often a substantial reduction in the salinity [*Lytle and Ackley*, 1996; *Takizawa*, 1985; *Weeks and Lee*, 1958], although this may remain quite high, as demonstrated by the wide range shown in Figure 2.2. The convective turnover of brine during freeze-up affects the nutrient fluxes within the ice [*Fritsen et al.*, 1994] and salt fluxes to the upper ocean [*Lytle and Ackley*, 1996]. Furthermore, due to crystal growth processes within the slush, there is isotopic exchange among the slush, ice and ocean during brine transport. The nature of this exchange is dependent on the permeability structure of both the slush and the underlying ice.

As discussed above, snow fractions based on oxygen isotope analysis are substantially lower than one would expect from a simple mixture of snow and sea water. If estimates of the quantities of snow ice are accurate, then there must be compositional changes in the flooded layer to produce many of the slightly negative $\delta^{18}O$ values observed. This implies that a large proportion of the water/ice mixture which is depleted in the heavy isotope has drained from the slush or snow ice into the underlying ice layers or to the

ocean and has been replaced by fresh brine from below during freezing. This has been inferred (although not with respect to isotopic composition) by *Fritsen et al.* [1994] and *Lytle and Ackley* [1996] during autumn freeze-up in the Weddell Sea, based on nutrient, salt, and heat transport. It is this process which casts some doubt on the determinacy of snow ice identification: if the isotopic composition is "diffused" along the ice thickness by convection during freeze-up, then snow ice layers will tend to lose their signature, while underlying ice layers may become depleted in the heavy isotope, leading to a possible ambiguity.

The notion that there is an effective diffusion of the isotopic composition has been explored by *Lange and Hubberten* [1992], motivated by the observation of a gradual increase in $\delta^{18}O$ with depth in sea ice cores (see Figure 2.1a). To achieve any sizeable effect, they require an exceptionally large diffusion coefficient. In the presence of fluid flow, such an effect may be plausible, and evidence for it may lie in the small fraction of congelation ice layers that displayed negative $\delta^{18}O$ values. Although many of these measurements may be explained by rapid growth (see Chapter 2), most of these layers lay immediately below a snow ice layer (Figure 3.1) While many congelation layers were immediately underneath a snow ice layer in an ice core, very few that had $\delta^{18}O < 0$ were underneath a frazil or congelation layer, except for those core samples from the 93-5 cruise (Figure 3.1a). This provides at least circumstantial evidence that $H_2{}^{18}O$ depleted brine may be transported downward through the ice. That most of the congelation ice retained a positive $\delta^{18}O$ value despite being below snow ice implies this phenomenon may occur infrequently.

3.2 Objectives

In this chapter, I develop a simple model of brine convection during freeze-up of a slush layer to examine the phase, solutal, and isotopic evolution of the flooded layer and the underlying sea ice during the freezing process. I investigate three key aspects of this problem: (1) What is the nature of the freezing interface in a flooded layer, i.e., is the thermohaline convection in the slush and ice strong enough to produce a well defined freezing interface, or is it more diffuse, with phase change occurring across a broader thickness? (2) How much salt is rejected from the flooded layer during freezing, how

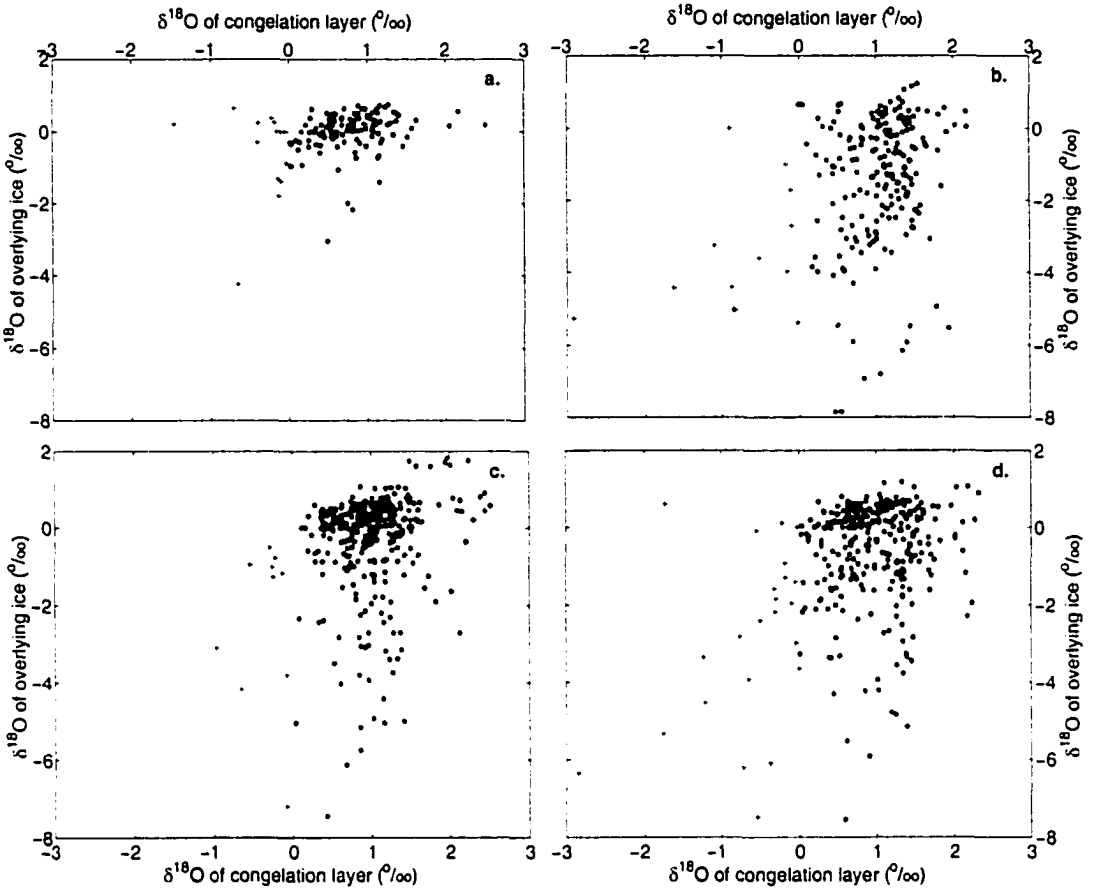

Figure 3.1: Transport of $H_2{}^{18}O$ depleted brine into congelation ice. $\delta^{18}O$ values for congelation ice layers are compared with those of the layer immediately above. (a) Aug-Sept 1993, (b) Sept-Oct 1994, (c) May-June 1995, and (d) Aug-Sept 1995. Symbols: + $\delta^{18}O < 0$, * $\delta^{18}O > 0$

much of this ends up in the lower portions of the ice, and what is the role of the ice permeability in this process? (3) Can isotopic changes in the ice during freeze-up cause substantial redistribution of the oxygen isotope composition? The first and second of these questions are important in understanding the evolution of the ice porosity and permeability structure during freezing. These parameters, as we shall see in chapter 4 and 5, are vitally linked to the flooding process through control of the percolation threshold. In this respect, redistribution of salt within the ice can affect the mass balance. The third question addresses the identification of snow ice, and as such this model aims to provide

guidelines for the identification of snow ice from oxygen isotope analysis.

3.3 Model formulation

The flooded layer and underlying ice are modelled as porous media with both convective and diffusive heat and mass transfer and phase change. Generally, the flooded layer is higher in porosity than the ice, so this problem is quite similar to the mushy layer problem often encountered in alloy solidification [e.g. *Worster*, 1997]. This has been extensively studied theoretically, experimentally and numerically [e.g. *Worster*, 1997; *Tait and Jaupart*, 1992; *Bennon and Incropera.*, 1967], and has recently been investigated with respect to the ice-ocean interfacial layer in growing sea ice [*Worster and Wettlaufer*, 1997; *Wettlaufer et al.*, 1997]. In some respects, our problem is simpler, in that rather than a mushy layer freezing into a liquid, we have one mushy layer (slush) freezing into another, less porous mushy layer (sea ice), and we can treat both regions with the same set of equations without resorting to complicated volume averaged equations [*Ni and Incropera*, 1995]. Ideally, however, a more robust method should be used, especially when porosities become very high or when drainage tubes are present and inertial effects become important in governing the flow [*Schulze and Worster*, 1997]. For computational convenience, we use a simpler formulation, and neglect inertial effects.

The basic equations for conservation of mass, momentum, heat and species transport in a porous medium are given by:
conservation of mass,

$$\frac{(\rho_b - \rho_i)}{\rho_b}\frac{\partial \phi}{\partial t} + \nabla \cdot \mathbf{u} = 0. \tag{3.1}$$

momentum,

$$\mathbf{u} = -\frac{K}{\mu}(\nabla P + \rho_b \mathbf{g}), \tag{3.2}$$

heat,

$$\rho_{si}C_{si}\frac{\partial T}{\partial t} + \rho_b C_b \nabla \cdot (\mathbf{u}T) = \nabla \cdot k_{si}\nabla T - \rho_b L\frac{\partial \phi}{\partial t}, \tag{3.3}$$

solute,

$$\frac{\partial(\rho_b \phi S_b)}{\partial t} + \nabla \cdot (\mathbf{u}\rho_b S_b) = 0, \tag{3.4}$$

isotopic composition,

$$\frac{\partial(\rho_b \phi \delta_b)}{\partial t} + \nabla \cdot (\mathbf{u}\rho_b \delta_b) = 0, \tag{3.5}$$

The reader is referred to appendix A for notation. Assuming local thermodynamic equilibrium, we have $S_b = F(T)$, which couples (3.1)-(3.4) by the phase relation. Note that we can neglect diffusion in (3.4) because the brine salinity is fixed by the temperature, and the thermal diffusivity is much larger than the solutal diffusivity. Diffusion in (3.5) is small and has also been neglected. Dispersive effects are not included in (3.1)-(3.5), although due to the large variability of pore volume on this scale, they may be significant. The method of solution of (3.1)-(3.4) is given in appendix B.

Equations (3.1)-(3.4) are applied to both the slush and the ice. To avoid steep temperature gradients at the base of the ice due to fixing the temperature of the lower boundary, a thin layer of 100% porosity is included to roughly simulate the oceanic boundary. This is merely a computational convenience and does not significantly affect the results. Ice property values, except where noted below, are taken from *Cox and Weeks* [1988]. The density of brine is assumed constant at 1050 kg m^{-3}, except in the buoyancy term. Thermal conductivity of the snow is assumed to be 0.3 W m^{-1} K^{-1}. There is a caveat regarding the application of (3.1)-(3.5) to thermohaline convection in sea ice. To be valid, we must assume that all the pore space is reasonably well connected so that pressure gradients due

to density variations vary smoothly. This is probably not the case in general, but here we are concerned with ice that has been warmed by the flooding process, and so brine volumes will be quite high, and therefore the fluid phase should be fairly continuous.

The thermal conductivity in the slush is taken as a weighted average of the upper and lower Maxwell bounds [*Kaviany*, 1995]

$$k = \frac{(2k_i + k_b - 2\phi(k_i - k_b))}{(2k_i + k_b + \phi(k_i - k_b))} k_i(1-\phi) + \frac{(3k_i - 2\phi(k_i - k_b))}{(3k_b + \phi(k_i - k_b))} k_b\phi. \tag{3.6}$$

This is valid for both high and low porosities.

The critical parameter in (3.1)-(3.5) is the permeability. Unfortunately, reliable measurements of sea ice permeability are few and may vary by an order of magnitude or more for the same porosity [*Freitag*, 1999]. Nevertheless, the Kozeny-Carman equation [*Bear*, 1972] with a grain size of 1 mm compares reasonably well with measurements by *Freitag* [1999] for new ice. However, it deviates substantially from his measurements of level arctic ice at high permeabilities. The ice permeability used in the model is summarized in Table 3.1, along with estimates for snow permeability, which are used for the slush layer. For very high porosities, the permeability of a circular tube of 5 mm diameter is used as an approximation of a brine drainage tube.

3.4 Isotopic fractionation model

In addition to transport of the heavy isotope of oxygen in the liquid phase due to brine transport, there is an exchange between the liquid and solid phase within a mixture volume. This is due to two main processes: (1) fractionation during freezing, causing heavy isotope enrichment in the solid phase, with a corresponding decrease in the liquid phase, and (2) isotopic exchange between the phases during snow grain coarsening in the presence of liquid water. The first process, in which the heavy isotope, ^{18}O, is preferentially incorporated into the solid phase during freezing, is the same process that occurs at the ice/ocean interface (Figure 3.2a). The second fractionation process was studied by *Raymond and Tusima* [1979]. Even without a net change in solid fraction, saturated wet snow will undergo grain coarsening in which smaller grains disappear at the expense of

Porosity	Permeability (m^2)	Comments
Snow		
< 0.05	1×10^{-15}	$\mathbf{u} \sim 0$
0.05 - 0.28	$1.2 \times 10^{-13} e^{18\phi}$	Kuroiwa (1968)
0.28 - 0.86	$1.096 \times 10^{-8} e^{(-8.79(1-\phi))}$	Sommerfeld and Rocchio (1993)
> 0.86	$9.86 \times 10^{-11} \frac{\phi^3}{(1-\phi)^2}$	Kozeny-Carman
Ice		
< 0.05	1×10^{-15}	$\mathbf{u} \sim 0$
> 0.05	$5.56 \times 10^{-9} \frac{\phi^3}{(1-\phi)^2}$	grain size = 1 mm
Maximum K	7.8125×10^{-7}	tube of diameter 5 mm

Table 3.1: Snow and ice permeability relations

larger grains as they round to minimize surface energy (Figure 3.2b). The shrinking grains will transfer mass to the liquid, depleting the melt. At the same time, the larger grains will grow, undergoing the equilibrium fractionation of the first process, further depleting the melt. In most instances, the second process dominates, as most of the ice grains vanish during coarsening [*Wakahama*, 1968] The first effect can be described by the equilibrium fractionation ratio, α_{eq}, given by the isotopic ratios in the solid and liquid phases:

$$\alpha_{eq} = \frac{R_i}{R_b}. \tag{3.7}$$

Eicken [1998] presented a model for this process for cooling sea ice using a Rayleigh fractionation model. Here we use a simplified discrete form. For each time step, for the freezing of a mass dm of brine, we may write the isotopic mass balance as

$$\begin{aligned} M_i R_i &= (M_i - dm)R_{io} + \alpha dm R_b \qquad dm > 0 \\ M_b R_b &= (M_b + dm)R_{bo} - \alpha dm R_b, \end{aligned} \tag{3.8}$$

provided dm/M_i is small. Using

$$\delta_{i,b} = \frac{R_{i,b}}{R_{VSMOW}} - 1, \tag{3.9}$$

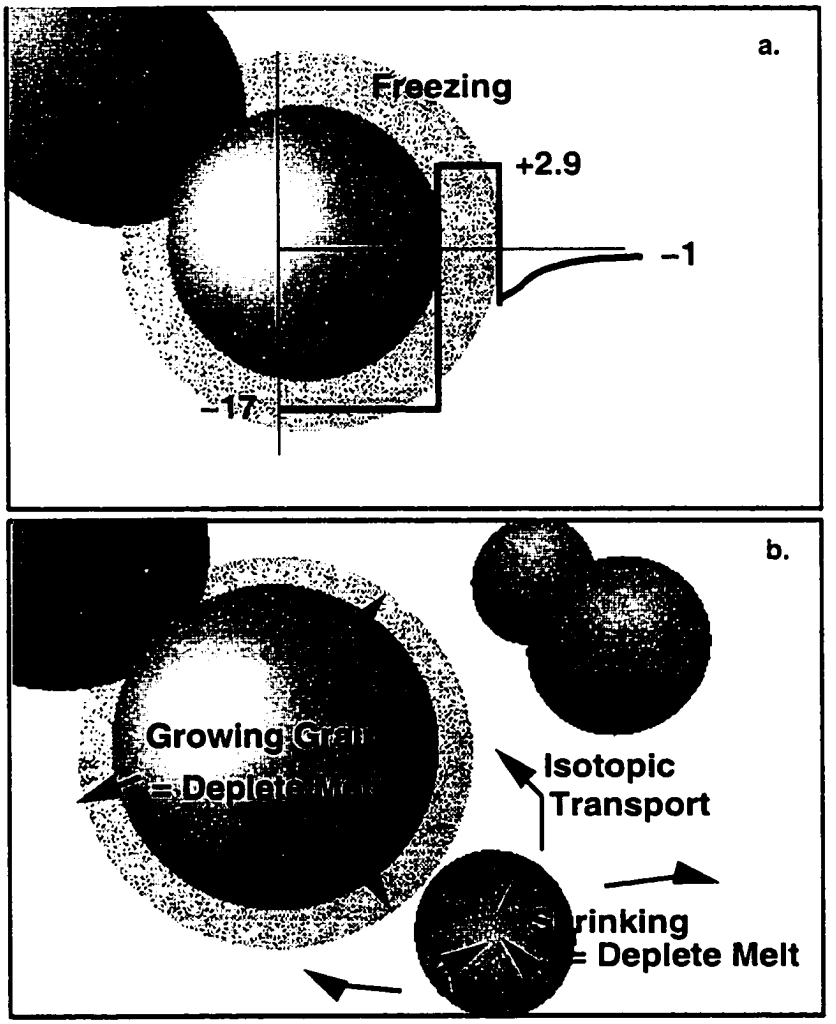

Figure 3.2: Modes of isotopic exchange in slush. (a) Freezing of the melt, (b) grain coarsening.

we obtain

$$\begin{aligned} \delta_{i,r} &= \delta_{io} + \frac{dm}{M_i}(\alpha\delta_{bo} - \delta_{io} + (\alpha_{eq} - 1)) \qquad dm > 0 \\ \delta_{b,r} &= \delta_{bo} - \frac{dm}{M_b}(\alpha\delta_{bo} - \delta_{bo} + (\alpha_{eq} - 1)). \end{aligned} \tag{3.10}$$

For the case of melting, no fractionation takes place, so we have

$$\begin{aligned} \delta_{i,r} &= \delta_{io} \qquad dm < 0 \\ \delta_{b,r} &= \delta_{bo} + \frac{dm}{M_b}(\delta_{bo} - \delta_{io}). \end{aligned} \tag{3.11}$$

Raymond and Tusima [1979] observed that the median particle size for their samples increased linearly with time, at a rate $dv/dt = 1.23 \times 10^{-6}$ mm^3 s^{-1}. *Nakawo et al.* [1993] used the results of *Raymond and Tusima* [1979] to derive an expression for the freezing fraction

$$\frac{dm}{M_i} = \beta ln(1 + \frac{1}{v_o}\frac{dv}{dt}t), \tag{3.12}$$

or, in discrete form

$$\frac{1}{M_i}\frac{dm}{dt} = \frac{\beta}{v}\frac{dv}{dt}, \tag{3.13}$$

where the constant $\beta \sim 0.41$ [*Nakawo et al.*, 1993]. We can then express the fractionation due to equilibrium grain kinetics as

$$\frac{dm}{M_i} = \frac{\beta\frac{dv}{dt}}{(1+f)v}dt, \tag{3.14}$$

where f is a scaling factor to account for the slowing of grain growth in the presence of impurities and is given by *Raymond and Tusima* [1979]

$$f = (1 + \frac{q_i}{q_b})\frac{k_b T}{\rho_b L D}. \tag{3.15}$$

q_i/q_b represents the ratio of the amount of heat transported in the ice to that transported in the liquid during grain coarsening. Since this process will take place in the presence of convective heat transport in the liquid, we assume this term to be zero. For the simulations presented herein, $f \sim 4$, so the rate of grain coarsening is about one-fifth of that of fresh water slush. Following (3.10), for fractionation due to grain coarsening, we may write

$$\begin{aligned} \delta_{i,c} &= \delta_{io} + \frac{dm}{M_i}(\alpha_{eq}\delta_{bo} - \delta_{io} + (\alpha_{eq} - 1)) \\ \delta_{b,c} &= \delta_{bo} - \frac{dm}{M_i}(\alpha_{eq}\delta_{bo} - \delta_{io} + (\alpha_{eq} - 1)). \end{aligned} \tag{3.16}$$

Nakawo et al. [1993] observed less fractionation in their samples than would be predicted by (3.12) and (3.16). They attributed this to the presence of a "diffusion layer" of low $\delta^{18}O$ melt surrounding growing grains during fractionation [e.g. *Eicken*, 1998]. In the presence of convection in the melt, we assume this diffusion layer will be largely absent, and that (3.16) adequately describes isotopic fractionation due to grain coarsening.

Although we have described fractionation due to equilibrium grain coarsening and bulk phase change as two separate processes, they certainly are not, in that bulk phase changes will affect the grain growth rates, and large scale thermal and solutal gradients will affect the equilibrium processes. However, it is unclear how to couple the two and they are left as separate phenomena to provide a likely upper bound on fractionation rates.

3.5 Simulations

All model runs were performed for a domain of 1m width and 0.5 m ice thickness. The dry snow depth was set constant at 18 cm with a density of 350 kg m^{-3}. Grid spacing was set at 5 mm, and the time step was set to 600 s. The latter was chosen as a compromise between computational speed and accuracy. Model runs lasted between 5 and 30 days, depending on the rate of freezing. The initial $\delta^{18}O$ values were set to -17‰ for snow, and -1‰ for the infiltrating sea water. These represent typical values for the Pacific Southern Ocean in winter [*Jeffries et al.*, 2001]. The initial median snow grain size was set to 0.5 mm. For the control simulation the surface temperature was set to $-20\,^{\circ}C$ and the initial salinity of the ice was set to 8‰. At the start of the simulation, it is assumed that the

ice has flooded and a slush layer 0.1 m thick has formed at the base of the snow, and the ice and snow are isothermal at $-1.85\,°C$, giving an initial ice porosity of 22% and slush porosity of 62%. This gives initial permeabilities for the ice and slush of 9.7×10^{-11} m^{-2} and 3.9×10^{-10} m^{-2}, respectively (see Table 3.1). During the early stages of the

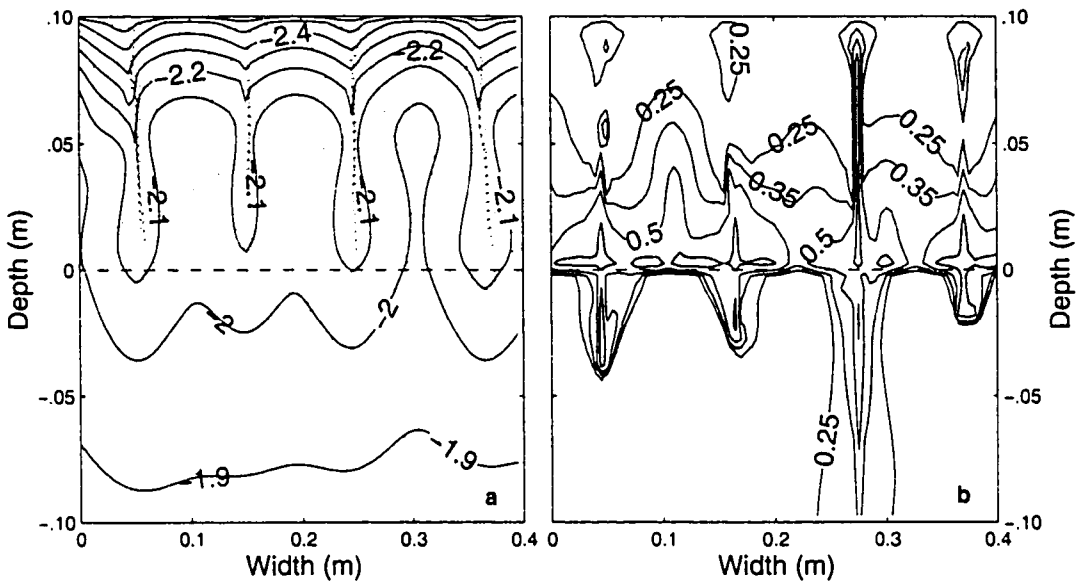

Figure 3.3: Convection and brine channel formation. (a) Convective pattern with streamlines showing salt finger formation for re-freezing slush at 1.5 days after flooding. Solid contours indicate temperature (°C) and dotted contours represent streamlines. (b) Brine volume (as a fraction of total volume) contour plot after 5 days. Focussing of convection produces highly porous columns (grey areas have brine volumes in excess of 80%) resembling brine drainage tubes analogous to chimneys formed during the casting of alloys.

modelled thermohaline convection plumes of cold, dense brine descend through the slush layer (Figure 3.3a). Along these plumes, streamlines tighten, indicating that the flow is being concentrated along the plume as it melts the ice matrix during descent. This increases the permeability along the plume, further concentrating the flow, leading to the formation of narrow columns of high porosity that act as channels for the flow. At the slush/ice interface, the stream lines begin to penetrate into the ice, and extend the channels into the ice (Figure 3.3b). The more vigourous salt plumes grow at the expense of their neighbours, as they draw brine from the other plumes. These channels strongly resemble the formation of chimneys which are a common feature in alloy casting [*Worster*,

1997]. Despite the formation of channels, the lower permeability of the ice provides an effective barrier to brine flow and dense brine remains at the base of the slush layer. A striking feature of this process is the influence of the dynamics in the mushy layer on the formation of channels in the underlying ice. As we shall see, the forcing provided by the highly convective slush may create channels where they would not otherwise form.

The onset of convection in the slush is governed primarily by the Rayleigh number,

$$Ra = \frac{\rho_b{}^2 g \Gamma K H^2 q}{\mu k_{si} k_{sn}}, \tag{3.17}$$

where Γ is a thermal expansion coefficient for brine density. Density variations due to brine salinity are tied to temperature via the liquidus relation so Γ is, in reality, an expansion coefficient for salt. q is the heat flux through the overlying snow layer. In practice, an appropriate Rayleigh number is difficult to determine because of the strong dependence of K on temperature and salinity and the coupling between the porosity and flow regime. The thermodynamic evolution of the system can be seen by examining the $-2.1\,^{\circ}\mathrm{C}$ isotherm of the simulated temperature evolution (Figure 3.4a). After an initial cooling of the upper few centimeters, convection begins and the slush layer is quickly cooled and becomes nearly isothermal in the convecting region. In many cases, as shown, the temperature gradient reverses, owing to a cold pulse to the slush/sea ice interface, consistent with field observations [*Hudier et al.*, 1995]. Dense brine begins to pool at the slush/ice interface raising the salinity there while lowering it at the top of the slush (Figure 3.4b). Initially the convection is confined to the slush only so that there is little heat transfer from the underlying sea ice to the slush. Consequently, the slush cools throughout its entire thickness despite the convecting portion remaining nearly isothermal. Between days two and four there is a slight increase in the salinity of the upper portion of the sea ice due to entrainment of dense brine as the convection slowly begins to penetrate into the underlying ice. Between days 4 and 10, channels begin to form in the underlying ice and convection penetrates through to the ocean beneath. The ice warms and rapid drainage of salt from both the slush layer and upper ice continues until the ice permeability drops sufficiently for convection to cease. Comparing the thermal evolution with convection to that without convection (Figure 3.4c) shows that although the advance of the isotherms is slowed during

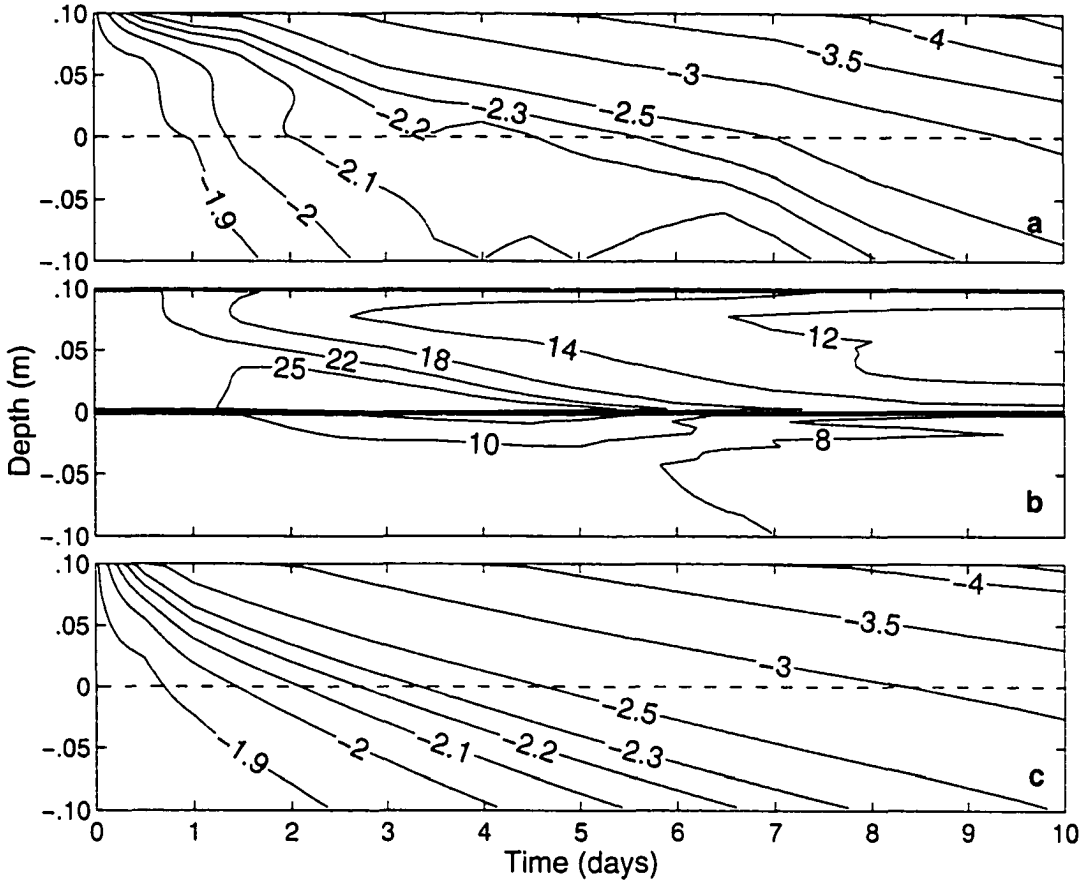

Figure 3.4: Thermal evolution of a slush layer. Time series of temperature (°C) and salinity (‰) for a re-freezing slush. Zero depth indicates the slush/ice interface. (a) Thermal evolution with convection of a 0.1 m thick slush layer for a fixed snow surface temperature of −20 °C. (b) Salinity profile. (c) Thermal evolution excluding convection. Note that contours are not evenly spaced.

convective events, there is only a moderate difference in the temperature profiles for the convecting and non-convecting cases. Generally, the convection provides a heat flux of only 2 to 4 W m^{-2} to the slush layer from below, while the conductive heat flux through the snow was approximately 25 W m^{-2}. The effect of convective heat flux to the slush is compensated by the increase in thermal conductivity due to brine drainage so that, after 10 days, the temperature profiles of the convecting and non-convecting case match closely.

In order to examine the effect of permeability on the amount of salt rejected from the slush layer during freeze-up we examine three main scenarios; one with high permeability

in both the slush and ice, a second with high permeability in the ice only, and a third with high permeability in the slush only (Figure 3.5a). For each group, there is only a modest dependence of brine rejection on forcing temperature, perhaps reflecting the competing effects of temperature on the amplitude of convection and permeability, which decreases with decreasing temperature. Primarily, however, the drainage is governed by the ice permeability. Although the amount of salt drained is smaller for those simulations with higher initial snow density (i.e., lower slush permeability), the final slush salinity is only slightly below that of the higher permeability case. The difference in salinity between the two cases is primarily a result of a 6‰ difference in initial slush salinity. In contrast, for lower ice permeability, drainage is substantially reduced. The results for variation of the isotopic composition of the frozen slush layer (Figure 3.5b) show less distinction, with increases of about 2 to 5‰, representing final compositions of -1.9 to -6.9‰. The increase in the $\delta^{18}O$ values is most dependent on the thermal driving force, since grain coarsening can progress further if the rate of freezing is reduced. Trajectories of the salinity and isotopic composition for typical results are plotted as arrows in Figure 3.6. The model can produce substantial shifts in the composition of the slush and demonstrate final salinity-$\delta^{18}O$ relationships within the observed range of values, although generally within the higher range of salinities. Most of the apparent snow ice samples shown in Figure 3.6 have salinities lower than those produced by the model. While the final salinity of the simulated snow ice layer is dependent on the choice of snow and ice permeability, this suggests that brine drainage processes continue to take place after the initial formation of the snow ice layer.

An important characteristic of the slush/sea-ice system is that it often consists of a highly saline layer immediately above a less porous layer of an often substantially lower salinity. Brine drainage from the freezing slush may then contribute to the salination of the upper layers of the ice, thereby increasing its porosity. To demonstrate the role of permeability on the drainage of salt from the slush and possible salination of the ice, several salinity profiles are shown in Figure 3.7a after a 10 day period. Curve A is the simulated profile for the same model run as Figure 3.4. Again, we note that the high permeability in both the slush and ice leads to efficient drainage of both regions. Once the convection has extended into the upper portion of the ice, the salinity there initially increased due to

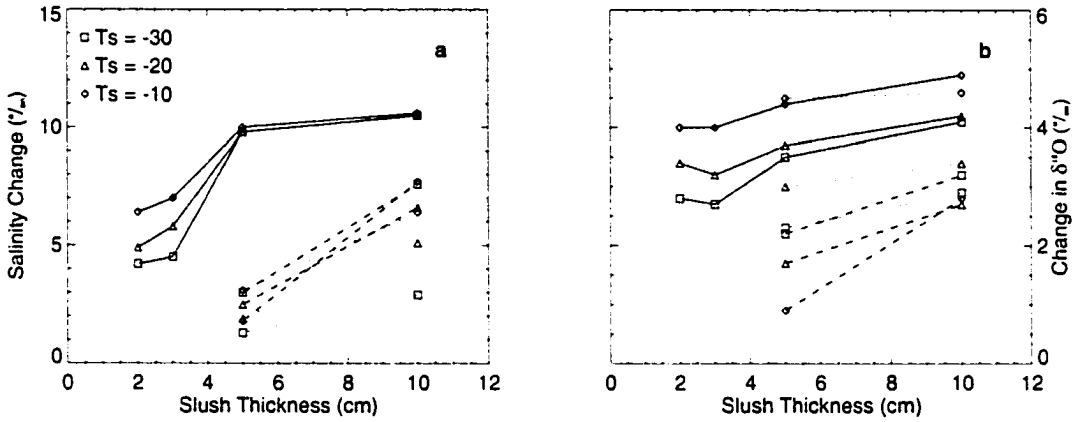

Figure 3.5: Salinity and isotopic changes during freezing. (a) Salinity decrease, (b) isotopic shift. Solid lines are for an ice salinity of 8‰ and initial snow density of 350 kg m^{-3} (high ice and slush permeability). Dashed lines are for an ice salinity of 5‰ (low ice permeability) and dotted lines indicate an initial snow density of 500 kg m^{-3} (low slush permeability). The legend indicates the surface temperature (Ts) forcing.

a salt flux from the slush. However, once channels penetrated to the ice/ocean interface, this excess salt drained rapidly, and there was little net change in the ice salinity. For curve B, the ice salinity is set to 5‰, rather than 8‰. This reduces the ice permeability, providing an effective barrier to drainage and, although the upper portions of the slush drained quite effectively, this salt was trapped at the slush/ice interface. Convection in the ice still occurred and drainage channels formed, but this was sufficiently slow that a modest increase in salinity (about 1‰) occurred in the upper part of the ice due to salination from the freezing slush. After 10 days, however, this salination slowed and slow drainage produced a net reduction in ice salinity. The simulation in curve C was the same as for B, except that the initial snow density in the slush was set to 500 kg m^{-3}, to reflect possible settling of snow during flooding [*Eicken et al.*, 1995]. Because of the relatively weak convection in the slush, channels did not form and convection into the underlying ice served to increase the ice salinity. The salinity of the slush layer remained quite high after freezing. Note the difference between runs B and C: no channels formed during run C, but in run B the focussing of the flow in the convecting slush allowed the initiation of drainage channels in the underlying ice, eventually allowing for partial drainage of the

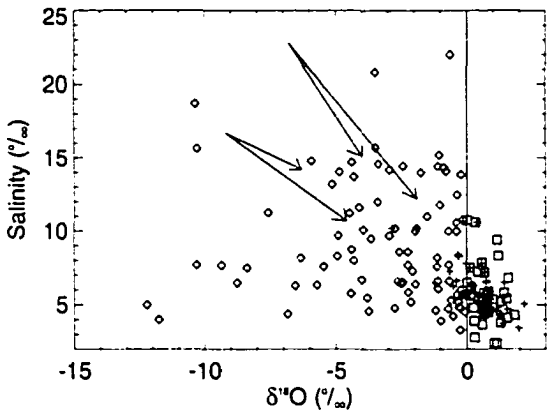

Figure 3.6: Simulated δ^{18}O-Salinity trajectories. Typical trajectories (arrows) are overlain on a scatter plot of ice salinity versus δ^{18}O for cores obtained during R.V. Nathaniel B. Palmer cruise 95-5 in the Ross Sea during the austral winter of 1995. The different symbols indicate ice type: ◇ snow ice, + congelation ice, □ frazil. For clarity, not all data points shown.

salt from the slush layer.

In real sea ice, brine drainage channels may be present before flooding (indeed, that may facilitate the flooding in the first place). Therefore, we present a simulation with channels placed *a priori* at 0.5 m intervals, shown in curve D. This demonstrates the importance of the spatial geometry of the ice permeability in governing the brine redistribution. Brine drained efficiently from the slush layer, without a substantial increase or reduction of the salinity of the bulk ice.

Isotopic profiles show the greatest increase in δ^{18}O for simulations A and D (Figure 3.7b). Isotopic ratios are increased throughout the slush thickness, but quite substantially near the ice interface, with values as high as -1‰. In curve C, note that there is some isotopic depletion in the upper regions of the ice due to slow convective transport into the ice, although at most this depletion amounts to a shift in isotopic signature of 0.6‰.

The evolution of the brine volume during freezing shows clearly the effects of permeability on the profiles in Figure 3.7. Brine volume profiles for three of the cases (A, B,

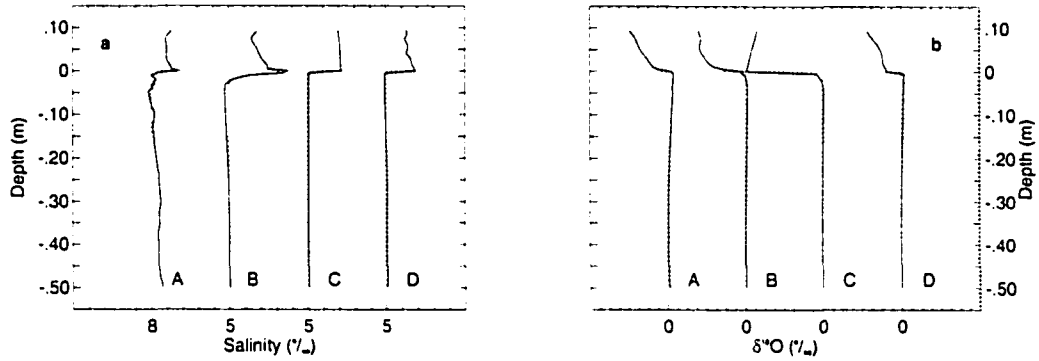

Figure 3.7: Salinity and isotopic profiles of freezing slush. Salinity (a) and isotopic (b) profiles are shown for various simulation runs. A: standard simulation. B: initial ice salinity of 5‰. C: initial ice salinity of 5‰ and snow density of 500 kg m^{-3}. D: same as simulation B, but with brine drainage tubes present. The dotted lines indicate the initial composition at the beginning of each simulation. The tick interval is 5‰ for salinity and 1‰ for $\delta^{18}O$.

and D) from Figure 3.7 are presented in Figure 3.8 at 5 and 10 days after the onset of freezing. As discussed above, convection penetrates more readily into higher permeability ice (contrast Figures 3.8a and b). As the ice freezes, and permeability decreases, the natural spacing of drainage tubes increases, in agreement with observations in new ice [*Saito and Ono*, 1980; *Wakatsuchi*, 1983]. In the more permeable ice (Figure 3.8b), the closely spaced channels can merge together, allowing efficient drainage of the slush layer. In the less permeable ice of Figure 3.8c-d, the channels are too widely spaced, and the slush cannot drain, resulting in the highly saline layer as described above. With brine tubes present (Figures 3.8e-f), the drainage in the slush is focussed towards the channel, and the slush can drain as effectively as it does through high permeability ice.

3.6 Implications of brine convection

The ability of a slushy layer to efficiently desalinate is primarily dependent on the existence of drainage channels; either existing channels, or those created through the flow focussing convective process. For the snow permeabilities used, the Rayleigh number for the flooded layer is above critical. The presence of convection does not guarantee the

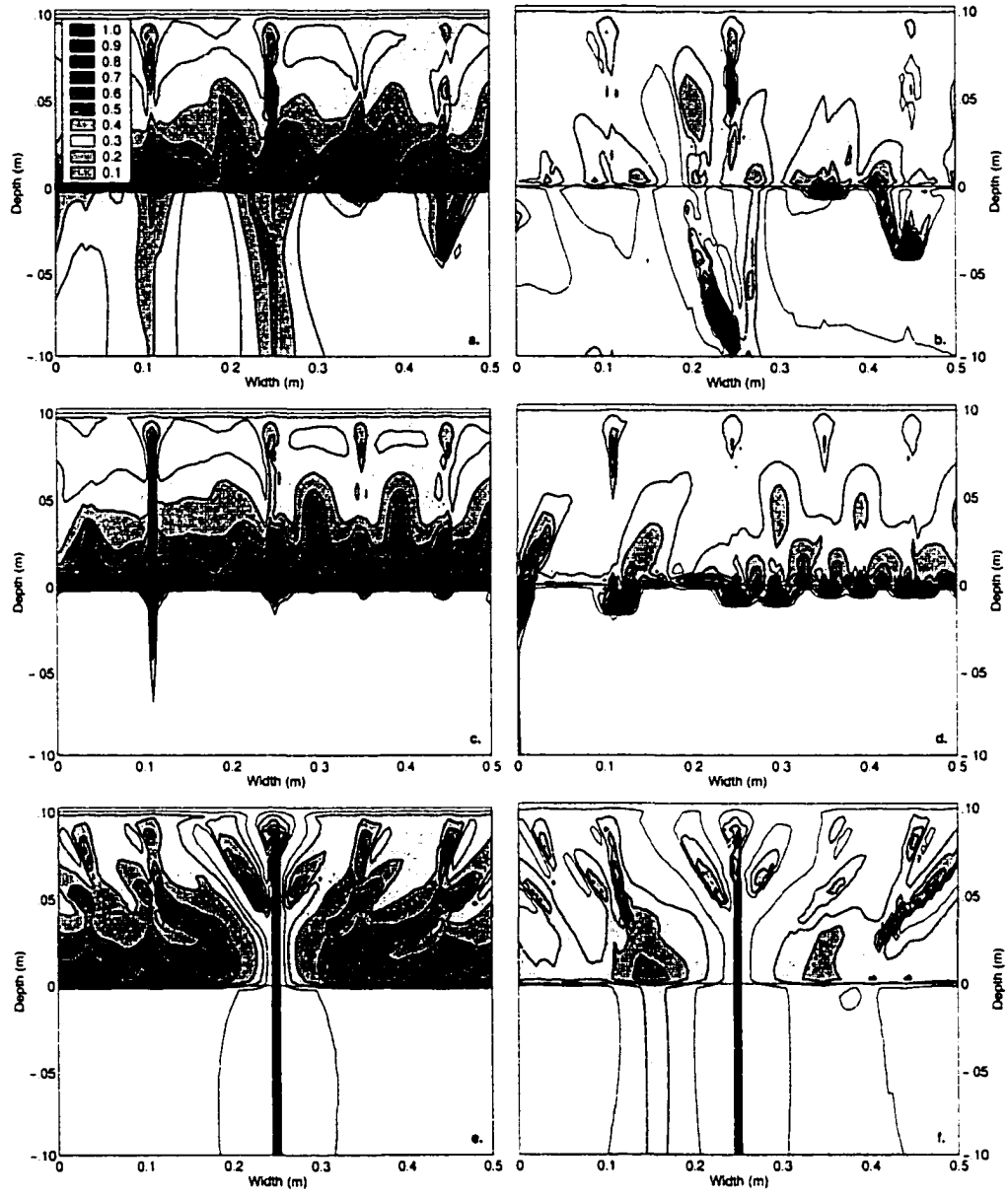

Figure 3.8: Brine volume contours of freezing slush. Three of the cases in Figure 3.7 are presented for two times: High permeability ice and snow (standard case) at 5 days (a) and 10 days (b); low permeability ice and high permeability snow at 5 days (c) and 10 days (d); and low permeability ice with existing brine drainage tubes at 5 days(e) and 10 days (f).

formation of channels. If the flow is slow enough, thermal diffusion will reduce the strong temperature, and hence, brine salinity gradients. This will reduce the amount of melting caused by a decending plume, keeping the local porosity relatively low. Without a strong effect on porosity, and hence permeability, the plumes may not focus sufficiently to create channels. In practice, this is unlikely, as the increase in snow grain coarseness with wetting will most likely increase the permeability above the values used in the present simulations. Observed snow permeabilities for coarse grained snow are much higher than for fine grained snow [*Kuroiwa*, 1968; *Shimizu*, 1970].

The simulated convection acts much like that described at the ice/ocean interface of growing sea ice [*Worster and Wettlaufer*, 1997]. Convection in the slush acts somewhat like a boundary layer mode, with salt redistributed within the slush, but confined within the slush layer until convection is initiated in the underlying sea ice. If convection is strong enough in the slush layer, it can penetrate into the ice, especially if the flow is focussed into channels, and can thus force convection in ice that would otherwise not convect on its own. This allows the slush layer, in effect, to create drainage channels of its own in the underlying ice that aid in the reduction of the layer's salinity.

An increase in the $\delta^{18}O$ values of the slush layer is also aided by the presence/formation of channels, but to a lesser degree. The shift in isotopic composition in the simulations is largely due to metamorphic changes within the layer itself, and the convective transport of the liquid fraction. Model results indicate a shift in isotopic fraction of several parts per thousand. In the extreme case, if a slow re-freezing is allowed to maximize the effects of metamorphic changes, bulk isotopic values can be raised to about -1.9‰, although local changes within the slush layer (for instance, at the slush/sea ice interface) can be larger. Since the transport of the liquid fraction is primarily through rapidly draining channels, negative shifts of the isotopic composition of the underlying ice layers are minimal, perhaps no more than 1‰. Although such shifts occur frequently during the freezing of the slush, the fractionation that occurs once the sea ice begins to cool increases the simulated $\delta^{18}O$ values, effectively cancelling the previous reduction.

Results described herein are highly sensitive to the underlying ice permeability. A reduction in permeability by a factor of five (based on salinity differences) can produce a similar contrast in the amount of salt drained (Figure 3.5). Unfortunately, the ice

permeabilities can vary by more than an order of magnitude [*Freitag*, 1999] and therefore predictive determinations of the salinity and isotopic profiles in flood-freeze cycles are presently not possible.

Although the formation of brine channels may be consistent with observations [*Worster*, 1997], there are several limitations in the model which need to be addressed. It should be noted that the resolution of the model does not allow a proper treatment of the channel dynamics, as they tend to be only one grid spacing in width, whereas actual drainage tubes may exhibit complex behaviour [*Niedrauer and Martin*, 1979]. In the slush, these channels may be affected by motion of the snow grains. The rounding of snow grains during coarsening will tend to reduce the structural strength of the snow pack so that grains may settle into voids, thus partially impeding the development of highly porous channels. At low brine volumes, discontinuities in the pore space may cause flow variations on the order of the scale of interest, and effects such as hydrodynamic dispersion may become important. There will likely be substantial variations in permeability on a small scale due to microstructural variations or, in the case of congelation ice, anisotropic permeability, which may have important effects on the fluid flow. Further laboratory and modelling work is needed to investigate the behaviour of thermohaline convection in sea ice.

We may note some general behaviour of the freezing slush/ice system. Thermohaline convection during freezing of the slush layer may be fairly effective at solute transport, but it is generally not vigourous enough to create a well defined freezing front, and cooling can occur through the entire slush layer before it freezes. The thermal evolution of the slush/ice system can be adequately treated by simple thermal diffusion provided a rough estimate of the brine rejected can be made. Brine drainage due to convection is primarily dependent on the permeability of the underlying ice, although if the convection in the slush layer is vigourous enough, it may penetrate into an otherwise impermeable ice layer and initiate the formation of drainage channels. Salt that has drained from the slush passes through channels that carry the salt effectively to the water column. Salination of the sea ice by the overlying slush may be minimal. These results suggest that this convection does not contribute substantially to maintaining a high porosity in the upper portion of the ice through the downward flux of salt. Simulated brine drainage reduced the salinity of the slush layer by as much as half, to as low as 10‰ in a few days. If the convection can

penetrate through the ice layer, slush salinities fall to 10-13‰ before convection ceases, though this range is a function of the prescribed snow permeability. This desalination is consistent with the findings of *Takizawa* [1985], but somewhat less than that observed by *Lytle and Ackley* [1996].

3.7 Compositional shifts and snow ice identification

The isotopic composition of the slush layer was raised by as much as 4-5‰ during freezing, to as high as -1.9‰. This should probably be viewed as an upper bound, as these simulations represent idealized fractionation conditions. Under natural conditions, the freezing process will likely mute grain coarsening effects by allowing the smaller ice grains to grow. If a slush persists under isothermal conditions for an extended period, however, the impact of grain coarsening may be enhanced. Further post-genetic changes to the isotopic composition are conceivable, as much of the simulated $\delta^{18}O$ values are due to ^{18}O depletion in the interstitial liquid. If subsequent flooding and re-freezing events or brine drainage processes over the long term could displace this brine, a moderate positive shift could result. The analysis of *Eicken* [1998] suggests that large changes are unlikely. After freeze-up, the liquid fraction in the slush layer is typically less than 15%, so even under ideal circumstances of slow freezing and flushing of brine, shifts of only about 0.1-0.3‰ in the bulk isotopic composition are possible.

As the compositional shift in the underlying ice was minimal, we do not expect isotopic shifts in congelation or frazil ice due to compositional convection to be large, and so the number of "false positives" when using isotopes to identify snow ice may be minimal. This suggests that the congelation layers with $\delta^{18}O < 0$ (Figure 3.1) may be due to rapid initial growth, rather than contamination with advected brine from above. In the slush itself, the model suggests a maximum $\delta^{18}O$ value of -1.9‰. Without a plausible mechanism to produce further shifts of about 2‰, caution should be taken in identifying snow ice as any granular sea ice with slightly negative $\delta^{18}O$ values.

3.8 Key results of modelling of flooded layer evolution

- Thermohaline convection during freezing of a slush layer provides an efficient means of desalination and brine exchange through the focussing of flow in narrow channels. Decreases in slush salinity of 10‰ can occur during freezing, though this drainage is highly dependent on ice porosity.

- If drainage tubes are present or form during freeze-up, drainage of $H_2{}^{18}O$ depleted brine can significantly raise the $\delta^{18}O$ value of the slush. This is primarily due to mass exchange between the liquid and solid phases during grain ripening in the slush.

- Brine drainage through the ice is primarily confined to narrow channels, so depletion of $H_2{}^{18}O$ in the ice due to the convection is small, though slight negative $\delta^{18}O$ shifts in the upper ice layers are possible.

- Based on model results, a $\delta^{18}O$ cut-off criterion for the identification of snow ice of no higher than -2‰ is recommended for the RAB seas.

Chapter 4

Flooding and snow ice formation with a one-dimensional model: Permeability controls on ice development

4.1 Permeability of sea ice and potential for flooding

The flooding/snow ice formation process has been the subject of some modeling studies [*Leppäranta*, 1983; *Eicken et al.*, 1995; *Crocker and Wadhams*, 1989; *Fritsen et al.*, 1998; *Saloranta*, 2000]. Early efforts [e.g., *Leppäranta*, 1983] assumed that a negative freeboard was the only requirement for flooding to occur. While this is certainly necessary, it is not the only requirement. There also must be established pathways from the ocean through to the snow/ice interface for sea water and/or brine to flow.

Freeboard data from one autumn and one winter cruise in the Ross Sea [see *Jeffries et al.*, 1998a] illustrate the fact that the snow/ice interface does not flood simply because the ice surface is below sea level (Figure 4.1). While 37% of the observed freeboards were negative, very few of the drilling sites were observed to be wet or flooded at the base of the snow pack prior to drilling. *Eicken et al.* [1995] noted similar results in the Weddell

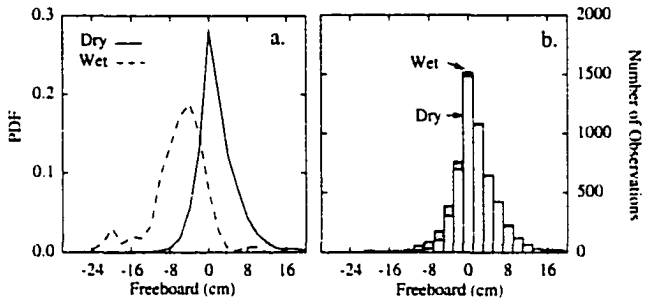

Figure 4.1: Freeboard distribution in the Ross Sea. (a) Probability distribution of freeboards for sites that were dry prior to drilling (solid line) and locations that were wet or flooded prior to drilling (dashed line) in autumn and winter 1995. (b) Frequency distribution of freeboards observed, indicating fraction that were wet or flooded prior to drilling.

Sea. Not until freeboards approached -6 cm did we observe a significant number of sites that were flooded prior to drilling. It should be noted that this flooding is not necessarily associated with areas of ice deformation [*Adolphs*, 1998, Figure 8]. Flooding is as likely to occur in areas of level ice where no obvious cracks or pathways for upward brine flow are apparent.

Obviously, the presence of a negative freeboard is insufficient to guarantee flooding. *Eicken et al.* [1995], based on unpublished permeability studies, speculated that under certain conditions, even though there is a negative freeboard, the underlying ice might be impermeable and prevent the upward movement of brine to the snow/ice interface. *Cox and Weeks* [1975], in their classic study of desalination processes, demonstrated that artificial sea ice becomes permeable at brine volumes exceeding 5-7%. At lower brine volumes, the brine pockets and channels are not sufficiently connected to allow brine flow. *Golden et al.* [1998], by analogy with electrical conductivity of compressed powders, suggested that the percolation threshold for columnar sea ice occurs at brine volumes of about 5%, and somewhat higher for granular ice. *Eicken et al.* [1995] showed that in the Weddell Sea, brine volumes may be below this threshold throughout much of the growth season.

As the porosity of the ice is closely linked to the thermal regime and the salinity characteristics of the ice, there is a strong coupling between the permeability and the flow

regime. While the importance of ice permeability in controlling the flooding process has been noted [*Crocker and Wadhams*, 1989; *Hudier et al.*, 1995; *Lytle and Ackley*, 1996; *Fritsen et al.*, 1998; *Golden et al.*, 1998], little attention has been paid to the complex relationships between flooding, desalination, and ice permeability.

4.2 Objectives

The aims of this chapter are (1) to investigate whether the percolation model for flooding is a plausible mechanism and whether it produces snow ice amounts similar to those inferred from ice core structural analysis and oxygen isotope data, (2) to identify the critical factors that control the flooding process and their consequences for the overall ice mass balance, and (3) to demonstrate the importance of the coupling between flooding and snow ice formation and the evolution of the salinity characteristics of the ice.

In order to investigate these processes and the factors controlling them, a one-dimensional (1-D), nonlinear sea ice growth model is developed. The evolution of the salinity profile is treated in a semi-heuristic fashion and is coupled to ice growth processes and flooding. The sea ice is modeled as a porous medium, and upward brine flow is described using a Darcian scheme. First, the governing equations of the model are presented, and different possible treatments of the brine flow regime are discussed. Model results of ice mass balance and salinity characteristics are presented and compared with field data, and the key parameters controlling ice growth are pointed out. The sensitivity of snow ice formation to several critical parameters is presented, and the importance of factors controlling brine percolation and the salinity profile is discussed. Finally, we point out gaps in our understanding of the flooding and snow ice formation process.

4.3 Model description

A one-dimensional nonlinear ice growth model was developed. The basic model builds on the previous work of *Maykut and Untersteiner* [1971], *Cox and Weeks* [1988] and *Wade* [1993]. The essential framework of the thermodynamics and salinity entrapment and desalination is based on that of *Cox and Weeks* [1975]. However, as we are interested

in complex thermo-physical interactions between the snow cover and brine network of the ice, the model is extended to allow for nonlinear temperature profiles and for upward brine flow through the ice and snow. As processes related to the snow cover are critical for resolving the phenomena of interest, the snow pack is treated in more detail than in standard sea ice growth models [e.g., *Cox and Weeks*, 1988].

4.3.1 Thermodynamics

The generalized one-dimensional heat equation for heat transfer in a porous medium is given by

$$\rho_{si,sn} C_{si,sn} \frac{\partial T}{\partial t} + \rho_b C_b \frac{\partial}{\partial z}(\phi u T) = \frac{\partial}{\partial z}(k_{si,sn} \frac{\partial T}{\partial z}) + \kappa I_o e^{-\kappa z}, \tag{4.1}$$

where $\rho_{si,sn}$ is the bulk density of sea ice or snow, $C_{si,sn}$ is the specific heat, $k_{si,sn}$ is the bulk thermal conductivity, ρ_b is the brine density, C_b is the specific heat of the brine, T is the temperature, ϕ is the effective porosity of the bulk medium, and u is the pore fluid velocity. Here, $C_{si,sn}$ is an effective specific heat, as it includes the latent heat due to changes in the volume fraction of entrapped brine. *Schwerdtfeger* [1963] gave $C_{si,sn}$ as

$$C_{si,sn} = -\frac{S}{\beta T^2} L + \frac{S}{\beta T}(C_w - C_i) + Ci. \tag{4.2}$$

Here, S is the sea ice salinity, L is the latent heat of fusion, C_w and C_i are the heat capacities for water and pure ice, respectively, and $\beta = -0.0182^\circ \mathrm{C}^{-1}$. The second term in (4.1) represents the heat transported by advection of brine upward through the ice during flooding events. Capillary wicking of brine up into the snow is neglected. To account for the phase change that occurs as brine is transported along temperature gradients in the ice, C_b also includes a latent heat term. C_b is most readily obtained from (4.2) by setting S equal to the brine salinity.

The second term on the right in (4.1) represents the absorption of short-wave radiation in the medium (Beer's law). Here, κ is the bulk extinction coefficient of light in the snow or ice, I_o is the net radiative flux at the surface, and z is the vertical depth. Strictly speaking, Beer's law is valid only for monochromatic light in an infinite medium. In the upper part of the snow cover, longer wavelengths are strongly absorbed. To accommodate this, we follow

the practice of *Maykut and Untersteiner* [1971] and define I_o as the fraction of radiation that penetrates beneath 10 cm. Below this depth κ is fairly constant [*Choudhury*, 1981], and exponential decay becomes a reasonable approximation. I_o is estimated based on the parameterization of *Grenfell* [1979]. This treatment is somewhat oversimplified; however, as this study concentrates primarily on the dark winter months, the effects of short-wave absorption on the heat balance of the ice are minimal.

Equation (4.1) assumes that the solid matrix and fluid are in thermal equilibrium, which may be true only for quite slow flow rates. As equation (4.1) is general, it applies to the snow cover as well as the ice below. Since we are concerned only with the fall and winter months, freshwater infiltration and snowmelt are not treated, although this may be an important process in the outer ice pack [*Sturm et al.*, 1998].

Ice growth at the base of the ice is given by

$$k_{si}\frac{dT}{dz} = \rho_{si}L_{si}\frac{dz}{dt} + F_w, \tag{4.3}$$

where L_{si} is the latent heat of fusion for sea ice and F_w is the oceanic heat flux due to heat transfer from the upper ocean to the ice. F_w is assumed to be 5 W m^{-2}. Temperature and salinity of the ocean are assumed to be -1.85 °C and 35‰, respectively. Material properties for (4.1) and (4.3) are taken from *Yen* [1981]. At the surface of the snow (or ice) the temperature is determined by balancing the surface heat fluxes [*Maykut*, 1978]:

$$F_l + F_E + (1-\alpha)F_r - I_o + F_s + F_e + F_c = 0, \tag{4.4}$$

where F_l is the incoming long wave radiation, F_E is the emitted long wave radiation, F_r is the incoming short-wave radiation, F_s and F_e are the sensible and latent heat fluxes, respectively, F_c is the conductive heat flux, and α is the albedo. The albedo of snow-free ice is taken from *Weller* [1972]. The albedo of ice with a snow cover is estimated from the measurements of *Allison et al.* [1993]. F_l is estimated by [*Key et al.*, 1996]

$$F_l = \sigma T_a^4(0.746 + 0.0066e)(1 + 0.26C), \tag{4.5}$$

where T_a is air temperature, σ is the Stefan-Boltzmann constant, e is the vapor pressure

(mbar), which is computed for an assumed relative humidity of 0.9, and C is the relative cloud cover, taken as 0.7. The short-wave radiation is computed after *Zillman* [1972], modified by a cloud factor of $1-0.6C^3$ [*Maykut*, 1978]. The turbulent fluxes are calculated from the standard bulk transfer parameterizations [e.g., *Maykut*, 1978], with bulk transfer coefficients taken from *Cox and Weeks* [1988].

4.3.2 Snow model

As the snow cover provides both very effective insulation for the ice as well as the necessary load to depress the ice for flooding to occur, the treatment of processes in the snow cover is critical for proper modeling of both congelation ice growth and the flooding/snow ice formation process. Since ice brine volumes and desalination processes are dependent on the thermal regime of the ice, the permeability, and hence flooding processes, are highly dependent on modeled snow/ice interface temperatures. Heat transfer through the snow cover is highly dependent on diagenesis in the snow pack [*Sturm et al.*, 1998]. The key processes of relevance to the present study are the mechanical deformation and diagenesis of the snow cover, including destructive metamorphism, such as the density increase due to settling and compaction, constructive metamorphism due to grain growth and depth hoar formation, and melt metamorphism in saturated snow and slush at the base of the snow pack. Depth hoar is a ubiquitous feature of the snow pack over sea ice in the Ross Sea region [*Sturm et al.*, 1998], and owing to its very low thermal conductivity, its formation is an important process in controlling the heat transfer through the snow pack. However, predicting production rates of kinetic growth grains is difficult [*Colbeck*, 1983b; *Sturm*, 1991], particularly so in this case where the base of the snow pack is often infiltrated by brine [*Sturm et al.*, 1998], which will affect the vapor transfer and crystal growth processes which control depth hoar formation. Because of these difficulties, depth hoar formation is not treated in the model. The possible consequences of this simplification are discussed below.

For densification due to settling, we use the formulation of *Anderson* [1976],

$$\begin{aligned} \frac{1}{\rho_{sn}}\frac{d\rho_{sn}}{dt} &= 2.8\times 10^{6} e^{0.04T} e^{-46(\rho_{sn}-150)} \\ &\qquad \rho_{sn} > 150\ kg\ m^{-3}, \\ \frac{1}{\rho_{sn}}\frac{d\rho_{sn}}{dt} &= 2.8\times 10^{6} e^{0.04T} \\ &\qquad \rho_{sn} < 150\ kg\ m^{-3}, \end{aligned} \tag{4.6}$$

where ρ_{sn} is the snow density (kg m^{-3}) and T is the temperature (°C). For densification due to compaction, we have [*Anderson*, 1976]

$$\begin{aligned} \frac{1}{\rho_{sn}}\frac{d\rho_{sn}}{dt} &= \frac{W_{sn}}{\eta} e^{0.021\rho_{sn}}, \\ \eta &= 1\times 10^{7} e^{(0.081T)}, \end{aligned} \tag{4.7}$$

where W_{sn} is the weight of the overburden and η (N s^{-1}) is the viscosity of snow. The initial density of new snow, 254 kg m^{-3}, is based on measurements of recent snow by *Sturm et al.* [1998]. This value was chosen because low-density, new snow was rarely observed in the study region, and the prevalence of high winds would tend to result in initial deposition of fairly dense snow.

The most critical parameter in the snow cover model is the thermal conductivity. Commonly, it is expressed as an effective thermal conductivity to account for both heat transport due to conduction and vapor diffusion. This has been the subject of extensive study, both theoretically and experimentally [*Arons and Colbeck*, 1995; *Sturm et al.*, 1997]. Here we use the equations given by *Sturm et al.* [1997],

$$k_{sn} = \begin{cases} 0.138 - 1.01\times 10^{-3}\rho_{sn} + 3.233\times 10^{-6}\rho_{sn}^{2} & 156 \le \rho_{sn} \le 600, \\ 0.023 + 0.234\times 10^{-3}\rho_{sn} & \rho_{sn} < 156, \end{cases} \tag{4.8}$$

where ρ_{sn} is the snow density in kg m^{-3} and k_{sn} has units of W m^{-1} K^{-1}. The uncertainty in (4.8) is ± 0.1 W m^{-1} K^{-1}. It should be noted that (4.8) gives effective thermal conductivities that are generally lower than those given by most other studies. For instance, for typical observed snow densities, (4.8) gives values about half that of those given by *Abel's*

[1893]. This difference may in part be due to the generally lower sample temperatures for the measurements of *Sturm et al.* [1997].

For slush, the thermal conductivity is calculated using a Maxwellian model [*Schwerdtfeger*, 1963],

$$k_{\text{wet}} = \frac{2k_i + k_b - 2v_b(k_i - k_b)}{2k_i + k_b + v_b(k_i - k_b)} k_i, \tag{4.9}$$

where k_i and k_b are the thermal conductivities of ice and brine, respectively, and v_b is the relative brine volume. Such a model is strictly valid only for a continuous ice matrix with small spherical brine inclusions. This is not true for slush, and so (4.9) may not be accurate. However, for typical slush brine volumes and ice and brine thermal conductivities, (4.9) gives values of k_{wet} quite close to that of a parallel plate model, so the error in k_{wet} is likely considerably less than the uncertainty in k_{sn}.

Erosion of snow due to wind drifting is not included in the model. While local redistribution is not germane to the mass balance in a 1-D model, loss to neighboring leads is. *Eicken et al.* [1994] estimated that these losses may be more than 10 cm over the course of a year in the Weddell Sea. However, they noted that hardening of the snow surface due to metamorphism may prevent the suspension of particles even in strong winds. *Sturm et al.* [1998] described a similar effect due to icing of the surface snow. In light of the uncertainty in precipitation estimates, we neglect the effects of snow redistribution.

4.3.3 Salinity model

The salinity of sea ice is normally governed by three main processes: the initial entrapment of brine during ice formation, the expulsion of brine due to the expansion of the ice as it cools, and gravity drainage [*Weeks and Ackley*, 1986]. Here we also investigate a fourth mechanism: upward flushing due to brine percolation through the ice during flooding events.

Initial salt entrapment is given by

$$S_{si} = k_{\text{eff}} S_w, \tag{4.10}$$

where k_{eff} is an ice growth velocity-dependent segregation coefficient, taken from *Cox and*

Weeks [1988], S_{si} is the initial salinity (‰) of the new ice, and S_w is the salinity of sea water. As the model formulation is based on the control volume approach [*Patankar*, 1980], the treatment of brine expulsion due to brine freezing in the interior of the ice is quite simple. If the total relative volume of components (ice and brine) within a control volume exceeds unity, the excess volume of brine is moved into the layer below, where volumes are recomputed and the process is then repeated for all ice layers. This treatment is essentially equivalent to the finite difference formulation presented by *Cox and Weeks* [1975]. Note that this does not allow for upward expulsion of brine into the snow cover. This can lead to a wet, saline snow layer at the snow/ice interface which may wick up several centimeters into the snow pack [*Sturm et al.*, 1998].

The most important factor in the evolution of the salinity profile of the ice is gravity drainage. Brine entrapped in sea ice forms a network of interconnected fluid pathways which tend to form elongated tubes that provide connectivity between the entrapped brine and the sea water beneath [*Bennington*, 1987; *Lake and Lewis*, 1970; *Niedrauer and Martin*, 1979; *Cole and Shapiro*, 1998]. Owing to the vertical density gradient of the brine, brine may become convectively unstable within the ice [e.g., *Wooding*, 1959; *Lake and Lewis*, 1970; *Niedrauer and Martin*, 1979]. This causes convective overturn of the brine within the pore space and an exchange of the cold dense brine with underlying sea water. Interception of the brine drainage network by isolated brine inclusions may enhance the rate of desalination [*Bennington*, 1987]. While no mechanistic model is currently available to account for this process, *Cox and Weeks* [1975] provided an empirical relationship based on observations of brine drainage in growing NaCl congelation ice. For brine volumes > 0.05, they give the rate of change of ice salinity (‰) as

$$\frac{dS}{dt} = (1.68 \times 10^{-7} - 3.37 \times 10^{-6} v_b)\frac{dT}{dz}, \tag{4.11}$$

where dT/dz is the vertical temperature gradient (°C m^{-1}). For brine volumes < 0.05, the ice becomes impermeable and no brine is drained from above the impermeable layer.

Unfortunately, (4.11) is not expressed in a conservative form; that is, although it permits calculation of the amount of salt lost from an individual ice layer, it tells us nothing about the brine fluxes between layers which govern the decrease in salinity. Since these

fluxes are likely dependent on ice microstructural variations and brine salinity gradients, proper treatment of brine drainage under a variety of natural conditions requires knowledge of how these factors control brine transport. For conditions similar to the experiments from which (4.11) was determined, namely, growing congelation ice with a constant thermal forcing [*Cox and Weeks*, 1975], the brine exchange should be implicitly accounted for by (4.11). For natural sea ice, we might expect that large differences in microstructure and porosity and highly nonlinear temperature gradients might affect the nature of this brine exchange so that, for example, brine draining from one layer may increase the salinity of a lower layer, and (4.11) will no longer adequately describe the salinity evolution of the ice.

Nevertheless, (4.11) has proven adequate to describe brine drainage in Antarctic sea ice, regardless of ice type [*Eicken*, 1992]. Furthermore, observations of bulk salinities show little difference based on ice structure (M. O. Jeffries, unpublished data, 1995). Presumably, this is because drainage features such as brine tubes form in both granular and columnar ice. Snow ice is similar in texture to frazil ice, and it is likely that, given time, similar drainage features could form in snow ice layers. Because of the current lack of any alternative, equation (4.11) is used to describe desalination by brine drainage in snow ice as well as columnar ice.

The treatment of brine drainage in the slushy layer is another matter. Although the slush forms a porous matrix similar in structure to frazil ice, the high brine volumes make it considerably more porous than most granular ice layers. Thus in contrast to congelation and granular sea ice, all the pores are well connected, and brine drainage may be enhanced. However, unlike in congelation and granular sea ice, there is likely a great contrast between the permeability of the slushy layer and that of the ice below; consequently, transport of brine draining from the slush into the underlying ice may be impeded, as shown in the previous chapter. Furthermore, convective overturn of brine as the slush layer re-freezes may be sufficiently vigorous to affect the heat budget of the slush layer and the underlying ice. Therefore the proper treatment of brine drainage from the flooded layer would require coupling of the equations for brine drainage and heat flow [e.g., *McGuinness et al.*, 1998]. However, since proper treatment of this problem is prohibitive in a simple 1-D model, equation (4.11) is applied to the slushy layers as well. The weaknesses and consequences

of this treatment of brine drainage are discussed in detail below.

4.3.4 Flooding and brine flow

When the snow load on the ice is sufficient to depress the ice surface below sea level, there is the potential for sea water or brine to infiltrate to the ice surface and flood the base of the snow pack. This condition is met when the freeboard becomes negative. The freeboard is calculated from the equation for isostatic balance,

$$fb = \frac{(\rho_w - \rho_{si})}{\rho_w} Z_{si} - \frac{\rho_s}{\rho_w} Z_s, \tag{4.12}$$

where fb is the freeboard, ρ_w and ρ_{si} are the densities of sea water and sea ice, respectively, and Z_{si} and Z_s are the ice and snow thicknesses, respectively.

Although a negative freeboard is a necessary requirement for flooding of the ice surface, it is not a sufficient one. There must also exist pathways for brine and sea water to infiltrate from the lower ice layers and the sea below into the snow pack. In the percolation model, we require the ice to be permeable throughout its entire thickness.

Figure 4.2 shows a representation of the mechanism for brine and sea water percolation. At equilibrium the brine within the ice is at its *in situ* freezing point. If a temperature gradient exists through the ice, any transport of brine along the gradient will result in heat transfer between the brine and ice and there will be phase change. Warmer, fresher brine moving up through a brine channel in the ice, despite carrying with it sensible heat, will tend to freeze against the walls of the channel as it loses heat to the colder ice, as observed by *Niedrauer and Martin* [1979]. They observed melting on one side of the channel as cold brine descended, while warm brine moved up the other side of the channel, plating it with ice. Under the influence of a potential head (due to the depression of the ice surface below sea level), sea water will begin to move up through the ice, provided it is permeable, displacing the colder, denser brine ahead of it, and thus modifying the salinity structure of the ice. The warm brine will lose heat to the colder, surrounding ice, freezing against the walls of the conduits and concentrating the brine. This freezing will restrict the fluid pathways, perhaps even closing them off, thus reducing the permeability of the ice. The release of latent heat will warm the ice adjacent to the channel, and heat will flow laterally

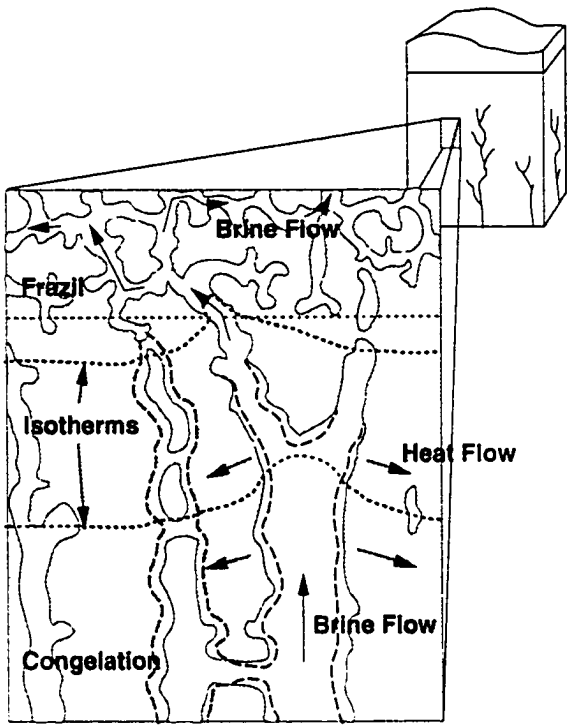

Figure 4.2: Brine percolation in porous sea ice. During upward flow of brine, the isotherms (dotted lines) are displaced vertically, and there is heat flow from the brine channel to the ice and isolated pores. This causes freezing and narrowing of the channel and a corresponding enlargement of the unconnected pores, indicated by the dashed lines.

along the temperature gradients (Figure 4.2). This heat transfer will warm the isolated brine pockets which, in turn, will grow in size by self-dilution, and they may coalesce and form additional hydraulic pathways. In this way the porosity and permeability of the ice are closely coupled with the flow itself. It should be stressed that while the influx of warm brine will tend to warm the ice and increase the brine volume, the infiltrating sea water is at its *in situ* freezing point. The only way it can transfer heat to warm the ice is by partially freezing. Then the overall effect will be to reduce the brine volume.

Obviously, solving the equations of fluid flow for such a complicated and essentially unknowable geometry is impossible. However, the average macroscopic flow may be de-

scribed using Darcy's law [*Bear*, 1972]

$$u = -\frac{K}{\mu}(\nabla P + \rho_b g), \tag{4.13}$$

where u is the area-averaged fluid velocity, which is related to the pore fluid velocity by

$$u = \phi u_p, \tag{4.14}$$

K is the intrinsic permeability, μ is the fluid viscosity, and ∇P is the pressure gradient due to the depression of the ice surface below sea level. Then, brine and salt transport may be expressed as

$$\begin{aligned} \frac{dM_b}{dt} &= \frac{d}{dz}(u\rho_b), \\ \frac{dM_s}{dt} &= \frac{d}{dz}(u\rho_b S_b), \end{aligned} \tag{4.15}$$

where M_b and M_s are the masses per unit volume of brine and salt, respectively, ρ_b is the brine density, and S_b is the brine salinity. In this way we need not know any details of the flow geometry provided we have a suitable method for estimating the permeability, assuming that the flow is homogeneous when averaged over a sufficiently large area.

Estimates for the permeability of sea ice are scarce. *Ono and Kasai* [1985] measured permeability in natural sea ice and observed a curious anisotropy in measured upward and downward permeabilities. This may be due to effects of the flow on the porosity; however, the results are the reverse of that expected. Unfortunately, they did not report brine volumes, and so any correlation between permeability and porosity is impossible to determine. *Saito and Ono* [1978] also did not report brine volumes; however, they may be crudely estimated based on the conditions under which the ice was grown. Figure 4.3 shows a plot of permeability measurements from several authors plotted against estimated brine volumes. The solid line shows a least squares third-order polynomial fit to the log transform of the data which were used to determine the permeability in the model. Note that only the data shown for the studies by *Saeki et al.* [1986] and *Kuroiwa* [1968] were used for the fit, as only these studies reported porosities. The brine volumes for the other two studies were estimated from the reported growth conditions and are shown only for

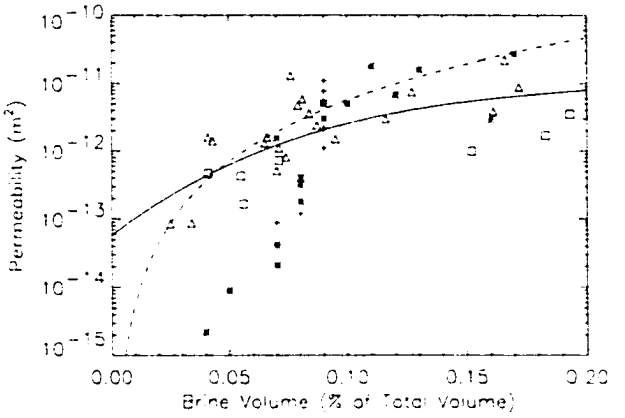

Figure 4.3: Permeability of sea ice. Data are from the following sources: asterisks, *Ono and Kasai* [1985]; triangles, *Saeki et al.* [1986]; pluses, *Saito and Ono* [1978]; and squares, *Kuroiwa* [1968]. The data from Kuroiwa are for artificially compressed snow. The solid line represents a best fit to the data. The dashed line is a fit of the Kozeny-Carman equation for a grain size of 1 mm [*Bear*, 1972].

reference. The most common parameterization relating porosity and permeability is the Kozeny-Carman equation [*Bear*, 1972],

$$K = \frac{d^2}{180}\frac{v_b^3}{(1-v_b^2)}, \tag{4.16}$$

where d is a representative grain size. This may not be valid for columnar ice, in which the permeability may be controlled by vertical drainage tubes, but may be reasonable for granular ice which is the controlling factor for the overall ice permeability since it will generally be present in the upper portions of an ice floe. The Kozeny-Carman relation for a grain size of 1 mm is shown in Figure 4.3 as a dashed line for comparison. There are pitfalls with this approach in that permeability is likely to be dependent not only on the porosity, but also on the thermal and brine flow history of the ice.

In light of the uncertainty in the brine percolation process, we explore two possibilities: (1) a standard model, where brine advection in the ice is governed by (4.13) and (4.15), and (2) a simple model, where flooding takes place by direct infiltration of sea water into the snow pack, and (4.15) is not used (there is no internal displacement of brine within the ice). To retain consistency, (4.13) is still used to determine the infiltration rate. In

the standard model, the bulk of the pore space is effectively connected, so, as the brine is advected upward, the higher-salinity brine ahead of it is flushed from the ice. This implies that the ice is reasonably horizontally homogeneous, so that the flow is essentially uniformly distributed throughout the ice sheet when averaged over a sufficiently large area. In the simple model, brine within the sea ice is isolated from the network of pathways through which flooding takes place, so there is no advection of brine or heat through the ice sheet. This would be the case if the flow was confined to only very localized areas, such as through cracks, or isolated tubes, and then spread laterally at the surface. These two regimes may be viewed as the end-members of the percolation model where the amount of pore space that is effectively connected varies from 100% to essentially 0%. Measurements by *Weissenberger et al.* [1992] indicate that approximately 80% of the pore volume is hydraulically connected for temperatures typical of the simulations presented here.

In the standard model, local thermodynamic equilibrium is assumed for the sea ice so that lateral heat flow from pore to pore is rapid enough to remove the horizontal temperature gradient due to flow (see Figure 4.2) during each time step. All the brine within a horizontal layer is then effectively of the same salinity. This means that the degree of connectivity is unimportant in the standard model, as the amount of salt transported with the brine is independent of the geometry of the flow. Consequently, brine volumes after a flow event will be the same regardless of the effective porosity. If the flow is restricted spatially, such as in isolated drainage tubes, the fluid pore velocity is proportionately higher, and horizontal temperature gradients will exist. In this case, brine salinities in the bulk of the pore space remain higher than those in the pore space in which most of the flow is taking place, and less salt is flushed from the ice. The simple model is the extreme case of this regime. This implies that the percolation threshold (and the permeability) will likely not be solely a function of brine volume, but will be time dependent, depending on the evolving pore geometry. In this study, however, the critical porosity for percolation is assumed to be constant at 5%.

As the flooded layer freezes, compositional (salinity) and temperature gradients may exist within the slush. Freezing may then occur over the entire thickness of the slush as it solidifies. This is akin to the so-called "mushy layer" problem that has received much

attention in metallurgy [e.g., *Worster*, 1986]. As the brine freezes, it rejects salt into the melt, thus concentrating the brine and allowing the slush to cool further, so that the temperature gradient propagates down through the slush and underlying ice, solidifying the slush throughout its thickness. Observations indicate, however, that convection of brine as the slush freezes is quite vigourous [*Lytle and Ackley*, 1996; *Hudier et al.*, 1995]. This is supported by the results of the 2-D model presented in chapter 3. In this paper we assume that the salt rejected during freezing drains quickly, so that the brine salinity at the freezing interface remains constant, as is the case at the ice/ocean interface. Therefore the temperature of the slush and ice is held constant by the eutectic condition until the entire slush layer freezes. The freezing interface is defined across a layer of finite thickness at the top of the slush layer. When this uppermost layer of slush reaches a solid fraction of 0.6, it is assumed to be frozen, and the freezing interface is moved down to the next layer. Note that this does not imply that the slush and underlying ice temperatures and brine salinities are those of the underlying sea water, but rather that they are determined by the upward transport of heat and salt during the flooding event, as indicated by (4.13) and (4.15). This can lead to very high salinities in the flooded layer, as has been observed in the field [*Sturm et al.*, 1998].

4.3.5 Numerical solution

The system of equations (4.1), (4.3), and (4.13) and (4.15) are solved using a finite volume method [e.g., *Patankar*, 1980], so that the quantities of interest (masses of salt, brine, and ice) are conserved. Although this essentially reduces to a finite difference method, mass of brine and mass of salt are the primary variables, rather than salinity. Equation (4.1) is solved using a semi-implicit scheme similar to that of *Goodrich* [1978] and *Wade* [1993]. Equation (4.15) is solved using a first-order upwind scheme. Layer thickness is nominally set to 2 cm. The bottom ice layer is of variable thickness so that the growth interface is tracked continuously. The snow layer thicknesses are also variable to accommodate densification. For each time step the brine velocity is determined first from (4.13). Then the energy equation, (4.1), is solved, and the mass transfers of salt and brine are calculated from (4.15). Next, the change in salt content due to brine drainage and expulsion is computed. There is assumed to be no brine drainage during a flooding event.

The masses of ice and brine are then updated for each layer based on the temperature and salinity following *Cox and Weeks* [1975]. In this way the equations for heat and mass transfer are decoupled and can be calculated independently for each time step. A time step of 0.5 hours is used when there is no upward brine flow and is reduced accordingly when there is brine flow. Verification of the solution technique by comparison of a simplified model with the analytic solution to the Stefan problem [*Hill*, 1987] showed agreement to within less than one layer thickness (¡ 2 cm).

Air temperature forcing fields were taken from automatic weather station data for Possession Island (71.9°W, 171.1°E). This was deemed the most representative and reliable data set for the region of interest that was continuous over the study period (April - November 1995) and most likely represents typical values for the region of the Ross Sea for which field measurements were taken [see *Jeffries et al.*, 1998a]. Although this station is quite close to the continent, and may not be truly representative of the ocean regions, temperatures were in good agreement with shipboard observations (Figure 4.4). Snow accumulation was estimated using National Centers for Environmental Prediction (NCEP) reanalysis precipitation rates, for the same time period and approximate location (71.4°S, 180°E). The total accumulation was scaled to give a yearly total of 400 mm, water equivalent, based on estimated precipitation rates for the Ross Sea [*Giovinetto et al.*, 1992]. The wind speed was set to 10 m s^{-1}. The effects of variation in the climatic forcing are discussed below. Simulations were run for climatic conditions for 1995, so that the results might be compared to field data from one autumn and one winter cruise in the Ross Sea in 1995 aboard the R/V *Nathaniel B. Palmer.*

4.4 Results

4.4.1 Flooding and snow ice formation

Figure 4.5 illustrates model results for both the standard model (Figure 4.5a) and the simple model (Figure 4.5b) for ice growth initiating on May 1 (Julian day 121). Ice growth is initially very rapid, with thicknesses approaching 40 cm within a few days. Once a snow cover has developed, however, little congelation ice is added throughout the growth season. This is particularly true for the standard model, which produces only 6 cm of congelation

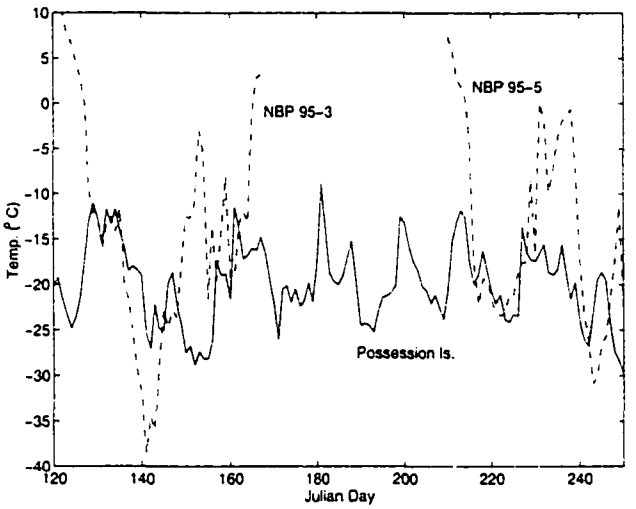

Figure 4.4: Winter Ross Sea air temperatures. Observed air temperatures in 1995 are shown along with automatic weather station data for Possession Island (71.9°W, 171.1°E). Vertical lines indicate days of closest approach of the ship to Possession Island.

ice during the last 5 months of growth, for a total of 52 cm. During the period of flooding and snow ice formation, approximately 4 cm of ice is melted from the bottom before the temperature gradient is reestablished. In the simple model, there is very little bottom melting; however, repeated flooding events keep the ice warm, preventing any substantial congelation ice growth.

Brine volumes are consistently above the critical value of 5% for the early stages of growth, except for a brief interval before significant snow accumulation. This is primarily due to the insulation provided by the snow cover, which maintains the ice at quite high temperatures. The average snow/ice interface temperature for the simulation in Figure 4.5a was -4.3°C. This is much higher than the average observed value of -9.8°C (M. O. Jeffries, unpublished data, 1995), in part due to the relatively thin ice (mean, 53 cm, of which 5 cm was snow ice) and deep snow (mean, 32 cm). The simple model produced more typical values of snow and ice thickness, with a mean ice thickness of 66 cm, including 17 cm of snow ice and mean snow depth of 22 cm. However, the average interface temperature was still quite warm (-4.4°C). For comparison, the mean ice thickness from the two winter cruises was 64 cm, with a mean snow ice thickness of 17 cm. Snow depths averaged 16 cm.

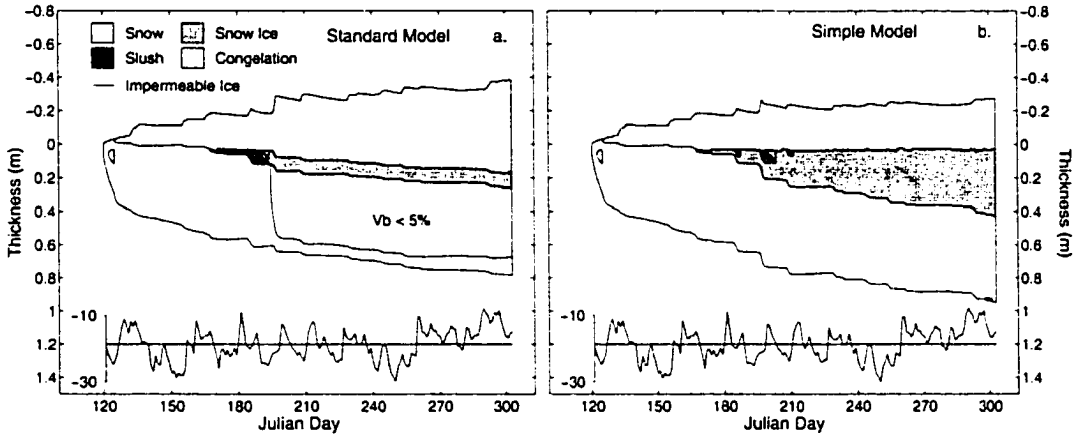

Figure 4.5: Simulated ice growth time series. (a) Standard model, including internal brine flow in the ice. (b) Simple model, without internal brine flow. The region of impermeable ice is indicated by the solid contours within the congelation ice layer. Depth is relative to sea level. Also shown is a trace of the air temperature (°C) record from AWS98495 (Possession Island).

The process of flooding and snow ice formation produces quite different results for the two regimes. First, in the standard model, after the initial flooding the slush layer persists for several days before freezing. The rate of freeze-up is very slow, since unless a cold front moves down through the ice, the brine salinity must be decreased by brine drainage for freezing to occur. In the simple model, freeze-up of slush is quite rapid, owing to the relatively low salinity of the incoming sea water. Some of this sea water is frozen initially upon contact with the cold snow, and as the temperature gradient is reestablished through the ice and snow after flooding, the low-salinity slush freezes quite readily. As a result, a slush layer rarely exists.

In terms of mass balance, the difference between the two flooding regimes is quite important. First, in the standard model, upward flow of brine through the porous brine network in the ice flushes more saline brine up onto the ice surface, replacing it with warmer, less saline brine. As the flooded layer freezes and the ice below cools again, the brine volume is correspondingly decreased, as shown by the impermeable layer in Figure 4.5a (see also Figure 4.6d). On day 195 the brine volumes in the congelation ice drop below the assumed critical value for permeability of 5% and remain below this value throughout the bulk of the congelation ice for the remainder of the simulation. Therefore despite

a negative freeboard, no further flooding or snow ice formation occurs. In contrast, in the simple model, where there is no upward flushing of brine, the brine volumes in the lower ice layers remain above the critical value for most of the simulation period, allowing repeated flooding and greater snow ice formation.

4.4.2 Salinity and brine volume

The effects on salinity and brine volume are more readily seen in Figure 4.6, which illustrates the vertical salinity profile for the standard and simple models. For comparison, three salinity profiles taken from ice cores sampled during the two cruises aboard the R/V *Nathaniel B. Palmer* in 1995 [*Jeffries et al.*, 1998a] are shown in Figure 4.6c. The profiles are taken from cores sampled on Julian days 157, 218, and 227. They were chosen because they consisted of a single layer of congelation ice topped with one or more layers of granular ice that can reliably be assumed to be snow ice due to their highly negative $\delta^{18}O$ values [*Jeffries and Adolphs*, 1997]. We can therefore expect that these cores experienced growth processes comparable to those in the simulations.

In Figures 4.6a and 4.6b we see that the profiles are generally S-shaped or slightly C-shaped [*Eicken*, 1992]. Brine drainage is quite efficient, and salinities decrease to below 5‰ in the lower portions of the ice before flooding occurs (day 165). This is due primarily to the insulating effect of the snow cover, which warms the ice and maintains high brine volumes even for low-salinity ice. This allows for efficient brine drainage, according to 4.11, despite small temperature gradients. As brine drainage will continue as long as brine volumes are greater than the threshold value of 5%, there will be brine drainage even for quite low salinities in warm ice. While low salinities are observed in ice cores [e.g., *Maksym and Jeffries*, 1996, Figure 1c], values below 3‰ are rare. In the standard model simulations, salinities in the lower portions of the ice are consistently below 3‰, largely because of the anomalously warm ice. In the standard model, there is a substantial drop in salinity during the main flooding event, as illustrated by the difference between profiles at day 165, before any flooding, and day 175, after the first flooding event. There is a drop in salinity throughout the entire ice thickness, but it is most pronounced at the top of the congelation ice layer, where the effects of upward brine flushing are greatest. After freeze-up of the flooded layer (day 195), a pronounced "knee" is evident in the salinity

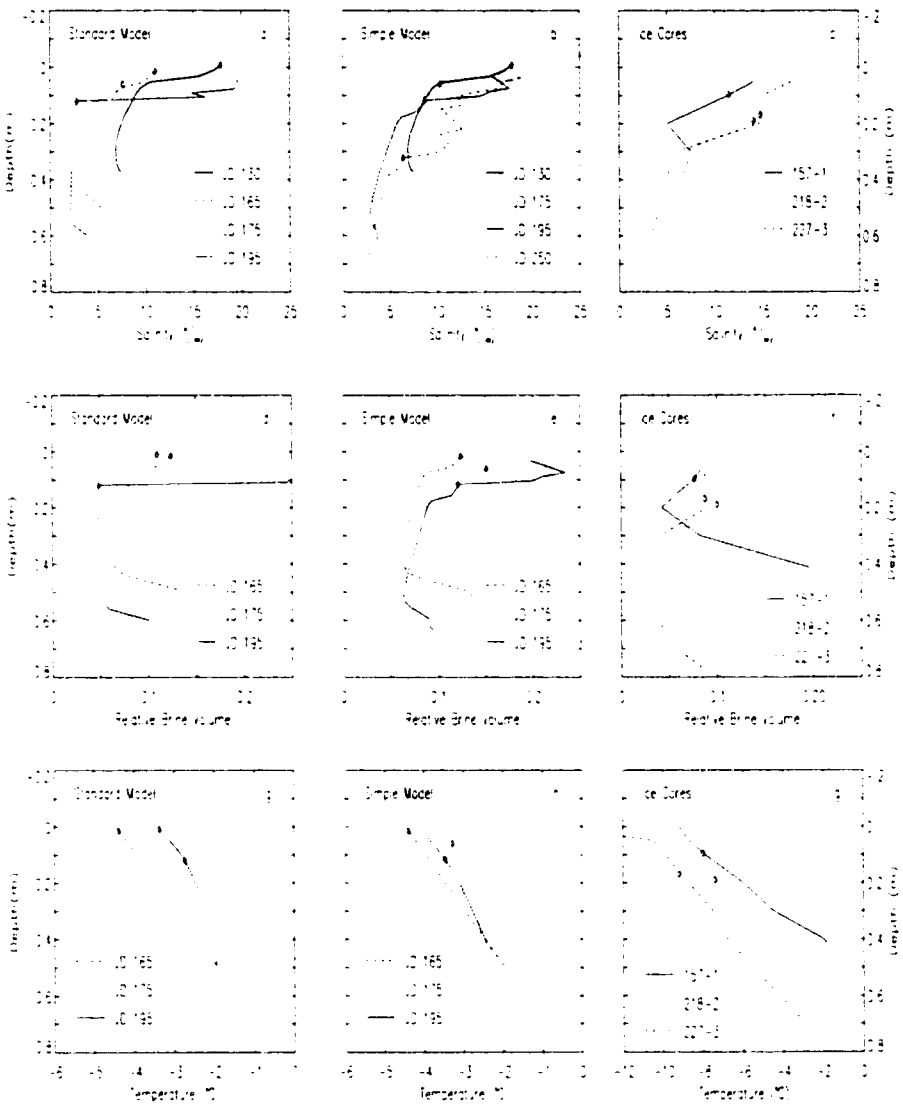

Figure 4.6: Salinity, brine volume, and temperature profiles. Vertical profiles are shown for the standard model (Figures 4.6a, 4.6d, and 4.6g respectively), simple model (Figures 4.6b, 4.6e, and 4.6h), and selected ice cores (Figures 4.6c, 4.6f, and 4.6i). Simulation results are shown for several different dates, as indicated by Julian day (JD), to show ice properties before and after major flooding events (refer to Figure 4.5). Core data (Figures 4.6c, 4.6f, and 4.6i) labels indicate date of sampling and identification number of core taken on that date. The depth scale is relative to the ice surface. The congelation/snow ice interface is indicated on each profile by the open diamond.

profiles between the congelation and snow ice layers, with very high salinities in the snow ice layer (15-20‰), and quite low (~3‰), nearly uniform salinities in the congelation layers. There is little change in the salinity after day 195, when freeze-up is complete, and the ice remains impermeable. The simple model shows similar salinities in the snow ice layers (approximately 15-17‰). However, the congelation ice layers show little change in salinity after flooding due to the lack of upward flushing. Brine drainage from these layers is reduced as the brine volumes approach the critical cutoff value of 5% (Figure 4.6e). Salinities at the base of the ice decrease primarily because of reduced ice growth rates, so initial brine entrapment is reduced [*Cox and Weeks*, 1988]. The salinity profiles from the simple model provide a closer match to the field data in Figure 4.6c in terms of overall shape and salinity in the lower portions of the ice.

Brine volumes for the standard model, simple model, and field data are presented in Figures 4.6d, 4.6e, and 4.6f, respectively. Figure 4.6d shows brine volumes just prior to flooding (day 165), after flooding (day 175), and after freeze-up and cooling (day 195). After the flooding event there is a slight decrease in brine volume in the lower congelation ice layers, despite the warming of the ice. This is caused by heat conduction maintaining a slight temperature gradient through the ice even as the brine moves upward, cooling this brine as it moves, causing some of it to freeze. After the ice is allowed to cool again and the temperature gradient is fully restored, brine volumes are significantly reduced (day 195). Note that brine volumes drop to well below the critical value for permeable ice (5%) despite the ice being very warm (> -4°C). This means that the ice is unlikely to become permeable again even with warmer air temperatures, unless the salinity is increased in some way. The enhanced reduction in brine volume at the top of the congelation ice layer is caused by flushing of brine from this ice combined with significant warming of the ice during flooding. Once the ice cools again, it is the ice at the top which cools the most, producing very low brine volumes. This produces the curious result that some of the lowest brine volumes in the ice often occur immediately adjacent to some of the highest.

In Figure 4.6e, for the simple model, there is no brine flushing. As the ice is warmed during a flooding event, brine volumes are increased, especially near the ice surface. High brine volumes are maintained throughout the growth season in part because repeated flooding events continually warm the ice surface. Both models have very high brine vol-

umes in the snow ice layers (approximately 15-25% for the simple model, 20-35% for the standard model). Neither model matches the field data particularly well (Figure 4.6f). This is due to the much colder temperatures of the ice cores (compare Figures 4.6g and 4.6h with Figure 4.6i). The average ice surface temperature for the three selected cores chosen was -10.4°C, whereas ice surface temperatures averaged only -4.3°C and -4.4°C for the standard and simple models, respectively.

4.4.3 Effect of initial ice formation date

The effects of varying the initial ice formation dates, and thus duration of ice growth, are illustrated in Figure 4.7. The total amount of each type of ice present at the end of the simulation (Julian day 304) is presented. The mean values in Figure 4.7a and 4.7b are the thicknesses of each ice type averaged over the entire growth period and over each start date. Note that this differs from the mean values at the end of the simulation. Also shown are the mean thicknesses of ice from all ice cores sampled in the Ross Sea during the two cruises aboard the R/V *Nathaniel B. Palmer* in 1995. Note that for these data, frazil and congelation ice are combined and represented as congelation only. Figure 4.7a shows results for the standard model, and Figure 4.7b shows those for the simple model. For both flow regimes the amount of congelation ice is almost completely independent of initial freezing start date, despite a sevenfold variation in the duration of ice growth. This reflects the fact that initial congelation growth is quite rapid, but once a significant snow cover forms, congelation growth becomes a very slow process, or there may actually be melting from the ice bottom, as is the case in many of the standard model simulations. Once the ice has thickened to approximately 40 cm, the bulk of any further ice thickening is by snow ice development. This value is obviously a function of the climatic forcing, however, and is discussed below.

For the simple model, there is an obvious decrease in total ice thickness as a function of start date. Brine volumes are consistently above the critical value of 5%, and freezing of the slush is quite rapid; hence snow ice develops readily as more snow accumulates. As the ice is generally permeable, snow ice formation is primarily a function of total snow accumulation. In general, there will be more snow ice the longer the growth period. In contrast, the amount of snow ice formed by the standard model does not necessarily

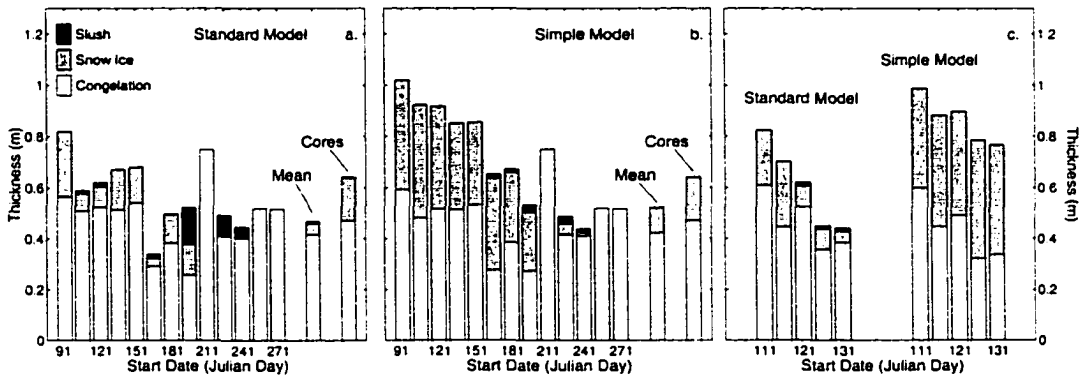

Figure 4.7: Ice thicknesses as a function of freezing onset date. Congelation ice, snow ice, and slush thicknesses at the end of the simulation for (a) standard model, (b) simple model, and (c) both models with a narrow range of start dates. Climatic forcing is the same as for Figure 4.5. The bars labeled "mean" are the mean simulation thicknesses for all simulations. The bars labeled "cores" are the mean thicknesses from field data.

reflect the length of the growth period. It reflects the dependence of snow ice development on the timing of the flooding event. An early flooding event may flush enough brine from the lower ice layers to render the ice impermeable after the temperature gradient is reestablished, thus inhibiting further flooding. The low quantities of snow ice for later start dates merely reflect low total snow accumulation.

Mean quantities of congelation ice produced in the simulations compare fairly well with observed values (mean snow, snow ice, and congelation ice thicknesses were 20 cm, 4 cm, and 42 cm, respectively, for the standard model, and 16 cm, 42 cm, and 10 cm respectively for the simple model). The mean quantities of snow ice produced by the simulations are, however, less than those observed, considerably so for the standard model. Caution must be exercised in comparisons with field data due to the uncertainty in actual growth conditions and since the sampled ice was subjected to substantial dynamic forcing, which is not accounted for in the model. Although the majority of the ice cores were taken from level ice areas, most consisted of multiple layers [*Jeffries and Adolphs*, 1997], which we attribute primarily to rafting events. While this will make the ice thicker than would otherwise occur for purely thermodynamic growth, we note that most of the rafting events occurred when the ice is relatively thin and such events are rare when the ice is thicker than 40 cm [*Worby et al.*, 1996; *Jeffries and Adolphs*, 1997; *Jeffries et al.*, 1997]. As the

simulated ice reaches this thickness very rapidly, the effects of rafting may be relatively minor in determining the long-term thickness of the ice.

The results of simulations run with a narrow range of start dates for both models are shown in Figure 4.7c. Results are shown for five simulations with ice growth initiated at 5 day intervals. Despite such a narrow range the standard model showed as much variation for both congelation and snow ice layer thickness as for the much broader distribution in Figure 4.7a. The simple model displayed similar variations in the congelation layer thicknesses, but the final snow ice layer thickness remains nearly constant, regardless of start date. This demonstrates that congelation ice thickness is strongly dependent on conditions during the early stages of growth. Snow ice thickness for the flow regime including upward brine flushing is dependent on the timing of flooding, whereas for the simple flow regime it is primarily dependent only on the rate of snow accumulation.

4.4.4 Sensitivity to climatic forcing

The importance of the nature of the flooding regime is illustrated well by the response of the two models to variation in climatic forcing. Figure 4.8 shows results for both flow regimes for various climatic conditions. Simulated ice thicknesses are shown for the same growth conditions as in the previous sections, but with variations in mean temperature (Figures 4.8a and 4.8b, standard model) and in accumulation rate (Figures 4.8c and 4.8d, simple model). These variations represent the typical range of climatic conditions found in the Ross Sea, with the lower temperatures being typical winter averages observed close to the Ross Ice Shelf, and the higher temperatures being typical temperatures near the outer edge of the pack. Accumulation rates are varied between 300 and 700 kg m^{-2} yr^{-1}, the expected range for the Ross Sea [*Giovinetto et al.*, 1992].

The simple model behaves much as we might expect; increasing the mean air temperature indirectly increases the amount of snow ice formed by controlling the amount of congelation growth, with lower growth rates for higher air temperatures (Figure 4.8b). As the thinner ice provides less buoyancy, the accumulated snow will depress the ice surface further below sea level and therefore produce more flooding and snow ice formation. For increasing snow accumulation rates (Figure 4.8d) there is a fairly linear increase in snow ice thickness for the simple model. Accumulation rate has a stronger effect on snow ice

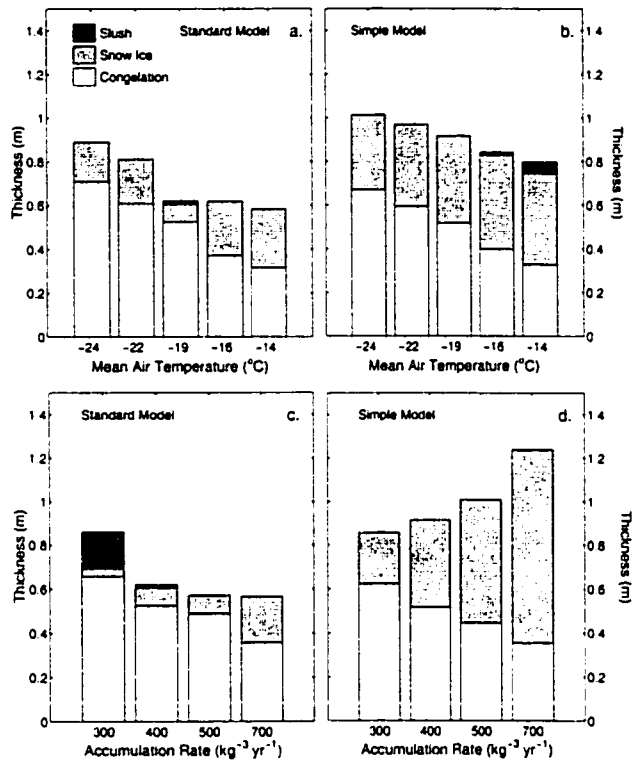

Figure 4.8: Snow ice thickness response to meteorological forcing. Dependence on temperature for (a) the standard model and (b) the simple model, and dependence on accumulation rate for (c) the standard model and (d) the simple model.

thickness than does air temperature, as it more directly controls the freeboard. Congelation ice thicknesses decrease steadily with increasing accumulation rate due to bottom melting. The ice is warmed both by the insulation from the snow cover and through the transport of heat to the snow/ice interface during flooding. This leads to an increase in bottom melting rates.

The situation for the standard model is quite different (Figures 4.8a and 4.8b). As before, the amount of snow ice formed is limited by the permeability of the ice. The upward flow of brine reduces the salinity in the lower portions of the ice and results in reduced brine volumes. Once a significant amount of flushing has occurred, the brine volumes are often reduced sufficiently below the critical value for percolation that the ice remains impermeable even with substantial warming. Figure 4.8a reflects this, with little dependence of snow ice thickness on temperature.

There is only moderate dependence of the snow ice thickness on accumulation rate in the standard model, since the ice becomes impermeable after the first or second flooding event, so there is no flooding with subsequent snowfall. The thick slush layer for the lowest accumulation rate (300 kg m^{-2} yr^{-1}) occurred at the very end of the growth period, when brine volumes increased due to warmer temperatures. This was only possible because the small degree of flushing that had occurred did not reduce ice salinities, and hence ice brine volumes, as severely as in the other cases. The dramatic differences between the simple model and the standard model show clearly the importance of brine transport processes in controlling flooding and snow ice formation.

In addition to air temperature and snow accumulation rate, ice growth and development is influenced by the oceanic heat flux. This is largely an unknown quantity, but it has been shown to have great variability in the Southern Ocean. In the Weddell Sea, winter estimates range from around 2 W m^{-2} along the continental shelf [*McPhee et al.*, 1992] to as much as 40 W m^{-2} [*Gordon and Huber*, 1990] in the eastern Weddell Sea. *Heil et al.* [1996] estimated the range to be 6-18 W m^{-2} in the east Antarctic. It has been suggested that the oceanic heat flux may be a significant controlling factor in ice development in the Ross Sea [*Jeffries and Adolphs*, 1997].

Figure 4.9 shows the effect of variations in ocean heat flux on both the standard and simple models. Other simulation parameters are the same as those in Figure 4.5. For both models the main effect is to cause an overall thinning of the total ice thickness and an increase in snow ice thickness for increasing ocean heat flux. With brine flushing included (Figures 4.9a and 4.9c) we again see low brine volumes throughout much of the ice thickness soon after substantial flooding and snow ice formation has occurred. This impermeable ice persists despite a warming of the ice with increased snow accumulation, so there is only modest dependence of snow ice thickness on ocean heat flux. Note that there is not necessarily a direct relationship between snow ice production and ocean heat flux, as less snow ice was produced in the run shown in Figure 4.5a, for an oceanic heat flux of 5 W m^{-2}, than for either 0 or 10 W m^{-2} (Figures 4.9a and 4.9c, respectively). The impermeable ice, however, allows a thick snow cover to develop without flooding. This insulates the ice and permits significant ablation from the base for the case of a high oceanic heat flux (Figure 4.9c).

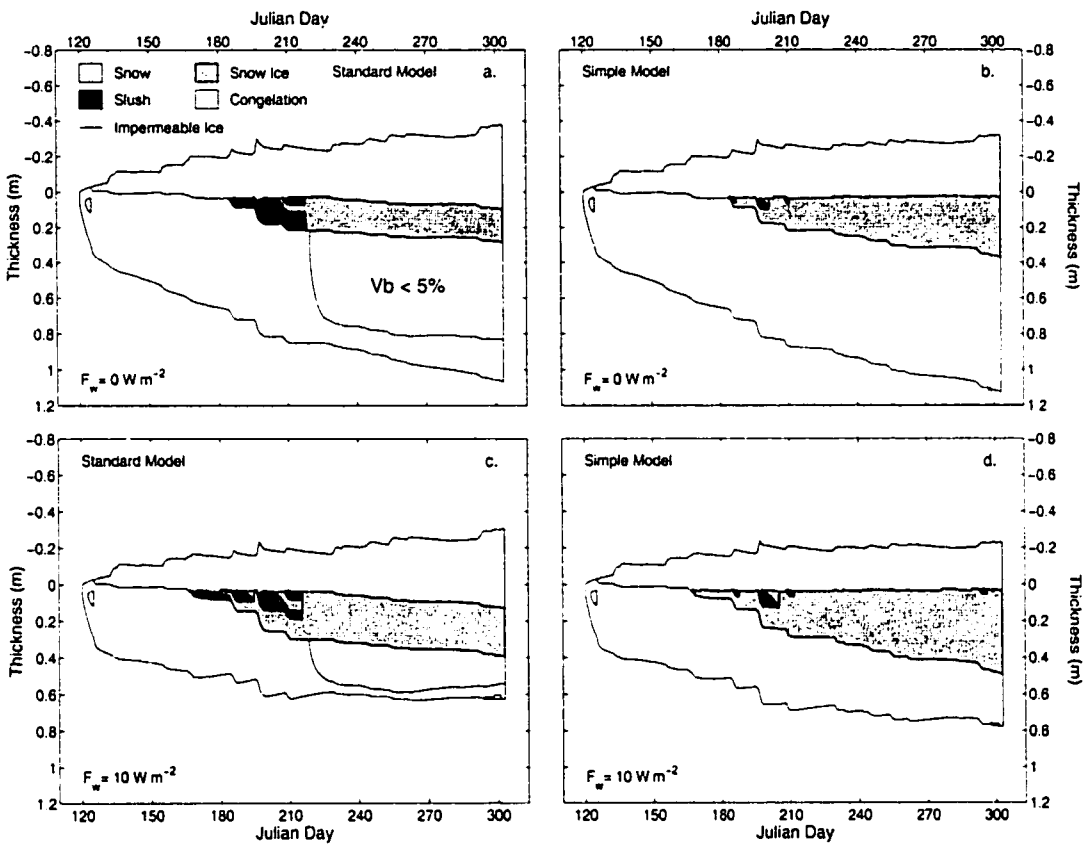

Figure 4.9: Effects of ocean heat flux. $F_w = 0$ W m^{-2} for (a) the standard model and (b) the simple model. $F_w = 10$ W m^{-2} for (c) the standard model and (d) the simple model. In Figure 4.5, $F_w = 5$ W m^{-2}.

Without brine flushing (Figures 4.9b and 4.9d), the main effect of the higher ocean heat flux is to slow congelation ice growth and even to promote basal melting. This amplifies the snow load, permitting increased flooding and snow ice development.

4.4.5 Effects of brine flow regime

As the conditions necessary for flow exhibit a critical behavior, in that the brine volume must be above a threshold value for flooding to occur, subtle influences on brine volume may have quite substantial effects. Variations in the nature of brine transport are quite important in controlling the mass balance, as shown above by the profound effects of brine flushing. However, the precise nature of this brine percolation, if indeed it even takes place, is largely unknown. For example, Figure 4.3 shows that the permeability of sea ice is not a well-defined quantity. Figure 4.10 shows the effects of variations in ice permeability, for three different dates of initial ice formation. Final ice thicknesses are shown for three regimes: the standard permeability, K, defined by the fit to the data from Figure 4.3, and a low- and a high-permeability regime, assigned permeabilities of $0.1K$ and $10K$, respectively, for the same brine volumes. Other parameters are the same as the simulation shown in Figure 4.5a. Contrary to what we might expect, there is a decrease in the amount of snow ice formed using the higher permeability. Flooding and re-freezing tends to occur in one major event, typically lasting several hours to a day, after which brine volumes in the lower portions of the ice are greatly reduced, usually rendering the ice impermeable for the remainder of the growth season. In this case the ice is permeable enough that the duration of the flooding event is governed by the rate of snow accumulation. In the case of low permeability, the flow velocity is so slow that the flooding is sustained over a period of many days, so that subsequent snow accumulation causes flooding events to overlap one another, and a continuous slow percolation of brine occurs. This provides a continual flux of heat to the ice and the slush, delaying the freezing of the flooded layer and thereby keeping the ice permeable. This sustained flooding increases the upward flushing of the brine network, so that despite the warming provided by the brine flow, enough salt is eventually flushed from the ice to reduce brine volumes below the percolation threshold. This prevents any further drainage of salt from the slushy layer, so it becomes much more difficult to freeze. As a result, in all three simulations shown

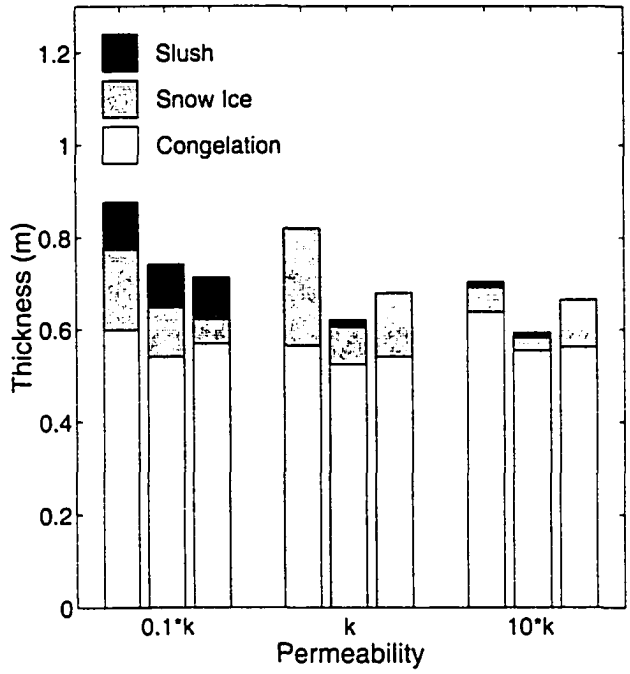

Figure 4.10: Effects of permeability. Thicknesses of congelation ice, snow ice, and slush for the standard model for variations in ice permeability. Standard permeability, K, is given by the fit in Figure 4.3. The high-permeability plot represents a tenfold increase in permeability; the low-permeability represents a tenfold decrease in permeability. Results for each permeability are shown for three different dates of initial ice formation (from left to right, Julian days 91, 121, and 151).

in Figure 4.10 for the low-permeability case, the flooded layer never completely freezes, even though it generally exists for 90 days or more. In the simulations using the higher permeability, flooding and subsequent re-freezing is relatively rapid (typically a few days). This allows temperature gradients to reestablish quickly after flooding, reducing brine volumes to below the percolation threshold. Hence we see very little snow ice formed in this regime.

It is evident that the nature of the processes involved in brine transport are vital in controlling both the timing and magnitude of flooding and snow ice formation. At this point, it would be prudent to examine the assumptions used in formulating the standard model. To this end we examine the effects of the convective exchange of brine during the freezing of the flooded layer. In Figure 4.11 we examine two cases: (1) Heat flux due to

convective overturn of brine from the flooded layer to the ocean below is neglected, which permits temperature gradients to propagate through the ice when a flooded layer is present (equivalent to treating the brine in the flooded layer in the same way thermodynamically as liquid inclusions in the ice below); and (2) salt drained from the slush is redistributed evenly among the ice layers below during freeze-up. This provides an estimate of the effects of possible salination of the ice from salt redistribution in maintaining ice permeability and allows an assessment of the effect of the limitations of equation (4.11) on the results.

Results are shown in Figure 4.11 for three different regimes: excluding convection (Fig-

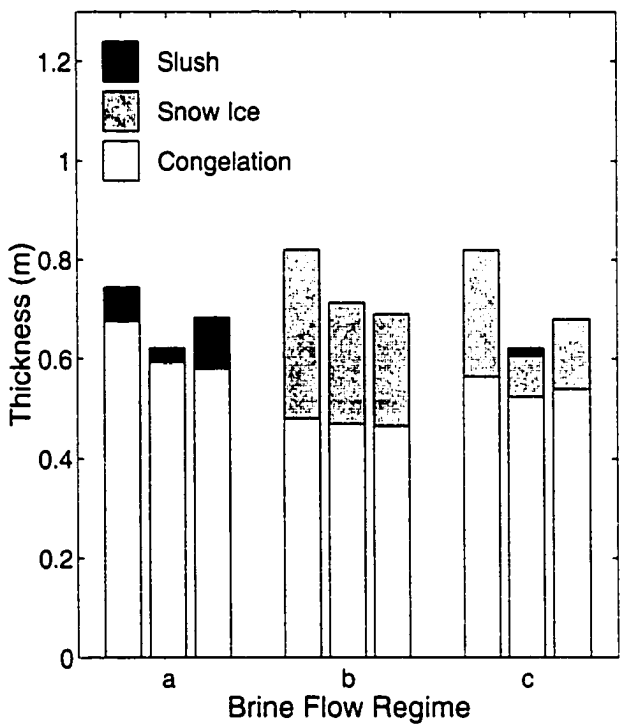

Figure 4.11: Effects of brine convection. Thicknesses of congelation ice, snow ice, and slush at the end of the simulation period for different parameterizations of the brine exchange between the slush and underlying ice: no convection between slush and ice (bars marked "a"), redistribution of brine drained from slush to the ice (bars marked "b"), and standard model (bars marked "c"). Results for each case are shown for three different dates of initial ice formation (from left to right, Julian days 91, 121, and 151).

ure 4.11a), including salt redistribution (Figure 4.11b), and the standard model (Figure 4.11c). Without convection, upward flushing of brine during flooding is very effective, so

that the ice becomes impermeable once the thermal gradient is reestablished. This leaves a thin, saline (30-40‰) slush at the base of the snow cover that cannot freeze without drainage of brine or a severe drop in air temperatures. As a result, without convection of brine, the standard model will rarely produce any snow ice at all. With salt redistribution included, the salt transferred from the slush layer to the ice increases the ice salinity somewhat, maintaining the porosity above the percolation threshold longer than for the standard model, allowing increased flooding. However, brine flushing is still a very effective process in reducing the ice salinity, so that the ice still becomes impermeable, and only a moderate increase in snow ice production occurs.

4.4.6 Sensitivity to snow thermal conductivity

It was noted above that the ice in the simulations was markedly warmer than is typically observed. While this is in part due to fairly thin ice and thick snow cover, this cannot account for all of the difference. We attribute this partly to the low snow thermal conductivity given by (4.8). *Yen* [1981] gives a relation for k_{sn} that fits the data a of number of investigators (included in the "others" data of *Sturm et al.* [1997]):

$$k_{sn} = 4.9211 \times 10^{-6} {\rho_{sn}}^{1.885}. \tag{4.17}$$

Simulated ice thicknesses were about typically 10 cm thicker than they were using the lower snow thermal conductivity since (4.17) gives thermal conductivities about 60% greater than (4.8) (Figure 4.12). For both models, the higher thermal conductivity allows more congelation growth once a snow cover develops because of an increased conductive heat flux. This reduces the relative snow load, delaying the initial date of flooding by several days to over a month. Consequently, less snow ice is produced. Once snow ice production begins, further congelation ice growth is minimal, amounting to only a few millimeters per day. Again, the standard model produces little snow ice due to the effects of brine flushing.

Simulated snow and ice thicknesses best match the data using (4.17), with the simple model producing the better fit. Results compare very well to the observations if a $\delta^{18}O$ criterion of -2‰ for snow ice identification is used. However, as noted above, a

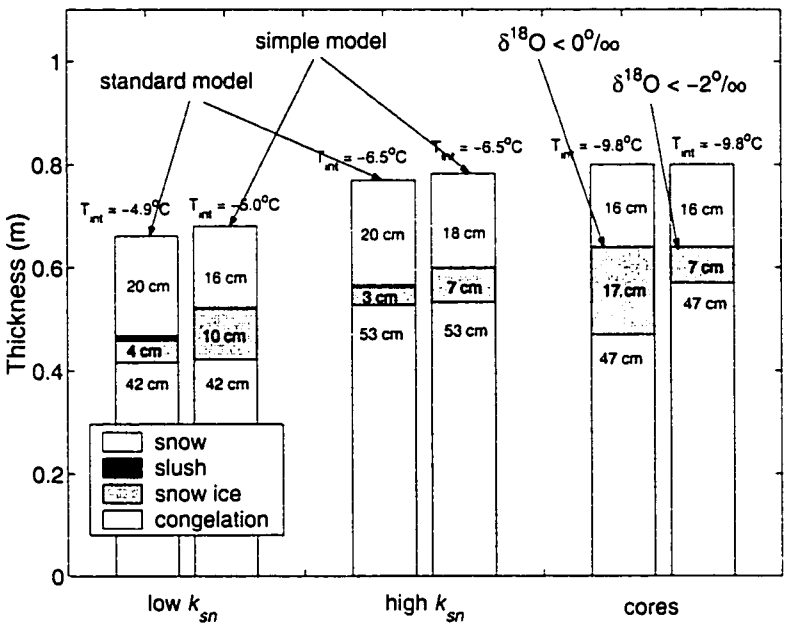

Figure 4.12: Effects of snow thermal conductivity. Average thicknesses of congelation ice, snow ice, slush and snow for the suite of simulations shown in Figures 4.7a and b. Results are shown for two thermal conductivities: low k_{sn} [*Sturm et al.*, 1997] and high k_{sn} [*Yen*, 1981]. Also shown are the mean thickensses from ice core samples from the Ross Sea in 1995. The snow ice thickness is given for both the $\delta^{18}O$ criterion from *Jeffries et al.* [2001] and the revised value recommended here of -2‰. Mean snow/ice interface temperatures are also given (T_{int})

direct comparison is difficult as true growth conditions are not fully represented in the model. Snow/ice interface temperatures are also more realistic using a higher snow thermal conductivity, although they are still several degrees below observed values. Part of this discrepancy is likely due to a cold bias in the data for the early winter 1995 cruise. Many measurements were taken on ice with little snow cover in very cold conditions close to the continent, which is not represented in the simulated results.

4.5 Summary

4.5.1 Ice and snow ice thickness

Snow, snow ice and total ice thicknesses were fairly well represented by the simple model, suggesting percolation is spatially inhomogeneous. Both models produced somewhat less snow ice than observed [*Jeffries et al.*, 2001], in part because flooding and snow ice formation did not occur on younger ice. The lower amounts of snow ice produced by the model reinforce the results of chapters 1 and 2, which suggest that a snow ice $\delta^{18}O$ criterion of 0‰ is too high. The simulation results are, however, strongly dependent on accumulation rates and ocean heat flux.

4.5.2 Effects of ice permeability on flooding

Flooding and snow ice formation are seen to be critically dependent on a number of factors. In particular, the nature of the flow process which brings brine and sea water to the surface during a flooding event is crucial in determining both the mass balance of the ice and its physical properties. Permitting interaction of the flooding brine with the porous ice matrix produces drastically different results than simple flooding of the surface with sea water. This is true in terms of the amounts of snow ice formed, and in turn, the thickness of the remaining snow cover, and in terms of the salinity and porosity (brine volume) structure of the ice. Upward brine flushing during flooding reduces ice porosity to such a degree that it generally restricts flooding to one major event or a series of closely spaced events. This typically restricts snow ice thicknesses to less than 20 cm. The overall mass balance is then controlled primarily by meteorological factors early in ice development. As flooding and snow ice formation are dependent on a critical percolation threshold, the nature of the physical processes involved is as important as meteorological effects in determining quantities of snow ice produced. With the simple model, brine volumes remained consistently above the percolation threshold, so snow ice thicknesses were primarily dependent on snow load, and the overall ice thickness was much less dependent on early growth conditions.

As presented, upward percolation of brine by uniform Darcian flow through a porous ice matrix seems an unlikely candidate to be responsible for the bulk of the flooding process.

Resultant snow ice thicknesses appear to be significantly lower than expected, and highly negative freeboards (as much as -20 cm) persist throughout much of the growth season, in conflict with observations (Figure 4.1). Large negative freeboards are generally associated with deformational features, and not level ice. Furthermore, the very low salinities that result from this upward flushing of brine are not consistent with observations. Brine volumes below the critical value for permeable ice are a ubiquitous result of this upward brine flushing and are typically present for most of the growth period after initial flooding. This is also inconsistent with observations, which show that most sea ice has brine volumes greater than 5% (M. O. Jeffries, unpublished data, 1995), despite lower ice temperatures than in the simulations. It should be noted that the choice of a percolation threshold of 7% [*Fritsen et al.*, 1998] will increase simulated brine volumes and salinities somewhat. However, the salinities will still tend to fall to near 3‰ throughout the congelation ice layers. Upward brine flushing is so effective in the standard model that flooding is generally restricted to a single event, or several closely timed events. It is expected, however, that multiple flooding events can occur.

If brine percolation through the ice does occur with any frequency in the Antarctic pack, it is undoubtedly not a uniform phenomenon. Horizontal inhomogeneities in the salinity and pore structure of the ice sheet will likely cause large spatial variations in the flow, so that only some areas of the ice sheet are affected internally by the flooding. If the permeable region is restricted spatially, or if the permeability is high enough in a given area, the flow may be sufficiently rapid that the assumption of local thermal equilibrium is not met. In this case the thermal response of the ice is reduced, and substantial flow may occur without the pathways freezing shut due to the brine transport. Modeling of the flow then becomes very difficult, since detailed knowledge of the porosity structure of the ice is required to account for both the flow and heat transfer, and the heat transfer relations become quite complicated. Furthermore, it may be necessary to account for horizontal transport of the flooding brine through the snow. Note that the extreme case of localized flow is roughly equivalent to the simple model presented here. Therefore the results of the two models represent bounds on the degree of variability that could occur in flooding and snow ice formation due to variability in the upward brine transport. In order to understand how variations in the degree of connectivity of the pore space affect the

flooding process and brine transport, it is necessary to account for the horizontal transfer of heat between connected and unconnected pores and the resultant evolution of the pore structure.

A significant area of weakness in the models is the treatment of brine drainage and convection in the ice. At present, the only parameterizations available to account for gravity drainage are those of *Cox and Weeks* [1975], which were derived for laboratory-grown NaCl congelation ice. Growth conditions are quite different for the modeled sea ice. First, the ice is generally warmer than that in the Cox and Weeks experiments, with temperature gradients generally lower than those measured in the laboratory. Second, model salinity profiles are "top heavy" after flooding, especially in the standard model, with very high salinities in the upper portions of the ice sheet (15-25‰), and very low, near-uniform values in the lower ice (~2.5‰ for the standard model, 3-5‰ for the simple model). It seems likely that brine drainage from the upper ice may have an impact on the salinity of the lower ice as it drains through the ice sheet [*Kovacs*, 1996]. Third, the very high porosities of the slush and snow ice layer could lead to brine pockets large enough for internal convection to permit them to migrate very quickly, possibly leading to significant resalination of the lower, low-salinity ice layers. Finally, convection of brine during freeze-up of the flooded layer will likely transport salt from the upper ice to that below. Observations indicate that brine convection may be quite important in brine transport for flooded ice [*Lytle and Ackley*, 1996], and may represent a significant redistribution of salt [*Hudier et al.*, 1995]. A simple parameterization of salt redistribution showed that while this process can increase the porosity of the ice temporarily, brine flushing during flooding is still the controlling process on the ice permeability. While it is possible that this simple approach underestimates the salt redistribution, results of the 2-D convective model (Chapter 3) indicate that salt redistribution is a small effect, as most of the drainage takes place rapidly through isolated tubes. It has been demonstrated that the salinity characteristics may play a crucial role in controlling the ice mass balance through the flooding and snow ice formation process; a proper treatment of brine transport in sea ice is essential to understanding the role of this process in Antarctic sea ice development.

If brine percolation through the bulk of the ice is a major component of the flooding process, then either significant convection and redistribution of brine must be occurring

to maintain the ice permeability, or upward brine flushing is spatially nonuniform. Either the process is restricted to areas of high ice permeability, such as in large drainage tubes or fractures, or local variations in pore geometry and thermal transport are significant in modifying the salt transport in individual pores.

4.5.3 Insulation effects of snow

Simulation results were in better agreement with observations using the higher (and more traditional value) for snow thermal conductivity, particularly for snow/ice interface temperatures. While we do not believe that (4.8) gives unrepresentative values, it may not account for all of the heat transfer through the snow. Enhanced vapor transport within warm snow may increase the effective thermal conductivity somewhat. Wind pumping and snow redistribution effects may cool the snow. As temperature gradients within the snow were very large, convection may have also played a role, although the presence of numerous icy layers [*Sturm et al.*, 1998] would seem to preclude this. Recent observations in the Arctic indicate that large lateral variations in snow depth may cause a focussing effect on the heat flow and may have a substantial effect on the thermal regime of sea ice (M. Sturm, personal communication, 2000).

The inclusion of depth hoar could have an important effect on the results due to its very low thermal conductivity. However, this would raise the ice temperatures even further. While this could render the ice permeable for a longer period, brine flushing would then remove even more salt from the lower ice layers, increasing the disparity between simulation results and field data.

4.6 Key results of 1-D percolation model

- Modelling of flooding produced more realistic results by treating the fluid pathways as isolated, high permeability regions hydraulically disconnected from the bulk of the ice pore space (the simple model). These might be large, open brine drainage tubes or cracks in the ice sheet. Percolation is most likely an inhomogeneous process over the ice sheet.

- Simulated snow and ice thicknesses provide the best match to observations if the

lower snow ice identification criterion of $\delta^{18}O < -2‰$ recommended in Chapter 3 is used. Snow ice production rates in the Ross Sea are likely modest in winter.

- Snow ice production is primarily dependent on snow accumulation rates. Once flooding and snow ice formation is initiated, little further congelation growth occurs and snow ice formation is the dominant thermodynamic growth mechanism.

Chapter 5

Spatial variability of brine percolation and snow ice formation

5.1 A 2-D model of brine percolation

In Chapter 4, we have seen that the assumption of uniform vertical brine flushing in the presence of a temperature gradient in the ice results in rapid desalination of the ice. Of course, sea ice possesses a complex microstructure, and hence, a heterogeneous permeability. The upward flow of brine is most likely restricted, at least in cold sea ice, to localized brine tube networks that formed during ice growth and drainage. Even if this is the case, percolation through cold ice will still cause freezing of the relatively fresh sea water resulting in constriction of the channels, with concomitant warming of the surrounding ice. As a result, during percolation the permeability of active pathways decreases, while that of the more constricted pathways increases. To examine the effects of this spatial and temporal variability on brine percolation and ice development, the 1-D model presented in Chapter 4 is extended to two dimensions.

The model physics is essentially the same as that discussed in Chapter 4, with ice growth, brine transport and drainage, and surface energy balance left unchanged. If the ice and snow cover are horizontally homogeneous, it reduces to the 1-D model described

in Chapter 4. To accommodate lateral heat flow, the heat equation, (4.1) is now given by

$$\rho_{si,sn} C_{si,sn} \frac{\partial T}{\partial t} + \rho_b C_b \nabla \cdot (\mathbf{u}T) = \nabla \cdot k_{si,sn} \nabla T + \kappa I_o e^{-\kappa z}, \tag{5.1}$$

where C_b is the same as in (B.4). Equation (5.1) is solved by considering horizontal and vertical heat fluxes separately. First, horizontal heat fluxes are computed explicitly and treated as a source function for the now 1-D vertical heat flow problem, which is solved as in the 1-D model. This allows for accurate determination of ice growth rates following *Goodrich* [1978], yet permits solution of 2-D problems. To avoid complications of differential rates of snow compaction along a floe, the snow density is set constant to 350 kg m^{-3}. Rather than use the snow thermal conductivity given by *Sturm et al.* [1997], which results in anomalously warm ice temperatures, the snow thermal conductivity is set to $k_{sn} = 0.3$ W m^{-1} K^{-1} based on *Yen* [1981].

To reduce the computational difficulties, brine flow in the ice is assumed to be in the vertical direction only. This is reasonable in that the external pressure gradient is in the vertical direction, and sea ice is much less permeable perpendicular to the growth direction [*Freitag*, 1999]. Once brine reaches the surface, it is permitted to spread laterally, provided it is not impeded by ice surface features. Water flow through snow is a complex problem and is affected by capillary forces [*Colbeck*, 1983a; *Marsh and Woo*, 1984], but for simplicity, it is approximated using the Dupuit approximation for flow in an unconfined aquifer [*Bear*, 1972],

$$u = \frac{K \rho g}{\mu} \frac{dh}{dx}. \tag{5.2}$$

Here, dh/dx is the slope of the phreatic surface. This is not truly valid when the phreatic surface moves vertically, though if the model is integrated slowly, it can provide a reasonable first approximation of the lateral spread of brine. The permeability of the snow is set to $K = 10^{-10}$ m^2. Horizontal flow is not permitted from the snow to an ice layer.

5.2 Localized percolation via high permeability pathways

First, we examine percolation on a small scale. If brine flow through the internal ice pore structure is a major source of fluid during flooding events, then this flow must be restricted to only a fraction of the pore space, and it must be sufficiently rapid to provide enough heat to maintain a high ice porosity. In Chapter 4, we have seen that if these conditions are not met, a flushing event will drastically reduce the ice salinity, if it occurs at all. This suggests that the flooding was restricted to isolated high permeability pathways. Therefore, the effects of these high permeability regions are examined to investigate the plausibility of this mechanism for percolation in cold winter sea ice and the possible flushing of salt during flooding events. To this end, the 2-D model is applied to a hypothetical floe with regions of high permeability periodically distributed throughout the ice. As the permeability will vary spatially in the ice, it is no longer appropriate to use a permeability determined for bulk sea ice.

5.2.1 Microstructure and permeability

In sea ice, the microstructure and porosity change as the ice temperature changes or when brine transport processes alter the salinity structure of the ice. Therefore, we need an expression for the permeability which takes account of the actual porosity evolution of the ice. For the present problem, sea ice can be considered a multiple porosity medium. Fluid inclusions in the bulk sea ice consist of small brine pockets trapped along the plate boundaries in congelation ice [*Perovich and Gow*, 1996], or between grain boundaries in frazil ice [*Weissenberger et al.*, 1992]. Although these pores comprise the bulk of the total pore space they may be responsible for only a portion of the total fluid permeability [*Freitag*, 1999]. This is, in part, because these conduits typically have diameters of a fraction of a millimeter, whereas the larger diameter brine drainage tubes that form during ice growth may be several millimeters in diameter [*Saito and Ono*, 1980; *Wakatsuchi*, 1983]. Yet these tubes represent only a small portion of the total brine volume. Based on the measurements of *Perovich and Gow* [1996], the smaller inclusions comprise 60-80% of the total brine volume. This is likely an underestimate because of the resolution of the imaging equipment.

In contrast, channels greater than 1 mm in diameter constitute a brine volume of less than 1% [*Saito and Ono*, 1978, 1980], though tube feeder structures can be a significant source of pore volume [*Cottier et al.*, 1999]. Large drainage tubes can be several millimeters to more than a centimeter in diameter, but they are sparsely distributed [*Bennington*, 1987; *Lake and Lewis*, 1970]. Obviously, the local permeability of these tubes is much greater than that of the bulk ice, but the spatial distribution of these features will be important in controlling fluid transport through the ice. *Martin* [1979] observed that percolation of oil to the surface of Arctic sea ice occurred principally through tubes spaced some tens of centimeters apart, yet ice samples clearly showed significant brine displacement by oil in the pore space between individual ice lamellae.

To treat the sea ice as a dual porosity medium, with a bulk permeability determined by the ice microstructure, we assume the brine pockets form an interconnected network of roughly vertical tubules [*Weissenberger et al.*, 1992; *Cole and Shapiro*, 1998; *Freitag*, 1999]. Using the hydraulic radius model [*Bear*, 1972], we may define the permeability as

$$K = \frac{\tau^2 \phi^3}{2B^2}. \tag{5.3}$$

For the vertical permeability, the brine pockets consist of an array of parallel tubes with an ellipsoidal cross-section. The specific surface, B may then be expressed as

$$B = \phi \frac{C}{A}, \tag{5.4}$$

where A is the pore area and C, the circularity of the pore, is about 30 [*Perovich and Gow*, 1996], representing an aspect ratio of about 5. Then, with the tortuosity, $\tau = \sqrt{2}$, we have

$$K = \frac{\phi A}{120}. \tag{5.5}$$

The distribution of pore sizes can be described by a log-normal distribution [*Perovich and Gow*, 1996; *Freitag*, 1999], so in principal one could determine the permeability by integrating (5.5) over all pores sizes. The connected pores will vary in size along the flow direction as well as spatially, so this treatment would tend to overestimate the true

permeability. Therefore, the median pore area, A_m, is used instead. On the scale of interest in this study, spatial variability of the pore size distribution should be small, since the number density of pores in this size range is $\sim$100 per cm^2.

During warming, both the porosity and pore area will increase, so (5.5) is modified to be a function of ϕ only,

$$K = \frac{\phi^2 A_m}{120\phi_m}. \tag{5.6}$$

Equation 5.6 might be reasonable at high brine volumes, where most of the pore volume is well connected. Near the percolation threshold, only a fraction of the pore space is connected. *Golden et al.* [1998] suggest that a power law behaviour near the percolation threshold is appropriate for bulk sea ice. Therefore, (5.6) is modified *ad hoc*, replacing ϕ by $\phi - \phi_c$, where ϕ_c is the percolation threshold,

$$K = \frac{(\phi - \phi_c)^2 A_m}{120\phi_m}. \tag{5.7}$$

Here, $A_m = 0.016$ mm^2 and $\phi_m = 0.065$, are best estimates for first year frazil and congelation ice [*Perovich and Gow*, 1996], and $\phi_c = 0.05$, as suggested by *Golden et al.* [1998].

The permeability from this model shows good agreement with the data of *Freitag* [1999] (Figure 5.1), matching new ice (laboratory ice) better at low porosities, and field data at high porosities. This is somewhat surprising, since the theoretical bulk permeability does not account for larger drainage channels. Also plotted are upper and lower bounds on the theoretical curve. The upper bound is calculated by integrating the pore size PDF over all pore sizes, while the lower bound is computed by integrating the pore size PDF along the direction of flow. The lower bound allows the maximum possible variation in cross-sectional area along a tubule. Also shown are the permeabilities for a 1 cm^2 piece of ice with a single vertical tube. The porosity is then approximately 0.2 for a 5 mm diameter tube. Note that the tube permeability is scaled by a factor of 1000. This means that compared to a large drainage tube, the bulk of sea ice is essentially impermeable.

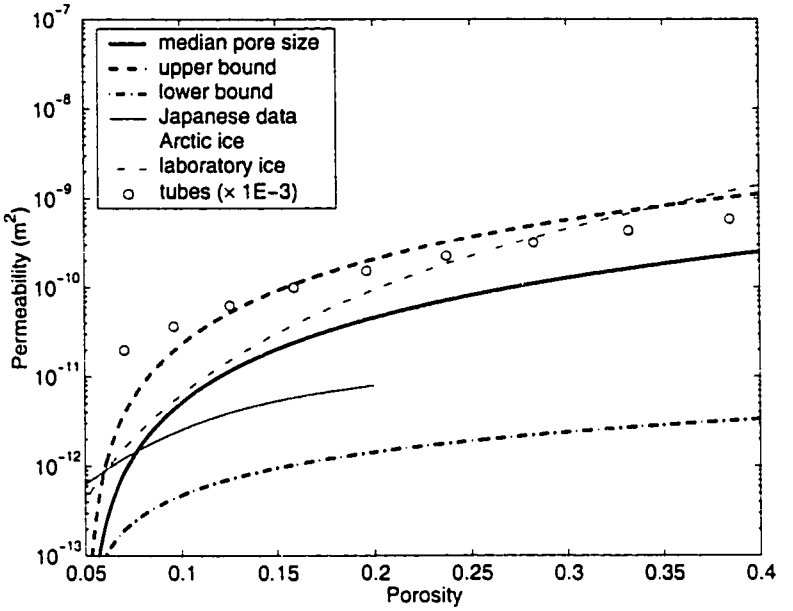

Figure 5.1: Permeability of bulk sea ice. Three theoretical curves are based on the data of *Perovich and Gow* [1996], using a median pore size, an integration over all pore sizes (upper bound), and an integration over pores in series (lower bound). The Japanese data is the fit from Figure 4.3, Arctic and laboratory ice are curves from *Freitag* [1999].

5.2.2 Simulation of inhomogeneous percolation

The model domain is a section of ice 65 cm thick, with a model resolution of 2 cm. The snow depth is set initially to 20 cm so that it is just at the freeboard threshold necessary for flooding. In the first case examined, the salinity of the ice is set to 6‰ in the lower regions of the ice. In the upper 20 cm, this is increased linearly to 10‰ at the ice surface. In the center of the model domain, a thin section (2 cm) of ice is set to a salinity of 10‰ throughout its thickness, so that its permeability will be much higher than the rest of the ice. The boundaries are periodic with a 10 cm spacing between the high porosity features. These ice properties are roughly similar to observations of spatial variability in ice structure observed in young ice [*Cottier et al.*, 1999]. The ice permeability is determined by (5.7) throughout the ice. As such, if the high porosity region is thought of as a brine drainage structure, this will underestimate the permeability.

Initially, the air temperature is set to -20 °C until the ice temperature equilibrates.

Then for the period of one day, the air temperature is raised to -5 °C and 20 cm of new snow are added at a constant rate. This forcing presents ideal conditions for flooding events for winter sea ice, and corresponds roughly to conditions under which extensive winter-time flooding has been observed [*Golden et al.*, 1998]. Initially, the ice is impermeable, but once

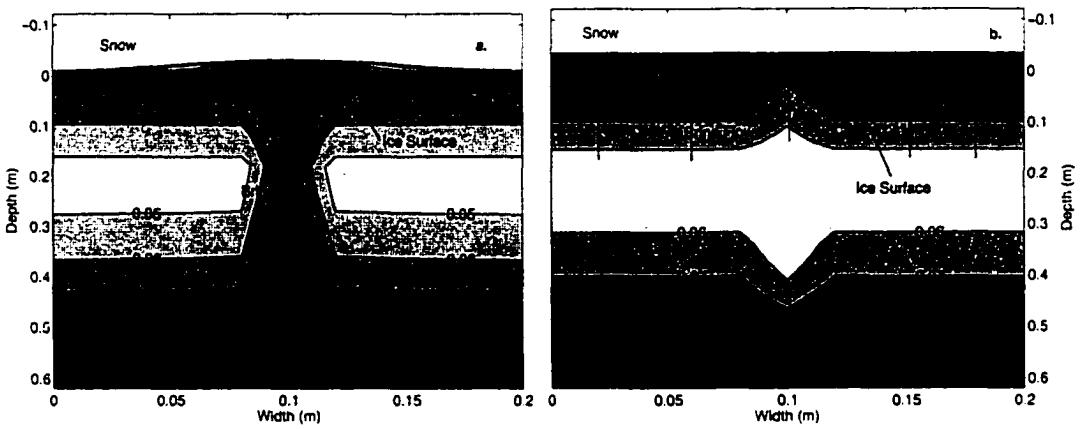

Figure 5.2: Brine percolation in a 2-D model. Initially, the ice is permeable only in the highly saline central region (a). Brine spreads laterally on the surface, warming the ice, allowing percolation to begin in the rest of the ice sheet (b). Brine volume contours are in percent.

the ice warms above the percolation threshold ($\phi_c = 0.05$), flooding takes place through the central channel (Figure 5.2). This flooding is very slow (a few centimeters per day), as it is in part limited by the rate of snow accumulation. As a result, there is only a moderate effect on the ice temperature and so the infiltrating brine is very saline, giving slush salinities of about 60‰. Since this salty brine will freeze slowly, it spreads laterally quite readily. This spreading, along with the warming of the ice due to the initial flooding, raises the temperature of the rest of the ice above the percolation threshold, and, after a day, brine flow begins through the entire ice sheet (Figure 5.2). Note that the porosity of the ice in the central channel has been reduced below that of the remainder of the ice due to the brine flushing. Eventually, this flow will reduce the ice salinity in the same manner as in the standard model of Chapter 4.

The tendency for percolation to reduce permeability through salt flushing appears quite strong. In order for it to occur in any substantial way, the flow must be rapid in order to maintain open fluid pathways. This can be facilitated either with warm ice, high

permeability channels, or a large hydraulic head (i.e., large negative freeboard) at the onset of percolation. Therefore, we explore an idealized case where several conditions are set that are most favourable to flooding. First, the permeability of the high salinity region is increased to simulate a brine drainage tube. An individual tube will have a permeability given by

$$K = \phi\frac{d^2}{32} = (\frac{\pi d^2}{4A})\frac{d^2}{4}, \tag{5.8}$$

where d is the tube diameter and A is the cross-sectional area in which the tube is embedded. Assuming a diameter of 3 mm, the permeability from (5.8) will be $5 \times 10^{-9}\text{mm}^2$ for an ice section 2 cm wide. This tube will comprise 7% of the volume of the 2 cm section. For typical ice temperatures, this will raise the local ice salinity by about 4‰, consistent with the salinity used here (10‰ vs 6‰).

Near the ice surface, brine channels narrow, and rarely penetrate to the surface except in very young ice or in the summer. Here, the permeability should be closer to that of the bulk sea ice; so, in the upper 6 cm, (5.1) is used. Although the manner in which the brine channel is modelled here is a simplification, the presence of this low permeability cap will reduce the rate of flow and allow more heat lateral transfer between the tube and the immediately surrounding ice. Therefore heat transfer, and hence, salt transfer via brine flow, should be roughly approximated in the model.

In the upper 20 cm, the percolation threshold is set to $\phi_c = 0.6$. This slightly higher threshold could result from a frazil ice structure, rather than congelation ice [*Golden et al.*, 1998]. The value chosen here was set in order to delay the onset of percolation until a thicker snow cover, and hence, hydraulic head, developed. To maintain ice porosity, the air temperature is maintained at -5 °C after the snow has accumulated. Finally, it is assumed that there is no salt transport from within a layer if the porosity is less than 0.5% above the percolation threshold. This prevents individual channels from freezing shut due to brine flow alone. These conditions provide what should be some of the most favourable circumstances for brine percolation that would be found in the Antarctic ice pack in winter.

In the simulation, the higher percolation threshold prevented flooding until after the

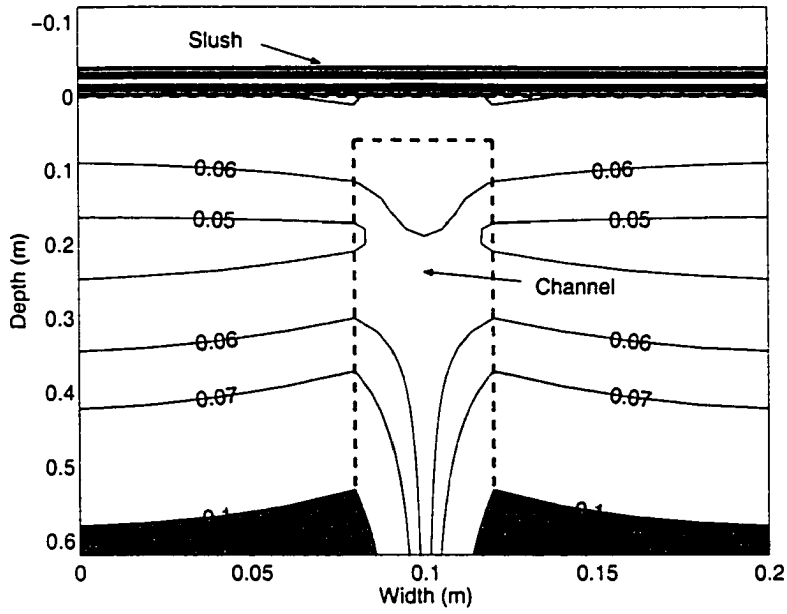

Figure 5.3: Percolation through a brine channel. Brine volume contours are shown during the early stages of pecolation. The location of the brine channel is shown by the dotted line.

snow had accumulated, resulting in a freeboard of -7 cm. Once the ice surface warmed above approximately -5 °C, relatively rapid fluid flow (several centimeters per hour) occurred through the channel, warming the ice and producing a saline slush of several centimeters after a few hours (Figure 5.3). Note that this is still slower than dramatic flooding events in which the snow surface is seen to "boil" as the brine infiltrates the snow cover [*Golden et al.*, 1998]. The bulk of the flow is through the channel until a day after onset of flooding, when the ice has been warmed enough for flow to occur through the bulk ice. While the porosity remains relatively high due to the warming effect of increased vertical heat transport, it only remains above the percolation threshold due to the imposition of a minimum porosity during flooding events.

These results support the conclusions of the 1-D modelling in Chapter 4. While percolation can occur in sea ice when a temperature gradient is present, it will tend to result in significant flushing of brine from within the bulk pore space and from any narrow channels that may exist. Ultimately, it is unlikely that conditions for sustained percolation can occur in practice, and any flow along a strong temperature gradient in the ice will tend

to cause closure of any smaller channels before much flushing can occur. Large drainage channels that penetrate to the surface (or at least through radial feeder tubes [e.g. *Lake and Lewis*, 1970]) are more likely to carry most of the fluid in a single rapid event. This implies that the simple model of Chapter 4 is more appropriate for large scale modelling of flooding, though criteria for the onset of percolation remain unclear.

5.3 Flooding and snow ice formation at the floe scale

While small scale processes affect the occurrence and mechanisms for brine percolation, spatial variability on the scale of individual ice floes likewise has an effect on the formation and distribution of snow ice, and in turn, on the development and mass balance of the floe. The 2-D flooding model is applied to ice floes sampled in the Ross Sea in 1995 to examine the role of spatial variation in snow and ice thickness on the formation and development of snow ice.

5.3.1 Floe modelling

To simulate the evolution of an ice floe, the model is first initialized with the snow and ice thicknesses measured at one meter intervals in the field. Since the freeboard will evolve with time, it is computed by the model using a modified version of (4.12), where the freeboard is referenced to an arbitrary constant level in the ice. This is necessary because parts of the floe may be out of isostatic balance, such as in a ridge, and the theoretical and true freeboard may be different. The computed freeboard can then be compared to a freeboard averaged over the entire floe to determine if the ice is locally above sea level. To allow for flexure of the floe, the local freeboard is computed by using an average freeboard over a 10 meter interval. This gave the best agreement between true and theoretical freeboards.

The flooding routine used is the simple model of Chapter 4, as this appears to give the best results and seems to be the most plausible mechanism for flooding. The percolation threshold is set to $\phi_c = 0.05$, though it is now uncertain what the meaning of this threshold is in the context of the simple model, where flooding must take place through relatively large scale features. The salinity of the ice is assumed to be 6‰. A linear vertical

temperature gradient is first set through the ice and snow, and the model is then integrated for several days to arrive at an initial temperature distribution. Snow is then permitted to accumulate. The ocean heat flux is set to 10 W m^{-2}. Other parameters and forcing conditions are the same as those used in Chapter 4.

5.3.2 Spatial distribution of flooding and lateral flow

The two floes presented in Figure 1.2 are re-examined here as they exhibit several salient features that provide insight into the problem of the spatial distribution of flooding. First, for both floes a significant portion of the ice surface is below sea level, yet flooding had not occurred at all of these locations. Many of these cases occur at local snow depth minima, implying a link between the ice temperature, and hence, porosity, and flooding. Second, the flooding is discontinuous, in that dry sections may lie immediately adjacent to flooded sections while there is no obvious impediment to flow from one location to the next through the snow-pack.

For each floe, the model is run for 10 days prior to the date of sampling. The air temperature used to drive the model is taken from the automatic weather station at Possession Island (See Section 4.3.5). The distribution of flooding is fairly well represented by the model (Figure 5.4) in each case, though it is generally more widespread in the simulations. For instance there is flooding above meter 80 on floe NBP138-1 (Figure 5.4c), and between meters 22 and 33 on floe NBP225-1 (Figure 5.4c). Of note, however, is that those regions where the ice surface is below sea level and no flooding occurred were also dry in the model. At these locations, the simulated ice porosity was below the critical threshold for percolation. The degree of agreement with the field data suggests that such a threshold may play a role in the flooding process.

In contrast to the small scale simulations above, lateral transport of brine was minimal. This is partly due to the relatively low salinity of the infiltrating sea water, which freezes rapidly upon reaching the cold snow pack. Any brine that spreads horizontally at the ice surface will tend to freeze as it comes in contact with more cold ice and snow, so it freezes before extensive lateral inundation of the snow-pack can occur. In actuality, the infiltrating fluid will be at least partially composed of denser brine, and the slush should persist longer, as in the observed profiles.

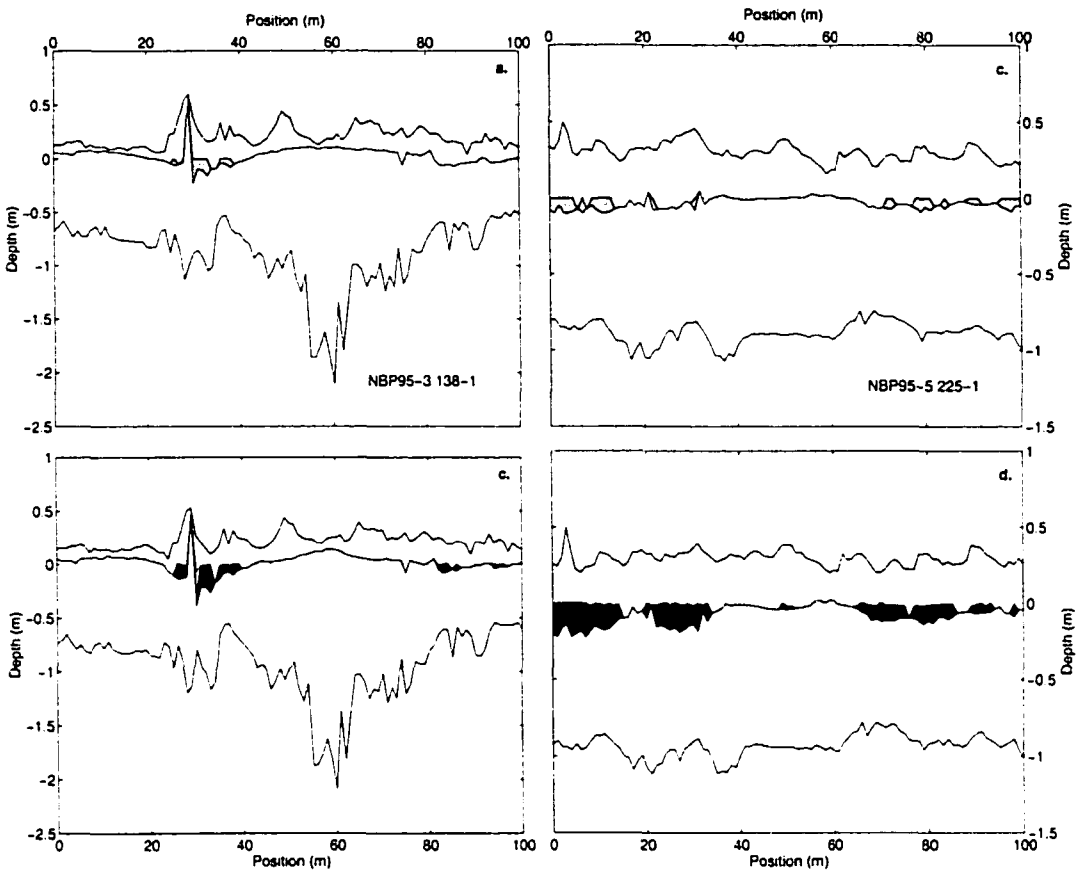

Figure 5.4: Flooding of ice floes. (a)-(b) Snow and ice thickness profiles of two selected floes from the Ross Sea with surface flooding present. (c)-(d) Simulated flooding and snow ice formation. New snow ice is black, slush is medium gray, and snow is light gray.

5.3.3 Evolution of an ice floe

Modelling the evolution of an existing floe provides a useful means of predicting the potential for future snow ice formation, since it is less likely to undergo significant dynamic thickening than young new ice and, therefore, is perhaps more amenable to simple thermodynamic-only models. Simulations of the evolution of floe NBP138-1 over a four month period demonstrate the effects of snow ice formation on ice development (Figure 5.5). Two snow accumulation rates are used in the simulation: (1) accumulation rates are from 1995 NCEP reanalysis data (Figure 5.5a); (2) NCEP data are scaled to match climatological estimates [*Giovinetto et al.*, 1992] (Figures 5.5b and c). Both accumulation rates

produce substantial quantities of snow ice, though more than twice as much is produced using the larger accumulation rate. Interestingly, the actual thickness of snow is greater at the end of the four month period for the lower accumulation rate. The reason can be seen by examining the evolution for snow of low thermal conductivity as predicted by (4.8) (Figure 5.5c). The insulating effect of the snow keeps the ice warm and permeable, while at the same time keeping it thin. This tends to enhance the rate of snow ice formation.

In general, snow ice formation tends to smooth out the thickness variation on an individual floe. Surface roughness is decreased as hollows are filled in by flooding as suggested by *Worby et al.* [1996] and the height of ridge sails above the surface is reduced. This may contribute to the low sail to keel thickness ratio that is often observed in Antarctic ridges. Thin ice will thicken by congelation growth if the snow cover is thin, while under a thick snow cover it will thicken through snow ice formation. The thicker ice grows slowly (e.g., the ridge at 60 meters), and due to its buoyancy, tends to form little snow ice. The net effect of these processes is to produce a more uniform ice thickness distribution. The effect on snow depth distribution is less clear. *Sturm et al.* [1998] has suggested that flooding increases the snow depth heterogeneity by thinning the snow at locations where flooding occurred. Model results suggest that this is true where there is a large variation in ice thickness, such as near a ridge (e.g. Figure 5.4c). For relatively uniform ice thickness (Figure 5.4d), flooding occurs preferentially at locations with a thicker snow cover. Flooding and snow ice formation cause a thinning of the snow pack at these locations, increasing the snow depth homogeneity. In essence, the spatially inhomogeneous flooding process results in increased spatial homogeneity in ice thickness. It is notable that although the amount of snow ice produced in the three cases (Figure 5.5) varies by a factor of three (12-36 cm snow ice), the variations in total ice thickness are small (115-123 cm).

5.4 Key results of 2-D modelling of percolation

- Percolation through isolated channels is limited by the permeability of the upper portion of the ice where the channel narrows. Unless the flow is very rapid, flushing of brine from this region and the channel below will cause a decrease in porosity and a reduction in the rate of flow to that of the brine in the bulk ice. For percolation

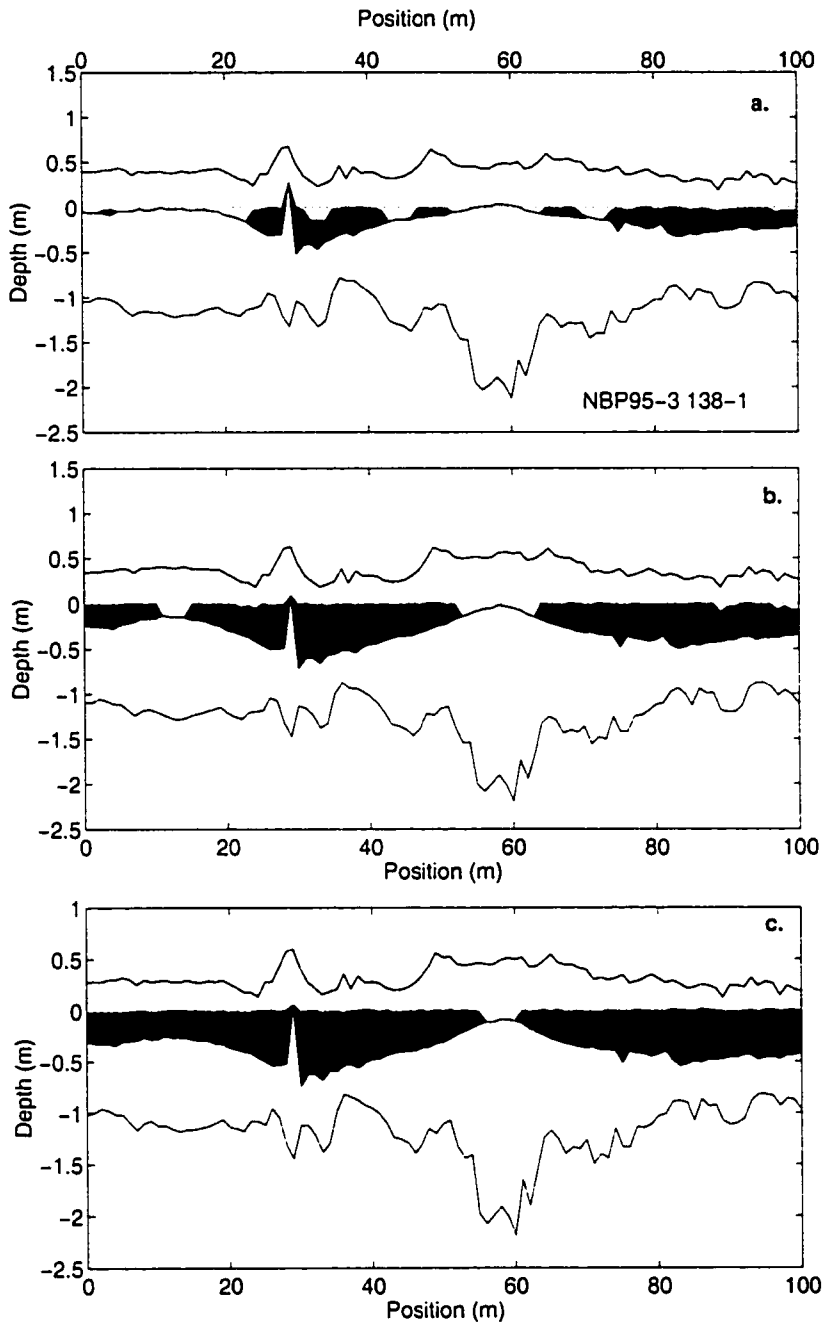

Figure 5.5: Evolution of ice floe thickness. Simulated thickness profiles of a selected floe after a 4 month period for different snow accumulation regimes: (a) 275 kg m^{-2} a^{-1}, (b) 400 kg m^{-32} a^{-1}, and (c) 400 kg m^{-2} a^{-1} with k_{sn} = 0.18 W m^{-i} K^{-1}. The snow is shaded gray, new snow ice is shaded black

to take place, channels must remain open when flow is initiated. It is uncertain how this can occur if a temperature gradient exists in the ice.

- Flooding of an ice floe does appear to be limited by a percolation threshold.
- Snow ice formation on an ice floe acts to increase the homogeneity in ice thickness distribution.

Chapter 6

Conclusions

6.1 Oxygen isotopes and snow ice observations

A reliable means of discriminating snow ice from frazil ice is an important tool in quantifying the impact of flooding and snow ice formation on the mass balance of sea ice in the Southern Ocean. Although currently the best means available is through the use of stable isotopes analysis, there is no clear line for distinguishing between the two ice types. Modelling of fractionation during the freezing of sea water shows that during rapid initial ice growth, isotopic fractionation may be minimal. A comparison of $\delta^{18}O$ of frazil and congelation ice samples samples suggests that this effect is more important in frazil ice. Therefore, in winter, granular ice samples with $\delta^{18}O$ values greater than that of sea water should be regarded as frazil ice. In the Ross, Amundsen, and Bellingshausen (RAB) seas, where the sea water $\delta^{18}O$ averages -1‰, this alone leads to a 40% reduction in quantities of snow ice inferred in previous studies [*Jeffries et al.*, 2001], in which samples with $\delta^{18}O < 0$ were assumed to be snow ice.

Modelling of isotopic exchange within the flooded layer suggest that significant changes in $\delta^{18}O$ values can occur within the slush during convective brine exchange through the ice. This is in marked contrast to previous work which showed that post-genetic isotopic shifts in sea ice are minimal [*Eicken*, 1998], although he did not consider snow ice. Mass exchange between the solid and liquid portions within a slush layer during grain coarsening leads to substantial isotopic exchange between phases. If the thermohaline convection in

the slush is strong enough to penetrate through the underlying sea ice, the ^{18}O depleted brine can drain and raise the $\delta^{18}O$ value of the slush by several parts per thousand. Fractionation during freezing will also contribute to this shift. Under the most favourable modelling assumptions, this was seen to raise the isotopic composition of the slush layer to as high as -1.9‰. While this is still well below the snow ice identification criterion use by *Jeffries et al.* [2001], it demonstrates that determinations of the meteoric ice fraction using oxygen isotopes [e.g. *Lange et al.*, 1990] may underestimate the contribution of snow to the ice mass balance.

Isotopic exchange during convective transport of brine can partly explain the distribution of $\delta^{18}O$ values observed in ice core samples, in particular, those values that fall between -2‰ and -5‰, which is an approximate upper limit for fresh slush. This leaves the provenance of those samples with $-2‰ < \delta^{18}O < -1‰$ as yet undetermined. Model results showed that efficient drainage of brine occurs primarily through isolated channels so that the isotopic composition of ice below a freezing slush layer is changed only slightly. For weaker convection in the absence of channels, a slight isotopic depletion of the ice is possible. In the simulations, this effect produced shifts of less than 0.6‰. It is proposed that this process, combined with a slow migration of brine depleted in ^{18}O through the discontinuous pore network throughout the growth season leads to a slow "diffusion" of the oxygen isotope signature downward into underlying ice. With only a slight additional shift, the full range of observed $\delta^{18}O$ values can be explained.

On the basis of these simulations, it is recommended that an upper limit for snow ice identification of $\delta^{18}O = -2‰$ be used in the RAB seas. This new criterion leads to a dramatic reduction in the amount of snow ice observed in the RAB seas (Figure 6.1), from 24-37% [*Jeffries et al.*, 2001] to a lower value of 6-18% of the total ice thickness. A corollary to the new estimate of snow ice percentage is an increase in the relative amount of frazil ice. If the snow ice identification criteria proposed here is correct, frazil ice is the dominant mechanism for ice formation in the RAB seas. A less supportable upper limit of -1‰ for snow ice changes the snow ice fraction to 15-25%. This criterion should be regarded as distinguishing between ice that formed by sea water freezing and ice that has had its composition altered by processes after initial formation, and does not distinguish by process. As such, for snow ice identification through the flooding process, the lower

value is preferred.

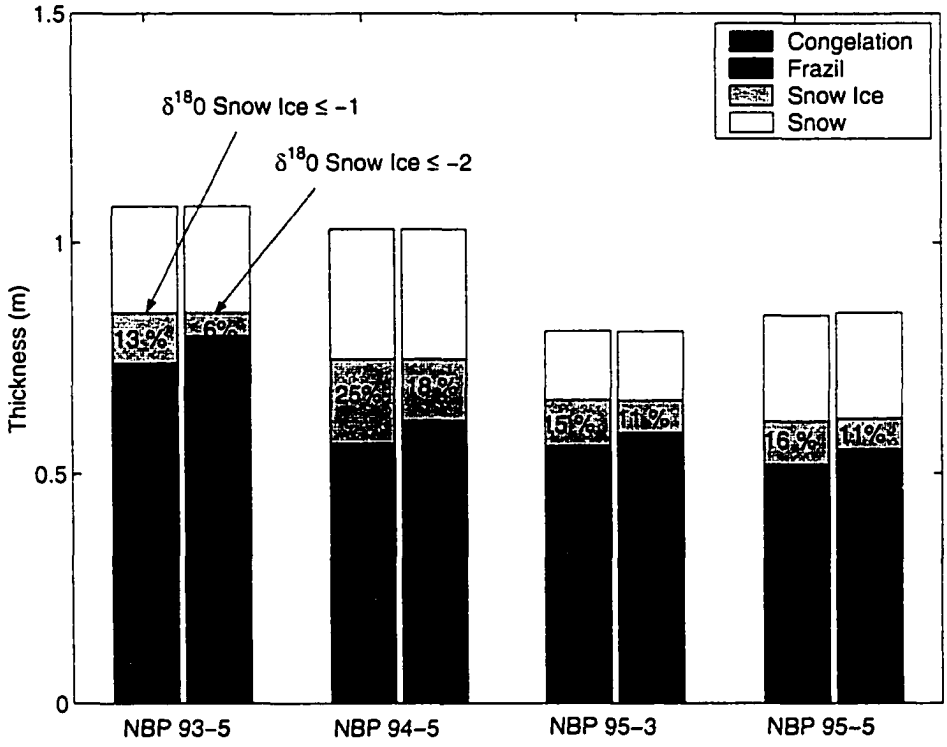

Figure 6.1: Revised ice composition for ice core samples. Structural composition is estimated for the RAB sea samples using two possible snow ice identification criteria, $\delta^{18}O = -1‰$ and $\delta^{18}O = -2‰$.

6.2 Brine transport and snow ice formation

6.2.1 Brine convection in slush

Results of the modelling studies described herein emphasize the importance of brine transport processes in controlling ice permeability and snow ice formation. Within a freezing slush layer, thermohaline convection can be quite vigourous, keeping the slush nearly isothermal. Since heat diffuses more rapidly than salt, cold, salty plumes of downward flowing brine will be more saline than brine at equilibrium with the surrounding ice. Therefore, the descending brine plume will partially melt the snow or ice matrix, forming a porous channel along the flow direction. Because of the strong dependence of

permeability on porosity, the flow will be highly focussed into these vertical channels. If the convection is vigorous enough, these channels will penetrate into the underlying ice, creating a pathway to the ocean for brine drainage. This process was found to be highly dependent on the initial permeability of both the ice and snow, so this effect is much more likely in warm ice. This process provides a means of rapid and efficient desalination of the slush, with decreases of as much as 10‰ in a few days. As the drainage is focussed into individual channels, salination of the upper ice will occur only if the ice has low permeability. This process may be an important factor in maintaining fluid pathways between the surface and the ocean.

6.2.2 Percolation in sea ice

Percolation of brine through sea ice during flooding events is a complicated and as yet unsolved problem. Uniform flushing of brine through the bulk ice cover is an unlikely mechanism for flooding. The resultant reduction in ice salinity and brine volume are too high to be realistic, and the process would render the ice impermeable throughout most of the growth season. Ice development is more realistic using a simple model in which flushing is ignored and sea water inundates the snow pack directly. If this is the case, then brine must percolate through isolated regions of high permeability, leaving the bulk of the ice nearly impermeable. Using a 2-D model of heterogeneous percolation, it was shown that even under idealized circumstances, brine flushing is still effective in closing off the fluid pathways. Unless large diameter tubes remain open all the way to the surface, it seems unlikely that brine percolation through the bulk of the ice pore space can be responsible for the few large scale flooding events that have been observed [*Golden et al.*, 1998]. While it is believed that the bulk of the flow takes place through a few isolated high permeability pathways, it is unclear how the evolution of this pore space occurs in such a way as to allow widespread flooding. This inhomogeneity in the distribution of percolation structures suggests that a simple percolation threshold determined for the bulk of the ice [*Golden et al.*, 1998] should be used with caution. Nevertheless, modelling of flooding on a floe scale shows compelling evidence that using such a criterion may indeed be useful, even if it is not clearly understood. Clearly more detailed work on ice microstructural controls of permeability during flow events is needed.

6.3 Response to meteorological forcing

Despite the uncertainty in the controlling mechanisms for the onset of percolation, several observations on the response of snow ice formation to meterological conditions can be made. For accumulation rates typical of the RAB seas, flooding and snow ice formation are of minor importance until about 2 months after initial ice formation. After the initial thickening, the insulation provided by the snow pack prevents any significant further congelation growth, and most of the remaining thermodynamic thickening is by snow ice formation. Snow ice formation is primarily dependent on snow accumulation rates. On the scale of an ice floe, local variations in snow and ice thickness cause a heterogeneous distribution of flooding and snow ice formation, though as snow accumulates, this process tends to reduce the heterogeneity of the ice thickness along the floe.

Appendix A

Notation

R	isotopic ratio ($^{18}O/^{16}O$)
δ	$\delta^{18}O = \frac{R_{sample}}{R_{VSMOW}} - 1$
α_{eq}	fractionation factor, $R_s/R_l = 1.0029$
ϵ_{eff}	isotopic fractionation coefficient = $\alpha_{eq} - 1$
M	mass (ice, brine or salt)
dm	mass undergoing phase change
f	scaling factor
v	mean snow grain volume
q	heat flux
f_{sn}	snow fraction
z_{bl}	boundary layer thickness
v_i	ice growth rate
k_{eff}	salt segregation coefficient
Z	ice or snow thickness
a	effective atmospheric boundary layer thickness
D	diffusivity of salt or $H_2^{18}O$
u	seepage (Darcy) velocity
u_p	pore fluid velocity
P	pressure
K	permeability
μ	brine viscosity
d	grain size or tube diameter
Ra	Rayleigh number
Γ	thermal expansion coefficient
T	temperature

S	salinity
ϕ	porosity (relative brine volume)
ρ	density
C	specific heat
L	latent heat of fusion
k	thermal conductivity
I_o	surface radiative flux
κ	radiative extinction coefficient
t	time
z	depth
F_w	ocean heat flux
F_l	incident long wave radiation
F_E	emitted long wave
F_s	sensible heat flux
F_e	latent heat flux
F_c	conductive heat flux
e	vapour pressure
σ	Stefan-Boltzmann constant
C	relative cloud fraction
v_b	brine volume
fb	freeboard
α	albedo
W_{sn}	snow overburden
η	snow viscosity
g	gravitational constant
τ	tortuosity
B	specific surface area
C	pore circularity
A	area

Subscripts

w	sea water
i	pure ice
b	brine
s	salt
si	sea ice
sn	snow
r	Rayleigh fractionation
c	fractionation due to grain coarsening
o	initial value

n.b. boldface indicates a vector quantity

Appendix B

Solution of convective transport equations

To solve (3.1)-(3.4), we first decompose $\mathbf{u}$ into solenoidal and irrotational constituents,

$$\mathbf{u} = \nabla \times \psi + \nabla\zeta \tag{B.1}$$

The second term on the right hand side of (B.1) represents brine flow due to volumetric expansion of water during freezing. Note that in 2 dimensions, the stream function, ψ, has only one component, perpendicular to the velocity. Taking the curl of (3.2) to eliminate the pressure term, we obtain

$$\nabla \times \frac{1}{\mathbf{K}} \nabla \times \psi = g \frac{\partial \rho_b}{\partial x} \tag{B.2}$$

This is strictly correct only for constant permeability, but typically $\nabla \times \psi >> \nabla\zeta$, so we neglect the influence of the smaller term on the Darcian flow. We can then express (3.1) as

$$\nabla \cdot \mathbf{u} = \nabla^2 \zeta = \frac{(\rho_i - \rho_b)}{\rho_w} \frac{\partial \phi}{\partial t} \tag{B.3}$$

The energy equation (3.3) can be simplified by noting that over the small range of temperatures of interest here, $S_b \sim T$. Then, combining (3.3) and (3.4), we obtain

$$(\rho_{si}C_{si} - L\frac{\rho_b\phi}{T})\frac{\partial T}{\partial t} + \rho_b(C_b - \frac{L}{T})\nabla \cdot (\mathbf{u}T) = \nabla \cdot k\nabla T \tag{B.4}$$

To solve the modified set of equations (3.4),(3.5),(B.1)-(B.4), we first solve for the stream function, ψ, from (B.2), calculate the velocities assuming $\partial\phi/\partial t = 0$, then solve (3.4) and (B.4). Material properties are updated to determine $\partial\phi/\partial t$, and (B.3) is solved. Using the total velocity, the final solution is calculated using (3.4),(3.5) and (B.4), and all material properties are recalculated. Only one iteration is performed for computational efficiency.

Equations (3.4),(3.5) and (B.4) are solved using an implicit alternating direction technique, while (B.2) and (B.3) are solved by an iterative under-relaxation Poisson solver. The vertical velocity at the upper boundary is set to zero, and the horizontal velocity is set to zero at the open lower boundary. Lateral boundaries are periodic.

Bibliography

Abel's, G., Beobachtungen der täglichen Periode der Temperatur im Schnee und Bestimmung des Wärmeleitungsvermogens des Schnees als Function seiner Dichtigkeit (Observations of daily temperature variations in a snow cover), *Rep. Meteorol. Herausgegeben K. Akad. Wiss.*, *15*, 1-53, 1893.

Ackley, S. F., Sea-ice pressure ridge microbial communities, *Antarct. J. U.S.*, *21*(5), 172-174. 1986.

Adolphs, U., Ice thickness variability, isostatic balance and potential for snow ice formation on ice floes in the south polar Pacific Ocean, *J. Geophys. Res.*, *103*, 24,675-24,691, 1998.

Allison, I., and A. P. Worby, Seasonal changes in sea ice characteristics off East Antarctica., *Ann. Glaciol.*, *20*, 195-201, 1994.

Allison, I., R. E. Brandt, and S. G. Warren, East Antarctic sea ice: Albedo, thickness distribution, and snow cover, *J. Geophys. Res.*, *98*, 12,417-12,429, 1993.

Anderson, E. A., A point energy and mass balance model of a snow cover, *NOAA Tech. Rep. NWS 19*, 150 pp., U.S. Dep. of Commer., Washington, D.C., 1976.

Arons, E. M., and S. C. Colbeck, Geometry of heat and mass transfer in dry snow: A review of theory and experiment, *Rev. Geophys.*, *33*, 463-493, 1995.

Bear, J., *Dynamics of Fluids in Porous Media*, Elsevier Sci., New York, 1972.

Bennington, K. O., Desalination features in natural sea ice, *Int. J. Heat Mass Transfer*, *30*, 2171-2187, 1987.

Bennon, W. D., and F. P. Incropera., A continuum model for momentum, heat and species transport in binary sold-liquid phase change systems. II. Application to solidification in a rectangular cavity, *J. Glaciol.*, *6*, 845–857, 1967.

Bromwich, D. H., R. I. Cullather, and M. L. Van Woert, Antarctic precipitation and its contribution to the global sea-level budget, *Ann. Glaciol.*, *27*, 220–226, 1998.

Burton, J. A., R. C. Prim, and W. P. Slichter, The distribution of solute in crystals grown from the melt. Part I. Theoretical, *J. Chem. Phys.*, *21*, 1987–1991, 1953.

Choudhury, B., Radiative properties of snow for clear sky solar radiation, *Cold Reg. Sci. Technol.*, *4*, 103–120, 1981.

Colbeck, S. C., The capillary effects on water percolation in homogeneous snow, *J. Glaciol.*, *13*, 85–97, 1983a.

Colbeck, S. C., Ice crystal morphology and growth rates at low supersaturations and high temperatures, *J. Appl. Phys.*, *54*(5), 2677–2682, 1983b.

Cole, D. M., and L. H. Shapiro, Observations of brine drainage networks and microstructure of first-year sea ice, *J. Geophys. Res.*, *103*, 21,739–21,750, 1998.

Cottier, F., H. Eicken, and P. Wadhams, Linkages between salinity and brine channel distribution in young sea ice, *J. Geophys. Res.*, *104*, 15,859–15,871, 1999.

Cox, G. F. N., and W. F. Weeks, Brine drainage and initial salt entrapment in sodium chloride ice, *CRREL Res. Rep. 345*, 46 pp., U.S. Army Cold Reg. Res. and Eng. Lab., Hanover, N.H., 1975.

Cox, G. F. N., and W. F. Weeks, Equations for determining gas and brine volumes in sea ice, *J. Glaciol.*, *29*, 306–316, 1983.

Cox, G. F. N., and W. F. Weeks, Numerical simulations of the profile properties of undeformed first-year sea ice during the growth season, *J. Geophys. Res.*, *93*, 12,449–12,460, 1988.

Crocker, G. B., A physical model for predicting the thermal conductivity of brine-wetted snow, *Cold Reg. Sci. Technol.*, *10*, 69–74, 1984.

Crocker, G. B., and P. Wadhams, Modelling Antarctic fast-ice growth, *J. Glaciol.*, *35*, 3–8, 1989.

Drinkwater, M. R., and V. I. Lytle, ERS 1 radar and field-observed characteristics of autumn freeze-up in the Weddell Sea, *J. Geophys. Res.*, *102*, 12,593–12,608, 1997.

Eicken, H., Salinity profiles of Antarctic sea ice: Field data and model results, *J. Geophys. Res.*, *97*, 15,545–15,557, 1992.

Eicken, H., Deriving modes and rates of ice growth in the Weddell Sea from microstructural, salinity and stable-isotope data., in *Antarctic Sea Ice: Physical Processes, Interactions and Variability*, edited by M. O. Jeffries, *Antarct. Res. Ser.*, vol. 74, pp. 89–122, AGU, Washington, D.C., 1998.

Eicken, H., M. Lange, H.-W. Hubberten, and P. Wadhams, Characteristics and distribution patterns of snow and meteoric ice in the Weddell Sea and their contribution to the mass balance of sea ice, *Ann. Geophys.*, *12*, 80–93, 1994.

Eicken, H., H. Fischer, and P. Lemke, Effects of the snow cover on Antarctic sea ice and potential modulation of its response to climate change, *Ann. Glaciol.*, *21*, 369–376, 1995.

Eicken, H., C. Bock, R. Wittig, H. Miller, and H.-O. Poertner, Magnetic resonance imaging of sea-ice pore fluids: Methods and thermal evolution of pore microstructure, *Cold Reg. Sci. Technol.*, 2000.

Fichefet, T., and M. A. Morales Maqueda, Modelling the influence of snow accumulation and snow-ice formation on the seasonal cycle of the antarctic sea-ice cover, *Climate Dyn.*, *15*, 251–268, 1999.

Freitag, J., The hydraulic properties of Arctic sea-ice - implications for the small scale particle transport, *Ber. Polarforsch. 325*, 150 pp., Alfred-Wegner-Inst., Bremerhaven, Ger., 1999.

Fritsen, C. H., V. I. Lytle, S. F. Ackley, and C. W. Sullivan, Autumn bloom of antarctic pack-ice algae., *Science*, *266*, 782–784, 1994.

Fritsen, C. H., S. F. Ackley, J. N. Kremer, and C. W. Sullivan, Flood-freeze cycles and microalgal dynamics in Antarctic pack ice, in *Antarctic Sea Ice: Biological Processes, Interactions and Variability*, edited by M. P. Lizotte and K. O. Arrigo, *Antarct. Res. Ser.*, vol. 73, pp. 1–21, AGU, Washington, D.C., 1998.

Giovinetto, M. B., D. Bromwich, and G. Wendler, Atmospheric net transport of water vapor and latent heat across 70°S, *J. Geophys. Res.*, *97*, 917–930, 1992.

Golden, K. M., S. F. Ackley, and V. I. Lytle, The percolation phase transition in sea ice, *Science*, *282*, 2238–2241, 1998.

Goodrich, L. E., Efficient numerical technique for one-dimensional thermal problems with phase change, *Int. J. Heat Mass Transfer*, *21*, 615–621, 1978.

Gordon, A. L., and B. A. Huber, Southern Ocean winter mixed layer, *J. Geophys. Res.*, *95*, 11,655–11,672, 1990.

Grenfell, T. C., The effects of ice thickness on the exchange of solar radiation over the polar oceans, *J. Glaciol.*, *22*, 305–320, 1979.

Heavner, M. J., Optical spectroscopic observations of sprites, blue jets, and elves: Inferred microphysical processes and their macrophysical implications, Ph.D. thesis, Univ. of Alaska Fairbanks, 1999.

Heil, P., I. Allison, and V. Lytle, Seasonal and interannual variations of the oceanic heat flux, *J. Geophys. Res.*, *101*, 25,741–25,752, 1996.

Hill, J. M., *One-Dimensional Stefan Problems: An Introduction*, *Pitman Monogr. Surv. Pure Appl. Math.*, vol. 31, John Wiley, New York, 1987.

Hudier, E. J.-J., R. Ingram, and K. Shirasawa, Upward flushing of sea water through first year ice, *Atmos. Ocean*, *33*, 569–580, 1995.

Jacobs, S. S., and J. C. Comiso, A recent sea-ice retreat west of the Antarctic Peninsula, *Geophys. Res. Lett.*, *20*, 1171–1174, 1993.

Jacobs, S. S., R. G. Fairbanks, and Y. Horibe, Origin and evolution of water masses near the Antarctic continental margin: Evidence from $h_2{}^{18}O/h_2{}^{16}O$ ratios in seawater, in *Oceanology of the Antarctic Continental Shelf*, edited by S. S. Jacobs, *Antarct. Res. Ser.*, vol. 43, pp. 59–85, AGU, Washington, D.C., 1985.

Jeffries, M. O., and U. Adolphs, Early winter ice and snow thickness distribution, ice structure and development of the western Ross Sea pack ice between the ice edge and the Ross Ice Shelf, *Antarct. Sci.*, *9*, 188–299, 1997.

Jeffries, M. O., R. Shaw, K. Morris, A. L. Veazey, and H. R. Krouse, Crystal structure, stable isotopes ($\delta^{18}O$) and development of sea ice in the Ross, Amundsen, and Bellingshausen seas, Antarctica, *J. Geophys. Res.*, *99*, 985–995, 1994.

Jeffries, M. O., A. Worby, K. Morris, and W. Weeks, Seasonal variations in the properties and structural composition of sea ice and snow cover in the Bellingshausen and Amundsen Seas, Antarctica, *J. Glaciol.*, *43*, 138–152, 1997.

Jeffries, M. O., B. Hurst-Cushing, H. R. Krouse, and T. Maksym, The role of snow in the thickening and mass budget of first-year floes in the eastern Pacific sector of the Antarctic pack ice, *Geophys. Inst. Rep. UAGR-327*, 34 pp., Univ. of Alaska Fairbanks, 1998a.

Jeffries, M. O., S. Li, R. A. Jaña, H. R. Krouse, and B. Hurst-Cushing, Late winter first-year ice floe thickness variability, seawater flooding and snow ice formation in the Amundsen and Ross Seas, in *Antarctic Sea Ice: Physical Processes, Interactions and Variability*, edited by M. O. Jeffries, *Antarct. Res. Ser.*, vol. 74, pp. 69–87, AGU, Washington, D.C., 1998b.

Jeffries, M. O., H. R. Krouse, B. Hurst-Cushing, and T. Maksym, Snow ice accretion and snow cover depletion on antarctic first-year sea ice floes., *Ann. Glaciol.*, 2001.

Kaviany, M., *Principles of Heat Transfer in Porous Media*, 2 ed., Springer-Verlag, New York, 1995.

Kawamura, T., K. I. Ohshima, T. Takizawa, and S. Ushio, Physical, structural, and isotopic characteristics and growth processes of fast sea ice in Lützow-Holm Bay, Antarctica, *J. Geophys. Res.*, *102*, 3345–3355, 1997.

Key, J. R., R. Silcox, and R. Stone, Evaluation of surface radiative flux parameterizations for use in sea ice models, *J. Geophys. Res.*, *101*, 3839–3849, 1996.

Kovacs, A., Sea ice part I. Bulk salinity versus ice floe thickness, *CRREL Rep. 96-7*, 16 pp., U.S. Army Cold Reg. Res. and Eng. Lab., Hanover, N.H., 1996.

Kuroiwa, D., Liquid permeability of snow, *IAHS Publ.*, *79*, 380–391, 1968.

Lake, R. A., and E. L. Lewis, Salt rejection by sea ice during growth, *J. Geophys. Res.*, *75*, 583–597, 1970.

Lange, M. A., and H. Eicken, Textural characteristics of sea ice and the major mechanisms of ice growth in the weddell sea, *J. Glaciol.*, *96*, 4821–4837, 1991.

Lange, M. A., and H.-W. Hubberten, Isotopic composition of sea ice as a tool for understanding sea ice processes in the polar regions, in *Physics and Chemistry of Ice*, edited by N. Maeno and T. Hondoh, pp. 399–405, Hokkaido University Press, Sapporo, Japan, 1992.

Lange, M. A., S. F. Ackley, P. Wadhams, G. S. Dieckmann, and H. Eicken, Development of sea ice in the Weddell Sea, *Ann. Glaciol.*, *12*, 92–96, 1989.

Lange, M. A., P. Schlosser, S. F. Ackley, P. Wadhams, and G. Dieckmann, $\delta^{18}O$ concentrations in sea ice of the Weddell Sea, *J. Glaciol.*, *36*, 315–323, 1990.

Leppäranta, M., A growth model for black ice, snow ice and snow thickness in subarctic basins, *Nord. Hydrol.*, *14*, 59–70, 1983.

Leppäranta, M., A review of analytical models of sea-ice growth, *Atmos. Ocean*, *31*, 123–138, 1993.

Lytle, V. I., and S. F. Ackley, Heat flux through sea ice in the western Weddell Sea: Convective and conductive transfer processes, *J. Geophys. Res.*, *101*, 8853- 8868, 1996.

Lytle, V. I., K. C. Jezek, S. P. Gogineni, and A. R. Hosseinmostafa, Field observations of microwave backscatter from the Weddell Sea ice, *Int. J. Remote Sensing*, *17*, 167–180, 1996.

Maksym, T., and M. O. Jeffries, Bulk salinity characteristics of first-year sea ice in the Pacific sector of the southern oceans, *Antarct. J. U.S.*, *31*(2), 99–101, 1996.

Marsh, P., and M.-K. Woo, Wetting front advance and freezing of meltwater within a snow cover 1. Observations in the Canadian arctic, *Water Resour. Res.*, *20*, 1853–1864, 1984.

Martin, S., A field study of brine drainage and oil entrainment in first year sea ice, *J. Glaciol.*, *22*, 473–502, 1979.

Martin, S., Y. Yu, and R. Drucker, The temperature dependence of frost flower growth on laboratory sea ice and the effect of the flowers on infrared observations of the surface, *J. Geophys. Res.*, *101*, 12,111–12,125, 1996.

Massom, R. A., M. R. Drinkwater, and C. Haas, Winter snow cover on sea ice in the Weddell Sea, *J. Geophys. Res.*, *102*, 1101–1117, 1997.

Massom, R. A., V. I. Lytle, A. P. Worby, and I. Allison, Winter snow cover variability on East Antarctic sea ice, *J. Geophys. Res.*, *103*, 24,837–24,855, 1998.

Maykut, G. A., Energy exchange over young sea ice in the central Arctic, *J. Geophys. Res.*, *83*, 3646–3658, 1978.

Maykut, G. A., and N. Untersteiner, Some results from a time-dependent thermodynamic model of sea ice, *J. Geophys. Res.*, *76*, 1550–1576, 1971.

McGuinness, M. J., H. J. Trohdahl, K. Collins, and T. G. Haskell, Non-linear thermal transport and brine convection in first-year sea ice, *Ann. Glaciol.*, *27*, 471–476, 1998.

McPhee, M. G., D. G. Martinson, and J. H. Morison, Upper-ocean measurements of turbulent flux in the western Weddell Sea, *Antarct. J. U.S.*, *27*(5), 103–105, 1992.

Nakawo, M., S. Chiba, H. Satake, and S. Kinouchi, Isotopic fractionation during grain coarsening of wet snow, *Ann. Glaciol.*, *18*, 129–134, 1993.

Ni, J., and F. P. Incropera, Extension of the continuum model for transport phenomena occurring during metal alloy solidification-I. The conservation equations, *Int. J. Heat Mass Transfer*, *38*, 1271–1284, 1995.

Niedrauer, T. M., and S. Martin, An experimental study of brine drainage and convection in young sea ice, *J. Geophys. Res.*, *84*, 1176–1186, 1979.

Ono, N., and T. Kasai, Surface layer salinity of young sea ice, *Ann. Glaciol.*, *6*, 298–299, 1985.

Patankar, S. V., *Numerical Heat Transfer and Fluid Flow*, Hemisphere, New York, 1980.

Perovich, D. K., and A. J. Gow, A quantitative description of sea ice inclusions, *J. Geophys. Res.*, *101*, 18,327–18,343, 1996.

Rapley, M., and V. I. Lytle, Brine infiltration in the snow cover of sea ice in the eastern Weddell Sea, Antarctica, *Ann. Glaciol.*, *27*, 461–465, 1998.

Raymond, C. F., and K. Tusima, Grain coarsening of water-saturated snow, *J. Glaciol.*, *22*, 83–105, 1979.

Saeki, H., T. Takeuchi, M. Sakai, and E. Suenaga, Experimental study on permeability coefficient of sea ice, in *Ice Technology, Proceedings: 1st International Conference*, edited by T. K. S. Murthy, J. J. Connor, and C. A. Brebbia, pp. 237–246, Springer-Verlag, New York, 1986.

Saito, T., and N. Ono, Percolation in sea ice, I. Measurements of kerosene permeability of NaCl ice, *Low Temp. Sci., Ser. A*, *37*, 55–62, 1978.

Saito, T., and N. Ono, Percolation in sea ice, II. Brine drainage channels in young sea ice., *Low Temp. Sci., Ser. A*, *39*, 127–132, 1980.

Saloranta, T., Modeling the evolution of snow, snow ice and ice in the Baltic Sea, *Tellus*, *52A*, 93–108, 2000.

Schulze, T. P., and M. Worster, A numerical investigation of steady convection in mushy layers during the directional solidification of binary alloys, *J. Fluid Mech.*, *356*, 199–220, 1997.

Schwerdtfeger, P., The thermal properties of sea ice, *J. Glaciol.*, *4*, 789–807, 1963.

Shimizu, H., Air permeability of deposited snow, *Contrib. Inst. Low Temp. Sci. Ser. A*, *22*, 32 pp., Inst. Low Temp. Sci., Sapporo, Japan, 1970.

Sturm, M., The role of thermal convection in heat and mass transport in the subarctic snow cover, *CRREL Rep. 91-19*, 82 pp., U.S. Army Cold Reg. Res. and Eng. Lab., Hanover, N.H., 1991.

Sturm, M., J. Holmgren, M. Konig, and K. Morris, The thermal conductivity of seasonal snow, *J. Glaciol.*, *43*, 26–41, 1997.

Sturm, M., K. Morris, and R. Massom, The winter snow cover of the west Antarctic pack ice: Its spatial and temporal variability, in *Antarctic Sea Ice: Physical Processes, Interactions and Variability*, edited by M. O. Jeffries, *Antarctic Research Series*, vol. 74, pp. 1–18, AGU, Washington, D.C., 1998.

Tait, S., and C. Jaupart, Compositional convection in a reactive crystalline mush and melt differentiation, *J. Geophys. Res.*, *97*, 6735–6756, 1992.

Takizawa, T., Salination of snow on sea ice and formation of snow ice, *Ann. Glaciol.*, *6*, 309–310, 1985.

Tison, J.-L., R. D. Lorrain, A. Bouzette, M. Dini, A. Bondesan, and M. Stévenard, Linking landfast sea ice variability to marine ice accretion at Hells Gate Ice Shelf, Ross Sea, in *Antarctic Sea Ice: Physical Processes, Interactions and Variability*, edited by M. O. Jeffries, *Antarctic Research Series*, vol. 74, pp. 375–407, AGU, Washington, D.C., 1998.

Ukita, J., T. Kawamura, N. Tanaka, T. Toyota, and M. Wakatsuchi, Physical and stable isotopic properties and growth processes of sea ice collected in the southern Sea of Okhotsk, *J. Geophys. Res.*, *105*, 22,083–22,093, 2000.

Wade, R. H., Studies of the geophysics of sea ice, Ph.D. thesis, Univ. of Alaska Fairbanks, 1993.

Wadhams, P., M. A. Lange, and S. F. Ackley, The ice thickness distribution aross the Atlantic sector of the Antarctic Ocean in midwinter, *J. Geophys. Res.*, *92*, 14,535–14,552, 1987.

Wakahama, G., The metamorphism of wet snow, *IAHR, pub. 79*, 370–379, 1968.

Wakatsuchi, M., Brine exclusion process from growing sea ice, *Contrib. Inst. Low Temp. Sci. Ser. A, 30*, pp. 29–65, Inst. Low Temp. Sci., Sapporo, Japan, 1983.

Weeks, W. F., and S. F. Ackley, The growth, structure and properties of sea ice, in *Geophysics of Sea Ice*, edited by N. Untersteiner, *NATO ASI Ser., Ser. 3*, vol. 146, pp. 9–146, Plenum, New York, 1986.

Weeks, W. F., and O. S. Lee, Observations on the physical properties of sea ice at Hopedale, Labrador, *Arctic*, *11*, 92–108, 1958.

Weissenberger, J., G. Dieckmann, R. Gradinger, and M. Spindler, Sea ice: A cast technique to examine and analyze brine pockets and channel structure, *Limnol. Oceanogr.*, *37*, 179–183, 1992.

Weller, G., Radiation flux investigation, *AIDJEX Bull.*, *14*, 28–30, 1972.

Wettlaufer, J. S., M. G. Worster, and H. E. Huppert, The phase evolution of young sea ice, *Geophys. Res. Lett.*, *24*, 1251–1254, 1997.

Wooding, R. A., The stability of a viscous liquid in a vertical tube containing porous material, *Proc. R. Soc. London, Ser. A*, *252*, 120–134, 1959.

Worby, A., and I. Allison, Ocean-atmosphere energy exchange over thin, variable concentration Antarctic pack ice, *Ann. Glaciol.*, *15*, 184–190, 1991.

Worby, A., and R. Massom, The structure and properties of sea ice and snow cover in east antarctic pack ice, *Res. Rep. 7*, Antarctic CRC, Hobart, Australia, 1995.

Worby, A. P., M. O. Jeffries, W. F. Weeks, K. Morris, and R. Jaña, The thickness distribution of sea ice and snow cover during late winter in the Bellingshausen and Amundsen Seas, Antarctica, *J. Geophys. Res.*, *101*, 28,441–28,455, 1996.

Worby, A. P., R. A. Massom, I. Allison, V. I. Lytle, and P. Heil, East Antarctic sea ice: A review of its structure, properties, and drift, in *Antarctic Sea Ice: Physical Processes, Interactions and Variability*, edited by M. O. Jeffries, *Antarctic Research Series*, vol. 74, pp. 41–67, AGU, Washington, D.C., 1998.

Worster, M. G., Solidification of an alloy from a cooled boundary, *J. Fluid Mech.*, *167*, 481–501, 1986.

Worster, M. G., Convection in mushy layers, *Ann. Rev. Fluid Mech.*, *29*, 91–122, 1997.

Worster, M. G., and J. Wettlaufer, Natural convection, solute trapping, and channel formation during solidification of saltwater, *J. Phys. Chem.*, *101*, 6132–6136, 1997.

Yen, Y.-C., Review of thermal properties of snow, ice and sea ice, *CRREL Rep. 81-10*, 27 pp., U.S. Army Cold Reg. Res. and Eng. Lab., Hanover, N.H., 1981.

Zillman, J. W., A study of some aspects of the radiation and heat budgets of the Southern Hemisphere oceans, *Meteorol. Stud. 26*, 562 pp., Bur. of Meteorol., Dep. of the Inter., Canberra, A.C.T., Australia, 1972.

Table 14. Student Opinion Survey 1999 Gender and Ethnicity for UWM Total Responses

Status	Gender		Ethnicity					
	Male	Female	Caucasian	African American	Hispanic	Native American	Southeast Asian	Other
No Responses	0	0	0	0	0	0	0	0
Freshmen	50	14	50	1	1	0	9	0
Sophomore	102	22	100	7	4	0	0	0
Junior	106	27	100	9	3	2	7	0
Senior	81	14	67	5	3	0	12	0
Totals	339	77	317	22	11	2	28	0

The review of the data in Table 13 (Gender and Ethnicity) has very little, if any value, other than the fact that 416 (94%) of the students responded to the question of gender and only 86 percent responded to ethnicity. The results showed that 339 (77%) male students responded to the survey. The number of male participants in the survey reflects what was found in the literature review indicating that the field of engineering and computer science is mostly male driven.

The number of Students of Color (ethnicity groups other than Caucasian) that responded in the survey by status was 11 freshmen, 11 sophomores, 21 juniors, and 20 seniors, totaling 63 (14%).

Moore and others (1983) indicate that those students with distinctive characteristics that are perceived by the academic community placed in with the vast majority of students that enter college are not only disproportional in

number but also need additional resources. The more resources available for students in the form of support mechanism, controlled specified study techniques implemented, and adequate study time allocated by students, the greater the retention rates among freshmen.

Again, studies by Tinto (1975) revealed that the forces that contribute to dropouts were the lack of commitments. These commitments were from the individual and the institution. The individual 's commitment took many dimensions but materialized from family, individual attributes, and pre-college training. These same elements became the forces that drove institutional commitment that led other researchers, authors, and educators to agree upon the six themes.

The findings and conclusions from the analyses of the instruments used in this study are discussed in chapter five. Chapter five provides a short synopses of the previous chapters along with suggestive measures, if implemented that would increase the retention rates of students in CEAS and help students achieve academic success or their academic goals. This increase would automatically increase the University's overall rating and increase its' ranking of retention between the Urban 13 List and those nationally.

CHAPTER FIVE: SUMMARY AND CONCLUSIONS

Summary and Conclusions

This chapter contains the summary of the previous chapters, findings and conclusions from the six instruments, and recommendations of the results of this study. The chapter summary provides only the overview of data presented. Since six instruments were used, conclusions regarding each instrument (variable) will be discussed, followed by some overall conclusions. The recommendations, if implemented, can be used to increase the retention rates of students in the College of Engineering and Applied Science.

Synopsis Review of the Problem

A number of arguments have been made regarding the retention of freshmen students. One of the primary arguments is that the retention of college freshmen is an indicator of a college's ability to meet the needs of the students. These needs are more diverse than the population of the institution.

One of the initial objectives for doing this research was to investigate the retention rates of similar institutions to UWM with higher retention rates and identify factors that affected retention. A second objective was to discover what students in engineering and computer science felt were major contributors or factors that impacted their decision to remain in school after their freshman year. The final objective was to use the literature review, results and the methodology found, and other schools retention practices to establish measures that would

increase the retention rate of students in the College of Engineering and Applied Science at the University of Wisconsin-Milwaukee.

This research becomes a benefit not only to the College, but also to the University. An increase in retention rate of CEAS increases the retention rate of the University. If more students remain in school, the graduation rate increases and more professionals enter into the workforce.

This research is also grounded in the essence of institutional commitment to higher education. The University of Wisconsin-Milwaukee is in the business of meeting students' expectations, and then they must create an environment where students are allowed to be successful.

The literature review focused on a brief history overview on when studies of retention began, what were some of the elements and factors that were found in various studies, what models were designed to provide measures, techniques and strategies to assist institutions of higher education to retain freshman. Once these entities were addressed, institutions used some of the measures listed and adapted models to address retention in their institution that had positive outcomes.

Studies of retention of students in higher education were identified as an issue as early as 1931 by the U. S. Department of Education. Theorists, educators, authors, and researchers found it impossible to pinpoint the single, specific reason why students did not return to college after their freshman year.

However, many agreed to think of causes that attributed to retention in terms of six themes. The themes were:

1. Academic boredom and uncertainty about what to study,
2. Transition/adjustment problems,
3. Unrealistic expectations of college,
4. Academic under preparedness,
5. Incompatibility, and
6. Irrelevancy.

Researchers and others felt that the solutions to these themes could be found in academic and student support services.

Researchers and others continued to study the causes of retention and in the late 1960s they found that the six themes were centered on three stages: Enrollment management, organizational development/supportive community, and action-oriented responses. The studies and works of researchers, authors, and educators focused on one or a combination of these stages. Figure 2.2 Literature Review Summary indicates the themes, stages, approaches and models used by individuals as they addressed the factors associated with retention. The figure also shows institutions that modified the models and implemented programs to address the retention issue in their school.

The main variables assessed in this study look at what causes students to stay or leave CEAS after their freshmen year. However, to achieve the objectives

in this study, chapter three outlined the designs utilized, the data collection methods, the sample, and instruments used to address this investigation.

The design of this research is a case study, using both qualitative and quantitative research. This case study (UWM/CEAS) is centered on the characteristics of a phenomenon (retention) that was investigated by the researcher on-site over a period of less than 16 weeks or one academic semester. The quantitative aspect of this research was using the factors that contributed to the students to remain in school as an explanation of the problem of retention and to predict what measures to use in retaining the students after their freshman year. This research was also correlational because the researcher looked at relationship of the retention rates between the different institutions.

The data collection method utilized the results from six different instruments other than the information found in the literature review.

The sample used in this study was from the population of students at the University of Wisconsin-Milwaukee in the College of Engineering and Applied Science in 1999

The six instruments used in this study were:

- Analysis of the advising Session Notes
- Results from the advising of student using the Re-Instatement Contracts for re-entering on final probation,
- Freshmen Orientation course evaluation results,

- Comparison of retention rates ranking data of the top 13 national engineering schools and the top three urban 13 schools with the retention rates and ranking of UWM,
- Interview with administrators in engineering schools of the three top urban 13 schools, and
- A Student Opinion Survey.

The results of the instruments used in this study were presented in chapter four. The summary of each instrument follows.

The advising session notes of 307 out of 783 (39%) inactive student files were reviewed by the researcher/advisor to reconfirm some of the reasons students stated attributed to the cause of them leaving. All of the reasons stated fit into one or more of the six themes defined by theorists, and others in the literature review. The researcher found 174 (57%) of the student's files with only one or two advising notations. Students are urged to meet with their advisor during the semester and notations were made from each session, the conclusion drawn is that either the student did not meet with the advisor during the year or the advisor did not record the event. Since the researcher was the only advisor from 1995 until 1999 and files for each appointment were pulled at the beginning of each day, the margin of error on the behalf of not making notations in the file is extremely small. A student file was generated prior to the student advising and registration (STAR) meeting with the student. Therefore, the student did not met with the advisor until a critical point was reached in their academic career.

The second instrument used was the Re-Instatement Contract signed by students returning on final probation. The nine out of 11 students that returned weekly with assignments and notes from each class improved their grade point average and were able to continue the next semester. The results from this instrument confirm what was found in the literature review especially noted by Lenning (1982). His work shows that good study skills and habits result in good grades connect with the theme of students leaving caused by academic underpreparedness. The results from this instrument were so positive that the contract has been modified and is being used by all advisors in CEAS.

Again, W. R. Habley (1981) indicated that intense advising-retention models provides the most significant mechanisms through which student achieve academic success.

Finally, one of the elements used in Thomas & Chickering (1984) study revealed that skill-building techniques are essential for academic success.

The results from the third instrument and results and comments from the students in the EAS 100 Freshmen Orientation course, indicate that the course is an effective method of reaching freshmen students. The topics discussed in this course address all of the themes found in the literature review associated with retention. According to the syllabus (See Appendix C), the topic: Keys to Success in Engineering Study, is discussed early in the class. This topic includes discussions centered on determination, effort, approach note taking skills, reading assignments, and test taking skills. The timing of the discussions is so

that student can implement the techniques in the beginning of the semester. The comments of the students are reviewed and some adjustments are made in the next year's syllabus.

The retention rates and ranking was the fourth instrument used in this study. The comparison of institutions on the Urban 13 List that had an engineering program older than five years, with a retention rate of five percentage points higher than UWM, and the institutions using the ACT scores resulted in three institutions. These institutions were compared with the top 13 national engineering institutions ranked by U. S. News and World Report for the years 1995 and 1998. Three categories other than retention were compared because studies found in the literature review revealed that institutions review the ACT/SAT and High School rankings of prospective students during the admission process. Another category used was the faculty/student ratio. Again, researchers have indicated that faculty commitment; support and involvement are crucial in the process of maintaining students (Tinto, 1975; Beal & Noel, 1980; Noel & Levitz, 1982).

The results from the comparisons of the retention rates showed that UWM's retention rates for both years were lower than any of the other institutions during the same period of time.

The second category compared in the ranking of the schools was the ACT/SAT. Schools that used the ACT 25th-75th percentile data were only used

in the comparison because the ACT scores were used for UWM. The results in this area revealed that UWM's ACT score (21) for accepting students was higher than one other Urban 13 school (University of Memphis, 20), but the retention rate of the other institution was 12-percentage points higher in the same year (1995). In 1996 the ACT score for UWM was the same as another Urban 13 school (19, 19), however the retention rate of the other institution (University of Memphis) was eight percentage points higher than UWM. In 1995 the ACT score for UWM and the University of Cincinnati acceptance level was the same (21, 21), but the retention rate for the University of Cincinnati for that year was six percentage points higher than the retention rate at UWM. These results indicated that the students that score lower on the ACT are accepted at another institution, but other institution's retention rates are higher.

According to a study based on the ACT Program's College Outcome Measures Program and research by Forrest (1982), the ACT is used to predict how well students may succeed in college. An analysis of the ACT scores of the schools in this study shows that schools with higher ACT scores had higher retention rates with the exception of UWM. UWM's retention rate is lower and the ACT score is high which indicates that either there are exceptions or there are other factors or measures not used in this analysis. Examples of others would be programs, strategies, and techniques the institution has in place to addresses factors associated with low retention. Another exception is that UWM does not fit the model. The literature review, formal retention programs implemented at

other institutions, along with the researcher's experience and knowledge of the College indicate that the problem is UWM.

The third category is the student/faculty ratio. The category can only be reviewed for the 1995 year because the data for all schools were not available in 1998. However, the results indicated that in 1995, UWM's student/faculty ratio was the same as the four other schools on the list, but the retention rates of the other schools were 14 to 21 percentage points higher. Of these institutions, one was an Urban 13 school with a retention rate of 14 percentage points higher, and one of the other Urban 13 schools was a University of Wisconsin System school with a retention rate of 21-percentage points higher.

The fourth and final category used in the comparison was the freshmen in the top 10 percent of their high school class. UWM's data for both years was the lowest of all the institutions. These data were consistent with information found in the literature. However, there were no data available on the following two statements. These statements were:

1. A comparison of these data cannot be used to accurately reflect the top 10 percent. Simply because the students in the top 10 percent of one high school may be different at another high school and the standard may differ among the high school (Pantages & Creedon, 1987).
2. The students that graduate from high school in the top 10 percent of their class are not the dominant population of the freshmen classes at UWM.

The researcher used the data from this category for informational purposes.

The information received from the interviews of the Urban 13 List schools revealed that the special programs that were implemented in their institution along with a combination of "the right people doing the right things in the right environment "contributed to their retention rate. A variety of pilot studies had been in place for several years and the institutions implemented some and discarded others but the administration felt that no one plan has attributed to the success of their retention rate. It was a combination of having the right people, in the right position, implementing the right programs, at the right time, in the right environment. A change in any one of these elements would have an impact upon their retention rate. All of these elements are constantly changing and they must be closely monitored or altered to compensate for the change. The literature revealed causal models by Spady and Astin (1971), theoretical model by Tinto (1975), and longitudinal models by Tinto (1987) designed for institutions to combat retention.

The results from the sixth instrument (Student Opinion Survey) revealed that 89.8 percent of the students felt that college advising was the "no influential" contributing factor that impacted the success of their freshman year. The students (84.1 percent) indicated that faculty involvement did not contribute to their freshman year success. The literature review revealed studies conducted by Beal & Noel, (1980) Habley (1981), Levitz, (1983), Crockett (1985) and others that academic advising is a powerful influence on student development and learning that fosters retention. The literature review also revealed that faculty members are key forces in the retention of students (Beal & Noel, 1980; Crockett, 1985).

Based upon the literature review and the percentages from the survey, one can conclude that college advising and faculty involvement are areas that the college needs to review and become a greater force to become a catalyst that influences the retention rate.

The students that participated in the survey felt that time management was the element that contributed most to the success of their freshman year experience. However, the main focus of this survey was to determine what factors contributed to the success of their freshmen year and students classified, as freshmen had not completed their freshman year, therefore they were eliminated from the remainder of the results. The opinions of the students with "other" status had a high response rate but they were few in number and were eliminated. The gender and ethnicity response data were also insignificant due to the low response rates that are also indicative of the lack of diversity with the field and College. Therefore, the responses evaluated are from sophomores, juniors, and seniors.

An analysis of the sophomore's responses that best represented the degree to which each component impacted the success of their freshmen year were ranked in order of the percentage indicating "very influential". The order is time management (37%), study habits (36%), study team (36%), reduced work schedule (30%), family support (29%), high school preparation (22%), faculty involvement (8%), and college advising (2%).

The juniors, seniors, and others were ranked in the order of the percentage indicating "very influential". The rankings from students classified as "others"

are not significant because there were only 12 students in this classification that participated in the survey.

The responses ranked "very influential from the juniors were time management (42%), study habits (38%), family support (36%), high school preparation (32%), reduced work schedule (25%), study team (20%), faculty involvement (18%), and college advising (9%).

In comparing the responses between the sophomores and juniors, the respondents indicated that the "very influential" contributing factors were time management and study habits. The "least influential" contributing factors were study team, faculty involvement and the very least being college advising.

The responses from seniors were ranked the order of very influential contributing factors that impacted the success of their freshman year. The respondents indicated family support (43%) first, followed by study habits (38%), and time management (37%). However, it is also important to note that they also considered the least influential to be study team (21%), faculty involvement (12%), and lastly college advising (8%).

A review of all responses from the sophomores, juniors, and seniors ranked the contributing factor that impacted the success of their freshmen year in the following order of significance:

1. Time Management (43.8%)
2. Family Support (43.9%)
3. Study Habits (40.9%)
4. High School Preparation (37.5%)

5. Reduced Work Schedule (35.3%)
6. Study Team (22.6%)
7. Faculty Involvement (15.9%)
8. College Advising (10.2%)

Each of the factors identified were found in the literature review as having an impact upon why students stay in school after their freshman year (Tinto, 1975). They also are fit into the themes that were discussed in the literature review. The analyses of the sophomores, juniors, and seniors that responded to the survey represented 32 percent of the total population of students in the College. These students ranked time management, as being the "very influential" factor that impacted the success of their freshmen year.

The factors that contributed to the retention in other institutions exist in CEAS and were documented in this study. The theories, strategies, and techniques used in other institutions, with modifications, if implemented, would perhaps improve the retention rate of freshmen in CEAS at UWM.

The catalyst that holds the key to implementing the programs, strategies, and techniques is the people (Tinto, 1975;Beal & Noel, 1980). Tinto and others supporters indicated that the commitment on behalf of the institution is one-half of the solution. There was no one reason why students did not return after their freshmen year and there is no one measure or quick fix that would have an impact upon retention. However, there are combinations of measures and strategies based upon this research and the researcher's knowledge that would

have an impact or contribute to retention. These recommendation, are based upon the collaborative efforts of people.

Recommendations/Conclusions

The recommendations/conclusions are in the form of measures, strategies and techniques resulting from this study and the knowledge and experience of the researcher as an advisor in the College of Engineering and Applied Science at UWM. These tools (measures, strategies and techniques), if implemented, would foster a cohesive working environment for staff, advisor and faculty to support the mission of the University.

These recommendations are discussed from the results of the six instruments.

Advising Sessions. All advising sessions should be recorded in each student's file. Freshmen students' files should be reviewed after six weeks into the semester and if an advising session has not occurred, the student should be contacted and asked to make an appointment. This session can be used for a variety of purposes: an introduction, establishing rapport, and assessing the needs of the student. If a student is having adjustment problems or academic problems, there is time to make adjustments. A notation should be made in the files if the appointment was not kept. A review of the freshmen eight-weeks grade report provides some indication of the performance of the student. Students with a grade report of "C" or less should be notified to make an appointment to discuss academic performance.

The six themes can be addressed during the advising sessions. The advisors can assist the student with boredom and uncertainty, transitional problems, provide the student with realistic expectations, assisting students to become better prepared, address the social and academic environment, and provide rationale for the content of the coursework.

Re-Instatement Contracts. Freshmen students should be admitted as pre-engineering or pre-computer science students. The first semester courses should be a selection from a group of standard courses: math, science, general education course, freshman orientation computer science, and English. These courses are selected during the STAR program. Students wanting to select a specific discipline must meet with an advisor to discuss the specifics of that discipline. The re-instatement contract should be modified into six different contracts, one for each discipline and signed during this session. The contract should be Pre-Mechanical or Pre-Computer Science and after satisfactorily completing the engineering/computer science core courses, the students meet again with the advisor and is admitted directly into the major after obtaining junior standing. The contract is used as a bonding tool between the student and the school through the advisor and must be completed before priority registration for the next semester.

It is noteworthy to mention that students entering CEAS prior to 1994 were initially admitted as pre-engineering majors. There were a number of factors that contributed to the failure of this status that would not be a factor

today. One of the failures was the lack of enough advisors. This has changed and the College has added three additional academic advisors.

First, the monitoring system of student's records was slow and cumbersome prior to 1994. Student's records were checked manually until 1994 and there was only one Academic Advisor. Since that time computerized programs have been designed and put into place to audit student's records. The College has added additional advisor.

Secondly, there has been a change in administration and more emphasis has been place on helping the students to succeed rather than just providing a curriculum. Previously, the focus was more on the institution and its curriculum rather than the students (Boyer, 1997).

Finally, the suggested new method utilizes the new computer program to monitor student records. The new computer program will also assist the student and will check the records and only allow the student to register for classes after prerequisites have been met. The new method provides an interacting and nurturing component to the pre-engineering or pre-computer science program that involves the faculty, other students (juniors) and advisor. This creates an academic environment that is inclusive for everyone that is a necessity for retaining students today (Tinsley, 1982).

Students taking ownership in their college commitments address the themes of incompatibility and irrelevancy. This ownership is emphasized and shown by signing the contract. Many of the students feel a sense of belonging and a part of the academic environment similar to what Tinsley (1982) stressed in

his work. Signing the contract will also assist the students to be more focused as indicated by Kuh, Schuh and others (1991).

EAS 100 Freshmen Orientation Course. This course should be redesigned and organized into a two semester series. All students entering the College for the first time should be required to enroll in the first series. This would also include transfer students admitted with less than 15 engineering core credits of a 2.0 GPA.

Transfer students that have completed more than 15 but less than 24 engineering core credits with a 2.0 GPA or above would be required to enroll in the second course. The first course should address the factors identified as the themes found in the literature review. Topics for discussion in the course would:

- provide solutions for boredom/uncertainty,
- address transition adjustment problems,
- provide unlimited realistic expectations parameters,
- assist students to determine if they are academically prepared, if not what resources are available to assist them,
- assist students in determining if the college is the best fit for them, and
- used explanations and examples that students can relate to and understand.

The instructor should utilize the comments found in the student evaluations to enhance the course. This class should also be structured so that it includes the design aspect for all the disciplines in the College.

The design aspect would be projects or assignments that encompassed computer science, mechanical, electrical, industrial, materials, and civil engineering concepts.

The course would also provide a mechanism that would allow the students to demonstrate that they are following the Guaranteed 4.0 Program (See next page). If students are not following the program, techniques and strategies should be in place so that the student can follow the program. The course should be changed from a one-credit course to a three-credit course

The second semester course should be designed or structured around a specific or a combination of specific disciplines. It should include a review of follow-up procedures from the first semester course. However, both of these courses must encompass a workshop that showcases faculty to student contact.

The research and studies conducted by Levitz (1983 & 1997), Gordon (1984), and Valverde (1985) support a freshmen orientation course for freshmen. At the University of Pittsburgh, freshmen students are required to take two freshmen courses, one in the fall semester and the other in the spring semester.

Retention Rates and Rankings. The retention rates and rankings instrument was used for informational purposes. It established a reference point and showed what rates national engineering institutions obtained. It also provided a reference as to what the retention rates and rankings of other institution on the Urban 13 List obtained as well as were UWM ranked.

Interviews. The interviews of the three top engineering schools on the Urban 13 List with the highest retention rates were also used for informational

purposes. Since these schools' retention rates were higher and other factors were lower, the researcher wanted to know what was in place that impacted their retention rates. Since the strategies and techniques in place at the University of Cincinnati and the University of Pittsburgh increased the retention rates at these institutions, and not at UWM, a similar program may have a positive impact upon the retention rate in CEAS.

Student Opinion Survey. The results from the Student Opinion Survey indicated what the students in CEAS felt were the contributing factors that impacted the success of their freshman year. Time management and study skill techniques were both crucial factors. Both of these factors are included in a Guaranteed 4.0 Program, co-sponsored by the College for Students of Color at UWM.

The Guaranteed 4.0 Program is an educational seminar that details a unique study method that guarantees the student a 4.0 GPA. It is a systematic approach to learning that is presented in a dynamic and motivational format providing highly effective and action oriented steps to ensure academic success. The program is based on the fundamentals premise that repetition yields retention and understanding. The seminar empowers students by enhancing their ability to learn principles and concepts. If a student follows the 4.0 plan and does not obtain all "A's", he or she will receive $100 from the program presenter and firm owner, Donna O. Johnson. This is a one-day seminar that is divided into two main segments. The first segment consists of introductions and general information regarding study techniques, time management, and stress

management. The second segment is in the format of a workshop were students design a study work plan for all courses and are provided one-on-one assistance from the presenter. The presenter gives an explanation as to how to implement the plan. If the plan is followed as designed, with on compromises, the student is guaranteed to receive a grade of "A" in each of the courses.

The recommendation of the researcher is that this program be extended to all freshmen engineering students. The follow up of the components of the program should be incorporated into the first freshman orientation course. Again, the action-oriented response is one of the stages found in the literature review by Harris & Antonnen (1986).

College Advising and Faculty Involvement were the factors ranked by the respondents in the Student Opinion Survey as the components that had the least impact on their decision to remain in school after their freshman year. Since other studies and research indicate that these factors are important element used in retaining students, it would be in the best interest of the College to improve both of these elements.

Forrest (1982) and others presented compelling evidence of the relationship between advising and student retention. The data also showed that good advising does not just happen; it is the result of a carefully developed institutional plan and commitment. Therefore, the recommendation is that a plan and/or training program should be developed, documented, implemented, and accessible for all advisors in the College.

The researcher recommends that a faculty member moderate Sophomore Interest Groups, clusters of the 20-25 students enrolled in two or more courses together with a common theme. This group is generated at the end of the second freshman orientation course. The faculty member and advisor work closely together so that any transfer students would be added to the group.

The researcher also recommends that a Tri-A-Thon be established in the College. The Tri-A-Thon is a group consisting of three different types or units focused on one movement or race. The components would be a small group (5 or less) of freshman students, a junior student with the same major, forming a coalition with a faculty member.

The Tri-A-Thon would provide a realistic expectation channel for freshmen, assist freshmen with transitional adjustments, and provide relevancy. The faculty would have a greater presence with the freshmen as well as with the junior students. Again, these are the issues addressed in the literature review that impacts retention (Tinto, 1987; O'Banion, 1983; Boyer, 1987; and Pantages & Creedon, 1978).

And lastly, one cannot overlook family support. UWM is an urban institution and many students commute or have ties with families within a 200-mile radius. The researcher recommends that a program, workshop, or seminar be offered to students and family to address their concerns and offer solutions to themes found in this research that contribute to the success of the freshmen year experience. This becomes extremely important to students that are first generation college students. The results of research conducted by Astin (1987) in

the literature review indicated that first generation college students do not have siblings or parents that have experienced the registration process or academic experiences; therefore, workshops and seminars are a necessity for academic success.

In conclusion, implementation of these programs, strategies, and techniques with a dedicated staff and College support would increase the retention rates of students in the College of Engineering and Applied Science at the University of Wisconsin-Milwaukee.

As freshmen enter the College, each student progress should be monitored and documented. After these strategies and techniques are implemented, reviewing the number of students that remain in the College after their freshman year can be one form of an assessment of the program. Another assessment tool would be to survey the returning students during the first semester of their sophomore year or a questionnaire that is a part of the registration for classes that ask the students to evaluate their freshman year.

Implications for Future Research

As a result of this study, the researcher identifies five major areas in which addition studies would be of benefit.

The first area would be to determine which high schools use the same standards and rankings among its students. If all high schools used the same standards those students graduating in the top 10 percent of their class in one area or district would meet the same standards as students in another area.

The second area in which studies would be of benefit is to determine which effective training programs are available to advisors in establishing a rapport with students. A study of the techniques and strategies used in advising to assist students would also be helpful in training new advisors.

The third area in which future studies would be of benefit would be to determine strategies or methods that would provide more faculty involvement at the freshmen level.

The fourth area in which future studies would be of benefit is a review or study of the freshmen retention rate and graduation rates.

Finally, determining how to increase the diversity in CEAS would be an additional benefit. Recruit more Students of Color and women into the College and add a more diversified faculty would increase the diversity in CEAS. As students enter the building or take classes, they can see someone that looks like them.

APPENDICES

Appendix A: U. S. News and World Report Best National Universities

BEST NATIONAL UNIVERSITIES

U. S. NEWS & WORLD REPORT, September 18, 1995

Section: American's Best Colleges

Data for institutions used in this study.

Key to Chart:
A=overall score
B=Academic reputation
C=Student selectivity
D= Faculty resources
E=Financial resources
F=Retention rank
G=Alumni satisfaction
H=SAT/ ACT 25th-75th percentile
I=Freshman in top 10 percent of HS class (shown in percentages)
J=Acceptance rate (shown in percentages)
K=Yield (shown in percentages)
M=Education expenditure per student
N=Freshman retention rate (shown in percentages)
O=Graduation rate (shown in percentages)
P=Alumni giving rate (shown in percentages)

H		I	J	A	B	C	D	E	F	G
O	P		K	L		M		N		
Stanford University (California)										
1270-1450		90	20	98.1	1	6	3	6	7	33
93	28		54	12/1		$36,450		98		
Mass. Institute of Technology										
1290-1470		94	30	98.0	1	4	6	7	10	16
91	38		51	10/1		$31,585		96		
Cornell University (New York)										
1180-1380		83	33	94.0	8	11	11	22	12	72
90	21		47	13/1		$21,864		96		
University of Michigan Ann-Arbor										
1060-1300		65	68	86.9	8	39	26	42	23	142
85	14		37	16/1		$15,470		94		

California Institute of Technology

1350-1480		100	25	95.5	8	5	2	1	28	24
81	32		46	6/1		$63,575		93		

Carnegie Mellon University (Pa)

1150-1360		74	24	87.2	20	34	19	18	50	25
72	31		22	9/1		$25,026		87		

KEY TO CHART
A=Overall Score
B=SAT/ACT 25th -75th percentile
C=Freshman in top 10 percent of HS class (shown in percentages)
D=Acceptance rate (shown in percentages)
E=Yield (shown in percentages)
F=Yield (shown in percentages)
G=Educational expenditures per student
H=Freshman retention rate (shown in percentages)
I=Graduation rate (shown in percentages)
J=Alumni giving rate (shown in percentages)
K=Academic reputation

H	I	J	K	A	B	C	D	E	F
	G								

University of California-Berkeley

93	78	10	4	86.4	1110-1370	95	40	40	17/1
	$15,140								

University of Illinois Urbana-Champaign

91	79	14	20	74.4	23-28	50	76	48	18/1
	$8,515								

University of Wisconsin-Madison

91	71	20	17	81.2	940-1230	40	69	45	15/1
	$11,857								

University of Southern California

89	67	12	36	75.7	1000-1230	40	72	18	15/1
	$17,822								

Georgia Institute of Technology

86	69	34	27	76.9	1170-1330	90	59	38	19/1
	$12,128								

University of Texas at Austin
86 62 16 20 N/A 10001240 44 66 53 19/1
$8,270

Purdue West Lafayette (Indiana)
84 69 15 32 N/A 880-1130 28 90 41 19/1
$9,066

University of Pittsburgh
84 63 12 58 N/A 890-1120 23 82 39 15/1
$15,016

University of Memphis (Tennessee)
82 33 12 195 N/A 20-24 N/A 64 61 18/1
$7,264

University of Cincinnati (Ohio)
76 47 18 115 N/A 21-26 22 85 44 17/1
$14,051

University of Wisconsin-Milwaukee
70 37 7 115 N/A 21-25 11 74 52 15/1
$8,473

Appendix B: Urban 13 List

Urban 13 List

University of Alabama-Birmingham
701 20th Street South, Suite 1064
Birmingham, AL 35924
Peter O'Neil, Provost
(205) 934-0622-phone
(205) 934-1221-fax
Mary Beth Adams
Institutional Research
(205) 934-3254
marybeth@uab.edu
(205) 934-4193, Dr Ernest D. Rigney

University of Cincinnati
101 Administration
P. O. Box 210097
Cincinnati, OH 45221-0097
Anthony J. Perzigian, Interim Sr. Vice President &
Provost for Baccalaureate & Graduation Education
(513) 556-2588-phone
(513) 556-7861-fax
Stan Henderson
(513) 556-6004

Cleveland State University
1860 East 22nd Street
Rhodes Tower 1209
Cleveland, OH 44115
Harold L. Allen, Provost and Senior Vice President
For Academic & Student Affairs
(216) 687-3588-phone
(216) 587-9290-fax
Pam Charity, Advisor
(216) 687-6912
(216) 687-2555, College of Engineering

Florida Agriculture & Mechanical University (A&M)
Foote-Hilyer Administration Bldg., Room #301
Tallahassee, FL 32307
James H. Ammons, Provost & Vice President for

Academic Affairs
(850) 599-3276-phone
(850) 531-2551-fax
(850) 410-6349,Dr. Sheldon White

University of Houston
4800 Calhoun #212
Houston, TX 77004-2162
Edward P. Sheridan, Provost
(713) 743-0988-phone
(713) 743-9108-fax
(713) 743-4242, Engineering
(713) 743-4203, Mary Schultz, Advisor

University of Illinois-Chicago
2832 University Hall MC-105
601 South Morgan Street
Chicago, IL 60607-7128
(312) 413-3450-phone
(312) 413-3455-fax
(312) 996-2375, Dean D. France
(312) 996-0520, Renata
(312) 996-2400, Marilette

Indiana University-Purdue
University at Indianapolis (IUPUI)
355 North Lansing Street, Room 108
Indianapolis, IN 46202-2896
William M. Plater
Executive Vice Chancellor/Dean of the Faculties
(317) 272-4500-phone
(317) 274-4615-fax
(317) 274-8703, Theresa Bennett
(317) 274-0802, Engineering
(317) 274-5555, General Number

University of Massachusetts at Boston
100 Morrissey Boulevard
Boston, MA 02125
Charles S. Cnudde, Vice Chancellor for Academic
Affairs and Provost
(617) 287-5600-phone
(617) 287-5616-fax

(617) 287-5420, Jennifer Brown, IR
(617) 287-6050, Engineering
The University of Memphis
360 Administration Building
Campus Box 526653
Memphis, TN 38152-6653
J. Ivan Legg, Provost
(901) 678-2119-phone
(901) 678-3643-fax
(901) 678-3258, Charles Bray
c.bray@memphis.edu
(901) 678-2171 Dr. Richard Warder, Engineering

University of Missouri-St Louis
8001 Natural Bridge
408 Woods Hall
St. Louis, MO 63121
Jack Nelson, Vice Chancellor for Academic Affairs
(314) 516-5371-phone
(314) 516-5378-fax
(314) 516-4010, Larry Westermeyer

University of Missouri-Kansas City
Administrative Center 300G
5115 Oak Street
Kansas City, Mo 64110-2499
Marjorie Smelstor, Interim Provost/Vice Chancellor
For Academic Affairs
(816) 235-1107
(816) 235-5509-fax
(816) 235-5926, Jennifer Spielvogel, Institutional Research

University of New Orleans
Lake Front
New Orleans, LA 70148
Louis V. Paradise
Executive Vice Chancellor & Provost
(504) 280-6723-phone
(504) 280-6020-fax
(504) 280-6667, Willie Kirkland, Institutional Research

City College of New York
138th and Convent Avenue

New York, NY 10031
Zeev Dagan
Provost & Vice President for Academic Affairs
(212) 650-6638-phone
(212) 650-6425-fax
(212) 650-5435, Engineering

University of Pittsburgh
801 Cathedral of Learning
Pittsburgh, PA 15260
James V. Maher
Provost & Sr. Vice President
(412) 624-4223-phone
(412) 624-9640-fax
(412) 624-1220, Jim Ritchie, Institutional Research

Portland State University
P. O. Box 751
Portland, OR 97207-0751
Mary Kathryn Tetreault, Provost and
Vice President of Academic Affairs
(503) 725-5257-phone
(503) 725-5262-fax
(503) 725-3434, David Burgess
(503) 725-3432, Institutional Research

Temple University
401 Conwell Hall
1801 N. Broad Street
Philadelphia, PA 19122
Corrine Caldwell, Acting Provost
(215) 204-4775-phone
(215) 204-5816-fax
(215) 204-8825, Dr. Ridenour, Undergraduate Engineering
(215) 204-5050, Dr. Tim Walsh, Director of Student Information Systems

The University of Toledo
University Hall 3340
Toledo, OH 43606-3390
(419) 530-2738-phone
(419) 530-4496-fax
(419) 530-5873, Dick Eastop, Enrollment Management

Virginia Commonwealth University
Box 852527
901 West Franklin Street
Richmond, VA 23284-2527
Roderick J. McDavis, Provost and Vice President
For Academic Affairs
(804) 828-1345-phone
(804) 828-1887-fax
(804) 828-1244, Dr. Henry Rhone, Retention Rate =86.7% (90 Students)
Pre-Engineering 93.8% (15 returned out of 16 students)
(804) 828-2925, Engineering

Wayne State University
4092 Faculty Administration Bldg.
656 Kirby
Detroit, MI 48202
Marilyn L. Williamson, Interim Provost and Sr. Vice Pres. For
Academic Affairs
(313) 577-2200-phone
(313) 577-5666-fax
(313) 577-3780 Engineering
(313) 577-3780, Dean Gerald Thompson

Some of the institutions listed on the Urban 13 list participated in a retention survey. The results of the survey are located at the University of Oklahoma.
Retention Information/Survey
University of Oklahoma
Theresa Smith
(405) 325-2158
Director of Consortium Data Exchange for Student Retention

Appendix C: EAS 100 Syllabus

College of Engineering and Applied Science
Introduction to Engineering and Applied Science
EAS-100, Spring, 1997*

Text: Studying Engineering, A Road Map to a Rewarding Career, by Raymond B. Landis, Publisher: Discovery Press.

Date	Topic	Assignment (Due next class period)
Jan. 14	**Introduction**: Establish classroom procedures, handout class materials, and discuss student worksheets.	Read Chapter 1 and complete problems 2, 11, and 22.
Jan. 21	**Keys to Success in Engineering Study**: Memory, note taking skills, reading and test tasking skills. Tour Computer Aided Engineering (CAE) Lab.	Read Chapter 2 and complete problems 1, 4, and 7. Also, complete computer problem given in class.
Jan. 28	**The Engineering Profession**: Discussion of specific engineering majors by a practicing engineer and a related laboratory tour.	Read Chapter 3. Assign the student tower of doom project (due Feb. 25, not next week).
Feb. 4	**Academic Success Strategies** I: Discussion of specific engineering majors by a practicing engineer and related laboratory tour.	Work on individual tower of doom project.
Feb. 11	**Academic Success Strategies II**: Discussion of specific engineering majors by a practicing engineer and related laboratory tour	Work on individual tower of doom project and read the CEAS Student Handbook.
Feb. 18	**In-class Group Dynamics Project**: Surprise group project. Learn the elements of group dynamics. Fun, fun, fun!!!	Read Chapter 4 and work on individual tower of doom project. Pass-out **Take-Home Exam** (to be done using class hand-out materials).
Feb. 25	**Student Tower of Doom Project Test**: Projects are tested to failure and reviewed by faculty members. Also, **Take-Home Exam due!**	None!!!
March 4	**Information on Diversity**: What is "diversity"? Also, discuss student group design project due April 22.	Work on group design project.
March 11	**Student GER and Course Planning**: Plan the courses you will take for the next few semesters.	Read Chapter 5 and work any 14 problems on pages 195-198.
March 18	**Broadening Your Education**: CEAS student groups.	Work on group design project.
March 25	**SPRING BREAK**	**None!!!**
April 1	**Pre-Professional Employment**: CEAS co-op program	Work on group design project.
April 8	**Graphing Hand Calculators - Why Do YOU Need One**: More fun stuff!!!	Work on group design project.
April 15	**Continuous Quality Improvement (CQI) Discussion**: Improving the quality of this course.	Work on group design project.
April 22	**Group Project Competition Tests.**	None.
April 29	**Final Examination and Course Evaluation.**	Whoopee!

Appendix D: Re-Installment Contract

Re-Installment Contract

Upon re-entering the University of Wisconsin-Milwaukee, College of Engineering and Applied Science, I_____, hereby establish a commitment with my Academic Advisor, Mrs. Johnson that I will meet and keep the appointments with her. I will also adhere to the instructions of my advisor.

This contract includes:

Worksheet for Planning your Time/Schedule
Course Outline for the next year
Homework assignments for each course
Appointment Schedule

I understand that if I forfeit this agreement by not keeping my appointments, not doing the work assigned by my advisor, and maintaining a grade of "C" or better, I will not be allowed to attend this University.

Option

I also permit my advisor to discuss my academic status with members of my immediate family, the Financial Aid Office and others that are part of the support mechanism in my college career.

_____

Student's Name Identification Number Date

_____ _____

Advisor's Name Date

Worksheet For Planning Your Time/Schedule

Time	Monday	Tuesday	Wednesday	Thursday	Friday	Saturday	Sunday
6:30-7:30							
7:30-8:30							
8:30-9:30							
9:30-10:30							
10:30-11:30							
11:30-12:30 PM							
12:30-1:30							
1:30-2:30							
2:30-3:30							
3:30-4:30							
4:30-5:30							
5:30-6:30							
6:30-7:30							
7:30-8:30							
8:30-9:30							
9:30-10:30							
10:30-11:30							
1:30 PM - 630 AM	Sleep	Sleep	Sleep	Sleep	Sleep	Sleep	Sleep

Homework Assignment Sheet

Student's Name_____ID #_____

Course_____

Week	Assignment	Started	Completed	Turned-I
1				
2				
3				
4				
5				
6				
7				
8				
9				
10				
11				
12				
13				
14				
15				

University of Wisconsin-Milwaukee

College of Engineering & Applied Science

Undergraduate Advising Semester Coursework Sheet

Student's Name_____ ID _____

Advisor: Ester Johnson Telephone # 229-3882

Fall Semester	Courses	Credits
	Total	
UwinterM		
	Total	
Spring		
	Total	
Summer		
	Total	

CEAS ADVISING NOTES

Student's Name_____ID #_____

Meeting Dates	Advisor	Advising Notes

Appendix E: Statement For Survey Administrators

Professor:

Thank you for taking the time to assist me with this survey.
As part of my dissertation, I would like to know what components contributed to the success of our students' freshmen year. The answers to this survey are a vital port of my data collection process.

To provide consistency in the procedure, I am asking that each professor read the following statement prior to giving the survey.

Hand out the survey and indicate to the students that "if you have participated in this survey before, please do not hand in your results."

READ:

Ester Johnson, the Academic Advisor, in the College, would like for each of you to honestly complete the following survey. The results of this information will be used in her study of the retention rates of students in our College.

Collect the survey

READ:

On behalf of Ester Johnson, thanks for your participation. If you have any questions or concerns, you can see her in the advising office in room E386.

Pleas return the completed surveys to me by the end of the week. You can also place them in my mailbox on the 5th floor or call me at X3882 or email me at ebj@uwm.edu, **and I will pick them up.**

Again, thank you.

Ester Johnson

Academic Advisor

EMS E386

Appendix F: Student Opinion Survey

Survey

Directions

Please circle the correct response:

1. Your status:

   Freshman Sophomore Junior Senior

2. Did you start your freshman year at UWM? Yes No

Select the response that best represents the degree to which each component impacted or contributed to the success of your freshman year.

3-Very Influential 2-Influential 1-Somewhat Influential 0-No Influence

A. Family Support.....	3	2	1	0
B. College Advising.....	3	2	1	0
C. High School Preparation.....	3	2	1	0
D. Faculty Involvement.....	3	2	1	0
E. Study Teams/Partners.....	3	2	1	0
F. Good Study Habits.....	3	2	1	0
G. Reduction of Work Schedule.....	3	2	1	0
H. Good Time Management Skills	3	2	1	0
I. Other:_____	3	2	1	0

Place an "X" for the correct response

4. **Male_____ Female_____**
5. **Caucasian____ African American_____ Hispanic_____**

   Native American_____ Southeast Asian_____

   International unknown____

Optional: Name_____ ID number_____

Appendix G: Fact Book Engineering Data Sheet

University of Wisconsin Milwaukee

Enrollment by Academic Area and Year Level

Fall 1999

Source: Budgets, Institutional Research and Space Management

Inst\ir\factbook\fb9900\ENROLL1.WK4

School/College	Freshmen	Sophomore	Juniors	Seniors	Specials	Totals
Allied Health	155	237	173	314	8	887
Architecture	156	165	137	165	6	629
Business Adm.	615	767	718	1,093	24	3,217
Education	301	398	277	517	313	1,806
Engr. & A. S.	356	404	248	469	9	1,486
The Art	345	421	210	417	1	1,394
Letters & Sci.	2,380	1,854	1,046	1,212	37	6,529
Library &Info	6	15	15	15	0	51
Nursing	159	201	167	254	0	778
DOCEx	0	0	0	0	1,112	1,112
Social Welfare	156	201	167	254	0	778
UWM Total	4,629	4,597	3,138	4,749	1,580	18,693

BIBLIOGRAPHY

A Comprehensive Approach to the Retention of Transfer Students. (1999). USA Group Noel-Levitz, Author.

Access Plus. (1999). USA Group Noel-Levitz, Author.

Aldredge, T. (1997). The Impact of a College Success Course on Students' Long-Term Academic Persistence (Retention, Dropout, Community College Students, High School. Unpublished doctoral dissertation, University of California-Davis.

Alexander, E. (Feb. 1998). An Investigation of the Results of a Change in Calculus Instruction at the University of Arizona (Doctoral dissertation, The University of Arizona, 1997). ProQuest - Dissertation Abstract, AAC9806815, 3049.

Anderson-Rowland, M. (1998). In Arizona State University, Effect of Course Sequence on the Retention of Freshmen Engineering Students: When should the intro-engineering course be offered? (pp. 252-257). Tempe, AZ: IEEE Piscataway, NJ.

Astin, A. (1975). Preventing students from dropping out. San Francisco: Jossey-Bass.

Astin, A. (1993, September 22). College Retention. Chronicle of Higher Education, 40(5), A48.

Astin, W. (1997, December). How 'good' is your institution 's retention rate? Research in Higher Education, 38(6), 647.

Atkinson, R. (1990, May 27). Supply and demand of scientists and engineers: A national crisis in the making. Science, 248(4954), 425.

Avenoso, E. & Totoro, K. (1994, Spring). Comparison of retention rates of first and second year co-op and non co-op students at a small institution. Journal of Cooperative Education, 29(3), 6.

Bagayoko, D., & Kelley, E. (1994, Fall). The dynamics of student retention: A review and a prescription. Education, 115(1), 31.

Baldo, T., & Softas-Nall, B.C. (1997, March). Student review and retention in counselor education: An alternative of Frame and Stevens-Smith. Counselor Education & Supervision, 36(e), 245.

Barr, R., & Tagg, J. (1995, November/December). From Teaching to Learning: A New Paradigm for Undergraduate Education. Change 101

Bean, J. (1982). Conceptual models of student attrition: How theory can help the institutional research. San Francisco: Jossey-Bass.

bfs.uwm.edu/DEPTS/BIRSPM/INTRANET [Departmental Planning Profiles Academic Division]. (1999-2000). Milwaukee, WI: Office of Budget, Institutional Research & Space Management [Producer and Distributor].

Boyer, E., (1997). College: The undergraduate experience in America. New York, NY. Harper & Row.

Boykin, W. (1983). Student Retention and Attrition in an Urban University. Unpublished doctoral dissertation, University of Wisconsin-Milwaukee.

Brown, N., & Cross Jr., E. (1993, Autumn). Retention in engineering and personality. Educational & Psychological Measurement, 53(3), 661.

Bunderson, E., & Christensen, M. (1995, fall). An analysis of retention problems for female students in university computer science programs. Journal of Research on Computing in Education, 28(1), 1, 18.

Busby, C. & Jackson, H. (1995). Student Retention Through Communication: Applying D'Aprix's Proactive Communication Model. NASP Journal, 32, 98-105.

Cabrera, A., & Nora, A. (1993). College Persistence: Structural Equations Modeling Test of an Integrated Model of Student Retention. Journal of Higher Education, 64, 123-139.

Campbell Jr., G. (1997). Engineering and affirmative action: Crisis in the making (SEQ61659). New York, NY: BBB22614 National Action Council for Minorities in Engineering. (ERIC Document Reproduction Service No. ED 422161)

Campbell, T., & Campbell, D.E. (1997, December). Faculty/Student mentor program: Effects on academic performance and retention. Research in Higher Education, 38(6), 727.

Chaffee, E. (1984). Successful Strategic Measurement in Small Private Colleges. Journal of Higher Education, 55, 212-241.

Chenoweth, K. (1999, February 18). HBCUs tackle the knotty problem of retention. Black Issues in Higher Education, 15(26), 38.

Collison, M. (1999, February 18). The new complexion of retention services. Black Issues in Higher Education, 15(26), 34.

Congos, D., & Schoeps, N. (1997, Winter). A Model for evaluating retention programs. Journal of Developmental Education, 21(2), 2.

Credle, J., & Dean, G. J. (1991, October). A comprehensive model for enhancing black student retention in higher education. Journal of Multicultural Counseling & Development, 19(4), 158.

Danhardt, G. (1995). Tracking student Enrollment Using the Markov Chain, Comprehensive Tool for Enrollment Management. Journal of College Student Development, 36, 457-462.

Dervarics, C. (1997, September 4). 'Super' Pell grant among Higher Education Act idea. Black Issues in Higher Education, 14(14), 5.

Drago, R., & Williams, J. (2000, November-December). A half-time tenure track proposal. Change: The Magazine of Higher Education, 32(6), 47-51.

Duncan, S. (1997). Personality and Cognitive Characteristics of Students In Science and Engineering (Technology Students). Unpublished doctoral dissertation, Indiana State University.

Durio, H., And Others. (1979). Mathematics Achievement Level Testing as a Predictor of Academic Performance in Engineering Students (SEQ30879). Austin, TX: University of Texas-Austin. (ERIC Document Reproduction Service No. ED 187548)

Etchison, J., (1998). Curriculum restructuring for freshman retention in the 1990's and beyond. ASEE Annual Conference Proceedings of the 1998 Annual ASEE Conference. .

Felder, R., & Others. (1994). Gender Differences in Student Performance and Attitudes. A Longitudinal Study of Engineering Student Performance and Retention (QXM64275). Raleigh, NC: North Carolina State University-Raleigh.

Forrest, A. (1982). Increasing Student Competence and Persistence: The Best Case for General Education. Paper presented at American College Testing Program: National Center for Advancement of Educational Practices, Iowa City, IO.

Freshman Year College: A Comprehensive Approach to the Retention of First-Year Student. (1999). USA Group Noel-Levitz, Author.

Fuertes, J., & Sedlacek, W. E. (1994, July). Using the SAT and non-cognitive variables to predict the grades and retention of Asian American. Measurement & Evaluation in Counseling & Development, 27, 74.

Gallagher, R., Golen, A. & Kelleher, K. (1992). The Personal, Career, & Learning skills Needs of College Students. Journal of College Student Development, 33, 301-309.

Gardner, C. (1998, September 7). Keeping students in school. Christianity Today, 42(10), 34.

Gateway Program. (1999). USA Group Noel-Levitz

Gay, J., & Rueth, T. (1993, Spring). The negative side effects of retention, academic competition, and punishment. Education, 113(3), 434.

Gebelt, J., & Parilis, G. (1996, Summer). Retention at a Large University: Combining skills with course content. Journal of Developmental Education, 20(1), 2.

Gee, P. (1976). The Minority Engineering Advancement Program at Indiana University Purdue University at Indianapolis (Session 2470). Indianapolis, IN: Indiana University-Purdue University at Indianapolis, Purdue School of Engineering.

Georges, A. (1999). Keeping what we've got: The impact of financial aid on minority retention in engineering. National Action Council of Minority in Engineering, 9, 1.

Georgia study cities hope for student retention, better grades. (1997, May 29). Towns, G. Black Issues in Higher Education, 14(7), 14.

Gerdes, H., & Mallinckrodt, B. (1994). Emotional, social & academic adjustment of college students: A longitudinal study of retention. Journal of Counseling and Development, 25, 315-320.

Gold, J. (1995). An Intergenerational Approach to Student Retention. Journal of College Student Development, 36, 182-187.

Gordon, V., & Grites, T. (1984). The freshmen seminar course: Helping students succeed. Journal of College Student Personnel, 25, 315-320.

Haag, S., & Rhoads, T. (1998). Assessing the effectiveness of integrated freshmen curricula in engineering. Frontiers in Education Conference Proceedings of the 1998 28th Annual Frontiers in Education Conference.

Haberman, M., & Dill, V. (1993, December). The knowledge base on retention vs., teacher ideology: Implications for teacher preparation. Journal of Teacher Education, 44(5), 352.

Habley, W. (1981). Academic advisement: The critical link in student retention. National Association of Student Personnel Administrators Journal, 18(4), 45-50.

Harris, H., & Antonnen, R. (1986, May). Assessing needs of male & female college freshmen. Journal of Counseling and Development, 227-279.

Harris III, J., & Ford, D. (1999, January). Hope deferred again. Education & Urban Society, 31(2), 225.

Heywood, J. (1998). Pupil's attitudes to technology: A review of studies which have a bearing on the attitudes which bring with them to engineering. Frontiers in Education Conference Proceeding of the 1998 28th annual Frontiers in Education Conference.

Hill, G. (1997). The experiences of African-American students majoring in engineering: Cognitive, non-cognitive and situational aspects (Retention). Unpublished doctoral dissertation, University of Pittsburgh.

Hossler, D. (1984). Enrollment management: an integrated approach. New York: The College Board.

House, E. (1991, February). The Perniciousness of Flunking Students. Education Digest, 56(6), 41.

Hudspeth, M., & Aldrich, W. (1998). Summer Bridge to Engineering. Paper presented at California State Polytechnic University, Pomona.

Iffert, R. (1958). Retention and withdrawal of college students. Washington, D.C.: U.S. Government Printing Office.

Johnson, I., & Otten, A. (1996). Leveling the playing field: Promoting success for students of color (Vol. 74). San Francisco: Jossey-Bass.

Johnston, C. (1997). Caring behaviors of college faculty and staff (Retention). Unpublished doctoral dissertation, University of Oregon.

Kenny, M., & Rice, K. (1995). Attachment to Parents and Adjustment in Late Adolescent College Students: Current Status, Applications, and Future Considerations. The Counseling Psychologist, 23, 833-456.

Kettering Minority Retention of Engineering Students Rank Third in Michigan. (1999, January). Hispanic Times Magazine, 35, Author.

Kluepfel, G. (1994, Spring). Developing successful retention programs: An interview with Michael Hovland. Journal of Developmental Education, 17(3), 28.

Kluepfel, G., & Parelius, R. (1994, Spring). Involving faculty in retention. Journal of Developmental Education, 17(3), 16.

Koerner, B. (1997, March 10). Top Schools. U.S. News & World Report, 122, 94.

Kostelaba, N. (1997). The Relationship of pre-enrollment factors on first year retention of community college students. Unpublished doctoral dissertation, The Pennsylvania State University.

Kuh, G., Schuh, J., & Whitt, E. (1991). Involving colleges: Successful approaches to fostering student learning and development outside the classroom. Jossey-Bass: 1991.

Kvam, P. (2000, May). The Effects of Active Learning Methods on Student Retention in Engineering Statistics. American Statistics, 54(2), 136.

Lambertz, G. (1998). An Analysis of Performance Gap Scores as Measured By The Student Satisfaction Inventory: The Relationship To Retention (Retention, Private Education). Unpublished doctoral dissertation, Montana State University.

Lemann, N. (1998, August 31). Universities use Rankings, too. U. S. News & World Report, 125, 81.

Levine, J., & Wycokoff, J. (1991, Summer). Predicting persistence and success in baccalaureate engineering. Education, 111(4), 461.

Levitz, N. (1999). Academic excellence awards. Noel Levitz, Author.

Lewallen, W. (1993). The Impact of Being Undecided on College Student Persistence. Journal of College Student Development, 34, 103-112.

Love, B. (1993, April). Issues and Problems in the retention of black students in predominantly white institution of higher education. Equity & Excellence in Education, 26(1), 27.

Low, C. & Handal, P. (1995). Relationship Between Religion and Adjustment to College. Journal of College Student Development, 36, 406-412.

Mason, H. (1998, December). A Persistence model for African American male urban community college students. Community College Journal of Research & Practice, 22(8), 751.

Mayer, A., & McConatha, J. (1982, November). Surveying Student Needs: A Means of Evaluating Student Services. Journal of College Student Personnel, 1, 473-476.

McDonald, L., & Gean, L. (1992, Summer). Thinking of retaining a student? Try one or more of the twenty-five alternatives to retention. Education, 112(4), 576.

McGrath, M., & Braunstein, A. (1997, September). The prediction of freshmen attrition: An examination of the importance of certain demographic factors. College Student Journal, 31(3), 396.

McLaughlin, G. & Brozovsky, P., et al. (1998, February). Changing perspectives on student retention: A role for institutional research. Research in Higher Education, 39(1), 1.

Melendez, J. (1998). Analysis of University Personnel's Perception of Persistence/Retention. Unpublished doctoral dissertation, Andrews University.

Mitag, K., & Mason, D. (1999, April). Cultural factors in science education--variables affecting achievement. Journal of College Science Teaching, 28(5), 307.

Moore Jr., W. (1970). Against the Odds: Higher Risk Student in the Community College. San Francisco: Jossey-Bass.

Morrison, C., And Others. (1995). Retention of Minority Students in Engineering: Institutional Variability and Success (BBB22614). : (ERIC Document Reproduction Service No. ED 401109)

Morse, R., & Flaning, S. (2000, September11). How we rank the colleges. U.S. News & World Report, 129, 10.

Mossa, J. (1995, July). Topic synthesis: A vehicle for improving oral communication skills, comprehension and retention. Journal of Geography in Higher Education, 19(2), 151.

Mutter, P. (1992). Tinto's Theory of Departure and Community College Persistence. Journal of College Student Development, 33, 310-317.

Naretto, J. (1995). Adult Student Retention: The Influences of Internal and External Communication. NSSPA Journal, 32, 90-97.

New Vision Program. (1999). USA Group Noel-Levitz, Author.

O'Branion, T. (1972). An Academic Advising Model. Junior College Journal, 42(6), 62, 64, 66-69.

Pantages, T., & Creedon, C. (1987). Studies of College Attrition: 1950-1975. Review of Educational Research, 48(1), 49-101.

Parker, C. (1997, February 20). Making retention work. Black Issues in Higher Education, 13(26), 120.

Perri-Petruolo, G. (1998). Mentoring of Undergraduate Students: The Assessment of Mentor Effectiveness (Quality of Mentoring) and Its Relationship to Student Outcomes [Abstract]. ProQuest, 251.

Reichert, M., & Absher, M. (1997, July). Taking Another Look at Educating African American Engineers: The Importance of Undergraduate Retention. Journal of Engineering Education, 63(4), 321.

Reinstein, A., & Garr, S. (1995, July/August). New Approaches to Recruiting and Retention in Accounting Programs. Journal of Education for Business, 70(6), 332.

Rendon, L. (1993, Fall). Eyes on the Prize: Students of Color and the Bachelor's Degree [Review of the book Community Colleges]. Community College Review, 21, 3, 11.

Reyes, M., Anderson-Rowland, M., & McCartney. (1998). Learning from our Minority Engineering Students: Improving Retention. Arizona: Arizona State University.

Reyes, N. (1997, February 20). Holding on to what they've got. Black Issues in Higher Education, 13(26), 36.

Richardson Jr., R. (1997, February 20). Accumulated wisdom on recruitment & retention. Black Issues in Higher Education, 13(26), 26.

Roach, R. (1997, November 27). Retention Pacesetter University of Virginia. Black Issues in Higher Education, 14(20), 35.

Roueche, J., & Kirk, R. (1973). Catching Up: Remedial Education. San Francisco: Jossey-Bass.

Rowser, J. (1997, May). Do African American student's perceptions of their needs have implications for retention? Journal of Black Studies, 27(5), 718.

Ruddock, M. (1996). The Efficacy of Prerequisite Courses in Mathematics for Minority and White College Students. Unpublished doctoral dissertation, University of Texas-Austin.

Rustagi, N. (1997, November/December). A study of the retention of basic quantitative skills. Journal of Education for Business, 73(2), 72.

Sanders, L., & Burton, J. (1996, October). From Retention to Satisfaction: New outcomes for assessing the freshman experience. Research in Higher Education, 37(5), 555.

Santarini, M. (1998, May 25). Panel: EE Educators Need to Raise Retention. Electronic Engineering Times (1008), 97.

Sayuri, T., Goodings, D., & Byrnes, J. (1998, July). Retention & Performance of Male and Female Engineering Students: An Examination of Academic Environmental Variables. Journal of Engineering Education, 87(3), 297.

Schroeder, K. (1998, February). Science Majors Defect. Education Digest, 63(6), 75.

Seymour, E. (1995). The Loss of Women from Science, Mathematics, and Engineering Undergraduate Majors: An Explanatory Account (Science Education: Issues and Trends). Boulder, CO: University of Colorado-Boulder, Bureau of Sociological Research.

Seymour, E. (1995, May). Revisiting the Problem Iceberg: Science, Mathematics, Engineering Students Still Chill Out. JSCT, 392-400.

Shea, C. (1992, July 15). Chronicle of New Mexico (Albuquerque NM. Chronicle of Higher Education, 38(45), A32.

Sherman, M. (1997). The New Vision for Continuing Higher Education: Creating Economic Wellness. San Francisco, CA: Jossey-Bass.

Sherman, T., & Giles, M. (1994, Spring). Assessment and Retention of Black Student in Higher Education. Journal of Negro Education, 63(2), 164.

Smith, F. (1997). Orientation Effects on African-American Engineering Students: The LSU Case (Louisiana State University, Undergraduates) (Doctoral dissertation, Louisiana State University, 1997). Higher Education, 0745(0537), 0631.

Smith, S. (1999, May 31). Researching Black Male Retention. Community College Week, 11(22), 24.

Spady, W. (1971). Dropouts from Higher Education. Interchange, 2(3), 38-62.

Spann, M., & Calderwood, B. (1998, Fall). Increasing student success: An interview with Edward Morante. Journal of Developmental Education, 22(1), 16.

Student Support Services Program. (1999). USA Group Noel-Levitz, Author.

Summerskill, J. (1962). Dropouts from College. In Meritt Sanford (Ed.) The American College. New York, NY: John Wiley & Son.

Swail, W. (1996). The Development of A conceptual Framework to Increase Student Retention In Science, Engineering, and Mathematics Programs at Minority Institutions of Higher Education. Unpublished doctoral dissertation, George Washington University.

Thomas, R., & Chickering, A. (1984). Foundations for Academic Advising. San Francisco: Jossey-Bass.

Thompson, J., & Morse, R. (1997). An Explanation of the U.S. News Rankings. U.S. News & World Report, 123, 98.

Tinsley, H., St. Aubin, T. & Brown, M. (1982). College Student Help Seeking Preferences. Journal of Counseling Psychology, 29, 523-538.

Tinto, V. (1987). The Principles of Effective Retention. Paper presented at Fall Conference of the Maryland College Personnel Association, Largo, MD.

Tinto, V., & Wallace, D. (1986). Retention: An Admission Concern (HE 521993). (ERIC Document Reproduction Service No. EJ349478)

Tinto, V., Russo, P., & Kadel, S. (1994, March). Constructing Educational Communities: Increasing Retention in Challenging Circumstances. AACC Journal, 26-29.

Weissberg, M., Bernsten, M., Cote, A., Cravey, B., Heath, K. (1982). An Assessment of the Personal, Career, and Academic Needs of Undergraduate Students. Journal of College Student Personnel, 33, 115-122.

White, K., & Hendrie, C. (1999, June 02). News in Brief: A National Roundup. Education Week, 18(38), 4.

White, W., & Mosely, D. (1995, Spring). Twelve-year pattern of retention and attrition in a commuter type university. Education, 115(3), 400.

Wiener, W., & Luxton, L. (1994, Spring). The Development of Guidelines for University Programs in Rehabilitation Teaching. Re: View, 26(1), 7.

Wilson, D., Woodhead-Lyons, S., & et al. (1998, February 10). Alberta's rural physician action plan: An integrated approach to education, recruitment and retention. CMAJ: Canadian Medical Association Journal, 158(3), 351.

Wilson, S., & Mason, T. (1997, July). Evaluating the impact of receiving university-based counseling services on student retention. Journal of Counseling Psychology, 44(3), 316.

Wilson, T., & Linville, P. (1985). Improving the Performance of College Freshmen with Attributional Techniques. Journal of Personality and Social Psychology, 49, 287-293.

Year One. (1999). USA Group Noel-Levitz, Author.

Zhang, Z. (1998) Prediction and Analysis of Freshmen Retention. AIR.